Politecnico di Torino

Corso di Laurea Magistrale in Ingegneria dei Materiali
A.a. 2020/2021
Sessione di Laurea luglio 2021

Giorno di Laurea: 13.07.2021

Niobium microalloying of press hardened steels for automotive applications

Relatore:
Prof. Paolo Matteis

Candidato:
Alessandro Pavesio

INDEX

Thesis purpose

In the last decades the role of safety in the automotive sector has become more and more relevant, in particular in the recent years, where it went at the same pace with the increase of attention to the environment.

Car manufacturers are strongly interested in enhancing the security level of their vehicles and at the same time in reducing emissions. New technologies have been developed, such as new propulsion systems, but one thing that is in common with every possible strategy in reducing the emissions is the vehicles weight reduction.

Naturally, the weight reduction must not compromise the safety of passengers.

That is the reason why a great contribution both to the weight reduction (and therefore to emissions reduction) and to the increase of safety was given by the invention of the press hardening process, which enables to produce stronger pieces with the use of less material.

The steels produced in this way are called “press hardened steels” (abbreviated “PHS”).

The martensitic microstructure achieved with these properties is responsible for better mechanical properties, but on the other hand it is sensitive to Hydrogen embrittlement and it is subject to grain coarsening, that reduces toughness. Moreover, Martensite shows little bendability, which limits its applications.

In order to reduce these side effects of press hardened steels, microalloying elements like Vanadium or Titanium are added to the steels.

Another innovative microalloying element that shows extremely good results in improving press hardening steels is Niobium. Its technology and application are more recent than the ones of the others microalloyers, but due to its outstanding outcomes Niobium recently caught the interest of the market, and its global demand has been constantly increasing in the last decades.

The purpose of this thesis is to describe the press hardening process in detail, referring to the production of sheet-steel parts dedicated to the production of the body-in-white in the automotive sector, usually made of 22MnB5 steel grade.

Then, after having outlined the main weaknesses of press hardening in terms of properties of the pieces produced, it is shown how a small addition of Niobium can drastically reduce the negative effects to whom press hardening is subjected.

1 - Press hardening

1.1 - Introduction

The press hardening process was invented in Luleå, Sweden, in 1973. It is also called "hot stamping", "hot pressing" or "die quenching"

Developed by Carl-Erik Ridderstråle, it was patented in 1974 and published in 1977 by the Swedish company *Plannja HardTech AB* (renamed *SSAB HardTech* in 1990), a subsidiary of *Norrbottens Järnverk AB* (nowadays part of the Spanish company *Gestamp HardTech AB*, which purchased it in 2005).

The basic principle of press hardening mentioned in the original patent [1] is the following one:

> *"A hardened steel article is formed by heating a hardenable steel blank to hardening temperature (750–1000°C, preferably 900°C) and then placing it in a forming apparatus in which the blank is deformed and simultaneously rapidly cooled to obtain a martensitic and/or bainitic structure while the blank remains in the apparatus which serves as a gauge for preventing distortion ... Cooling is by cooling parts of the forming device and/or by direct cooling with salt water or oil".*

The original patent stipulated the use of Boron steels, and nowadays the 22MnB5 Boron-alloyed steel is the most widely used for press hardening, due to its acceptable hardenability and to the fact that it produces a fully lath martensitic structure, without anu Ferrite or Pearlite left.

At the very beginning, press hardened steels were mainly used in agricultural industry and in construction industry, for applications such as lawn-mower blades, saw blades, ploughshares, mouldboards, disc harrows, forks and spades.

But PHS were soon largely used in the automotive field, with two main purposes:

- Vehicle weight reduction;
- Safety improvement.

1.2 - Press hardening steels for vehicle weight reduction and safety enhancement

In the last years, the problem of global warming is becoming more and more serious; so, since the cars are for sure one of the biggest causes of emissions of greenhouse gases such as Carbon dioxide, the automotive industry is expected to give a strong contribute to reduce the environmental pollution, by limiting for instance vehicles emissions.

This can be done by increasing the fuel efficiency of the traditional internal combustion engine-powered vehicles.

Although several innovative technologies have been developed and alternative fuels and powertrains have been introduced in the automotive field (like liquid petroleum gas, electric and petrol-electric hybrid), one of the best ways in order to increase the fuel efficiency remains the simple vehicle weight reduction, also known as lightweighting.

In fact, a 10% of lightweighting can result in 2,5% increase of fuel efficiency [2].

Typical passenger vehicles owe the 30% of their weight to the body structure, called “body-in-white” (abbreviated “BIW”). It also represents the safety cell of the vehicle.

Fig. 1: Car body-in-white.

Then, since the BIW represents a relevant percentage of the vehicle weight, the automotive industry has been concentrating its efforts on it in order to reduce the weight and then to enhance the fuel efficiency.

It is possible to reduce the weight of the BIW by acting on the properties of the sheet-steel materials, by means of two strategies:

- Use of sheet-steel materials that show **lower density**;
- Use of sheet-steel materials that are **thinner** (this strategy is called “downgauging”).

Before the introduction of press hardening, the BIW was made of single cold-stamped parts of sheet-steel materials, joined together and finally assembled in the BIW.

The typical materials involved were hypoeutectoid ferritic low-Carbon low-alloy steels (like Carbon-Manganese steels), high-strength low-alloy steels (HSLA) and multiphase low-Carbon low-alloy steels (such as dual phase steels and complex phase steels).

The main reasons behind the choice of these kind of materials were their relative low cost, the ease in manufacturing them and their high yield strength.

Since the materials are given, the easier and mostly adopted strategy would be the downgauging, i.e. a thinning of the sheet steels, as said.

But of course, downgauging itself would have negative consequences on the improvement of passengers safety and crashworthiness, which are fundamental aspects of automotive engineering as well, that have to meet more and more stringent compulsory crash standards over time.

Indeed, during a crash collision the BIW must act as a barrier between the people inside the car and the object hit in the accident, in order to protect the passengers from the crash by absorbing the energy of the impact. So, by reducing the BIW thickness, stiffness and structural strength of the BIW are obviously degraded, and it would be a less efficient barrier.

Another negative effect of the downgauging is the so-called “springback”, which consists in a geometric distortion of the piece as it is reduced in thickness.

Moreover, the downgauging makes the formability inferior.

1.2.1 - Ultra-High Strength Steels (“UHSSs”)

Weight reduction by downgauging and enhancement of passengers’ safety may then seem in contrast with each other.

The solution to these issues related to downgauging, which anyway must be exercised, comes from the invention of the press hardening process, which allows to manufacture ultra-high strength steels (abbreviated “UHSSs”), such as Boron steels, giving them the desired shape quite easily.

Actually, there is not a univocal way to define the UHSSs, but it is possible to place a steel with a Yield Strength higher than 550 MPa in the category of the UHSSs.

This category embraces various types of steels, which are the following ones [3]:

- Medium Carbon low-alloy hardening steels;
- Medium alloy hardenable or tool and die steel;
- High alloy hardenable steels;

- High nickel maraging steels;
- Martensitic stainless steels;
- Semi austenitic precipitation hardenable stainless steels.

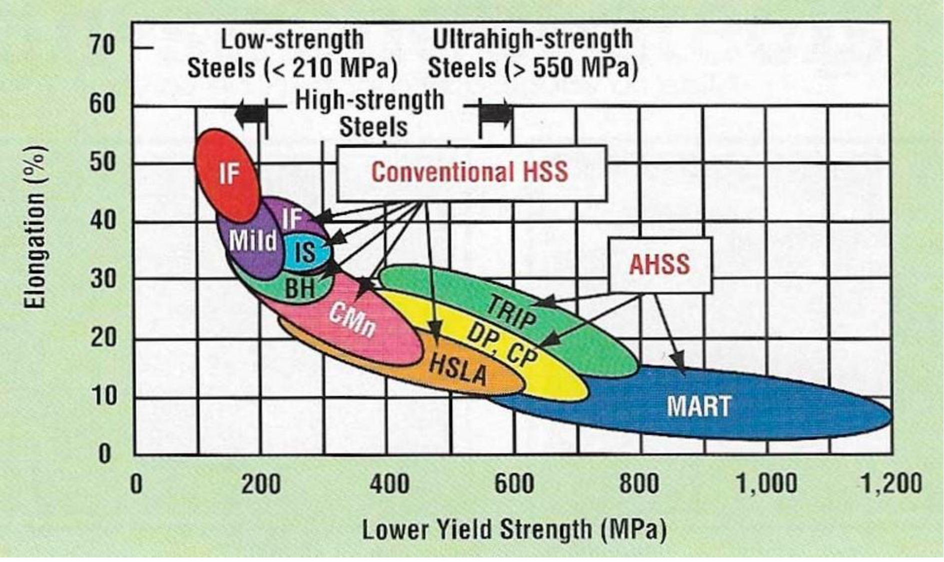

Fig. 2: Lower Yield Strength and Elongation for several types of steels.

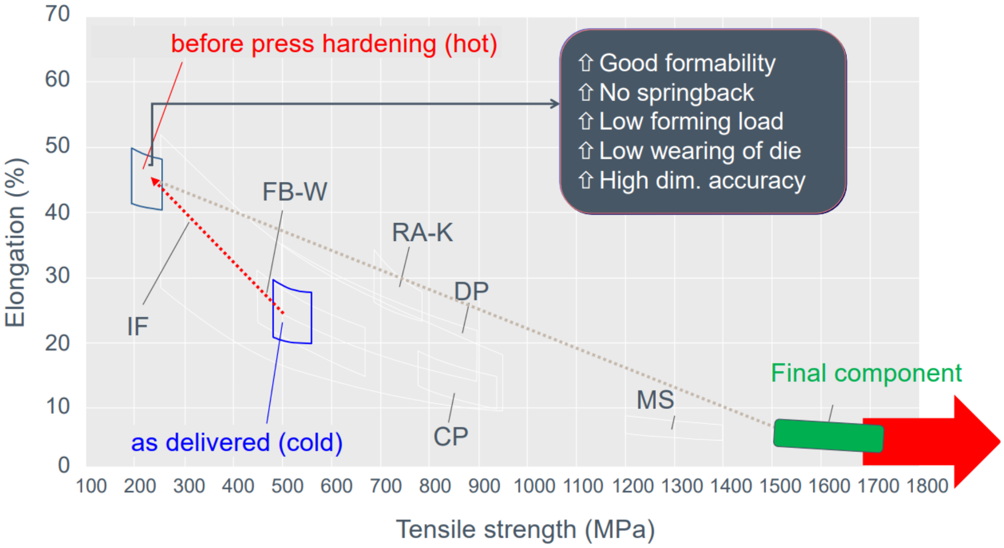

Fig. 3: Improvent of Tensile Strength provided by means of press hardening.

The ultra-high strength is achieved by some strengthening mechanisms such as [4]:

- Solid solution hardening by interstitial and substitutional elements like C, Mn, Si;
- Precipitation hardening (Ti, Nb, V);

- Grain refinement;
- Dislocation hardening;
- **Transformation hardening (Martensite).**

By means of press hardening it was then possible to produce the UHSSs suitable for the body-in-white.

The most widely UHSS used by hot stamping, as mentioned before, is the 22MnB5, which is a Boron-alloyed steel with acceptable hardenability that gives place to a fully martensitic microstructure.

Carmakers appreciate the hot-pressed ultra-high strength steels because they show a higher Yield Strength (up to even 1200 MPa) and a higher Ultimate Tensile Strength (up to approximately 1500 MPa), allowing to reduce the quantity of material (and therefore the weight) while offering an extremely high strength that improves the vehicles safety.

Moreover, compared to cold pressed steels, hot stamped UHSSs have further advantages like good repeatability in long production runs, excellent shape accuracy, good welding properties (since UHSSs are low-Carbon steels) and, above all, the absence of springback.

The avoidance of springback is due to the Austenite-to-Martensite transformation that happens during hot stamping, so the pieces do not tend to return to their initial shape.

The press hardened components in a vehicle are mainly the anti-intrusion structural elements belonging to the safety cell (the BIW).

They are, for instance, A-pillar and B-pillar reinforcements, front and rear bumpers, roof rails, rocker rails, tunnels, bumper beams, automotive door beams, side-impact beams, reinforcing beams and more various components of the auto body.

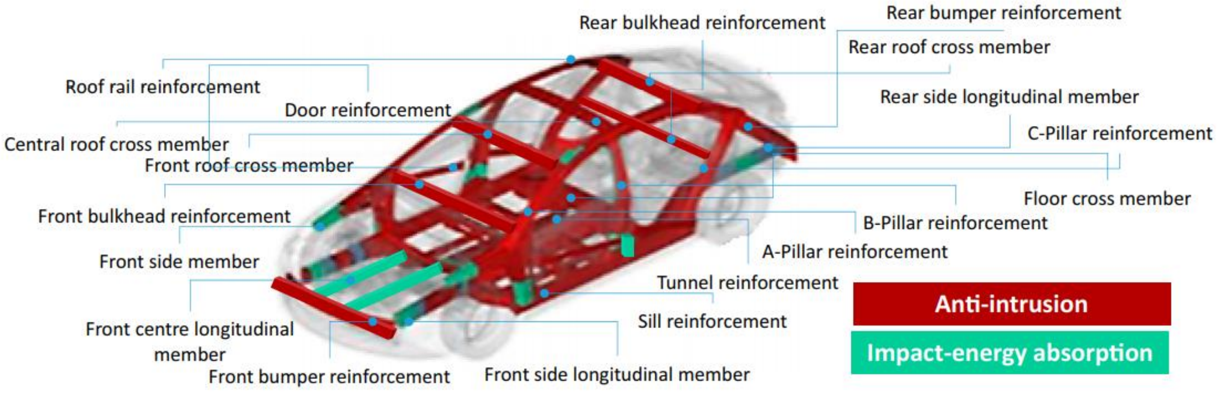

Fig. 4: Hot stamped parts of the body-in-white.

In addition to their use in the automotive field, which is probably the most relevant one, press hardened steels are also used for machinery for agriculture, public works, mining, and for heat-treated and wear-resistant parts.

As a brief recap, some general advantages of UHSSs are the following ones:

- Really high formability during stamping operation;
- Possibility of forming very complex geometries;
- Ultra-high strength steel parts after process;
- High toughness;
- High elongation at brake;
- Material properties independent of forming depth;
- Acceptable dimensional tolerances;
- Good weldability;
- Well suited for crash applications [5].

1.2.2 - A brief history of the use of press hardened steels ("PHS") in automotive industry

Press hardening technology began to look forward automotive industry from 1975 on, thanks to collaborations between *Plannja HardTech AB*, *Volvo Trucks AB* and the *Luleå University of Technology*, which promoted research and development automotive-oriented.

But it was only in 1980 that the first contract between *Plannja HardTech AB* and some carmakers like *Saab Automobile AB*, *Rover Corporation Limited* and *Jaguar Cars* were signed, in order to develop hot stamped Boron-steel side-impact beams (which are door reinforcements).

In fact, this ultra-high strength steel was considered really suitable for anti-intrusive parts of the body-in-white, due to the absence of springback and the possibility of downgauging, as said before.

So, in 1982 started a close collaboration between *Plannja HardTech AB* and *Saab Automobile AB* focused on developing the hot stamped Boron-steel side-impact beams for the car model *Saab 9000*, which was unveiled in 1984, May 24^{th} and released in the following autumn.

Saab 9000 was then the first passenger vehicle to use parts manufactured with hot stamped Boron steels.

Fig. 5: 1984 Saab *9000*: it was the first production passenger vehicle to use the hot-stamping Boron-steel technology. It was the first case of automotive series application of press hardened UHSS components.

Hot stamped parts were expensive, about three times more than the conventional cold-stamped steel alternatives, such as ferritic low-Carbon low-alloy steels.

Moreover, hot stamped steels had the problems of scratching and warping, and of the formation of oxide scale, since there was not any coating applied. This oxide scale was removed through shot blasting. In addition, the hot stamped parts were considered pretty unweldable, so they were held in place by three large rivets in the ending areas of each side-impact beams.

On the other hand, the ultra-high strength of the martensitic Boron steel used allowed to downgauge the side-impact beams by 50%, if compared to the cold-stamped steel alternatives, still being able to meet the severe requirements of the American side-impact tests.

For these reasons, after the 1984-1985 period, when the hot stamped parts production was low, in 1986 *Plannja HardTech AB* started out the series production of hot stamped Boron-steel side-impact beams, reaching 3 millions of manufactured parts in 1987, mainly addressed to *Saab Automobile AB*.

From 1991 to 1995 *SSAB HardTech* (previously *Plannja HardTech AB*, until the name change in 1990) signed contracts with many OEMs (Original Equipment Manufacturers) of the automotive industry, for hot stamped Boron-steel parts supply.

An OEM is a society that produces the final product for the consumers, such as cars. For instance, the carmakers are OEM societies producing vehicles.

Among these OEMs involved there were *Ford*, *Volkswagen AG*, *Mazda*, *Volvo*, *Seat SA* and *Porsche*.

In the meanwhile, the types of parts produced in hot stamped Boron steel were increasing over time: the production did not involve anymore only the side-impact beams, but also other components like rear reinforcements and bumper reinforcements.

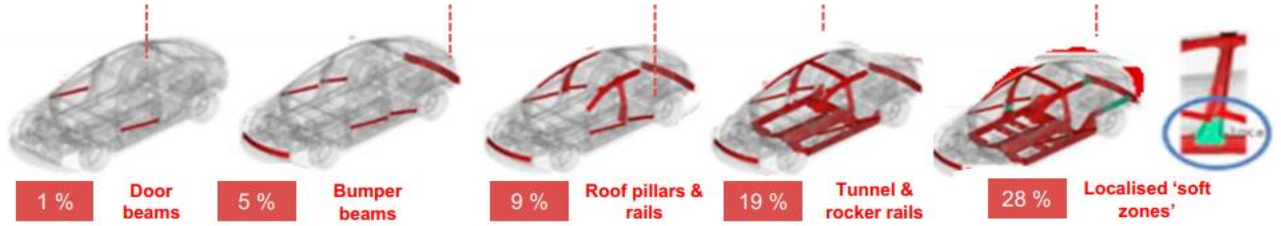

Fig. 6: Percentage increase of the parts of the body-in-white produced with hot stamped Boron steels.

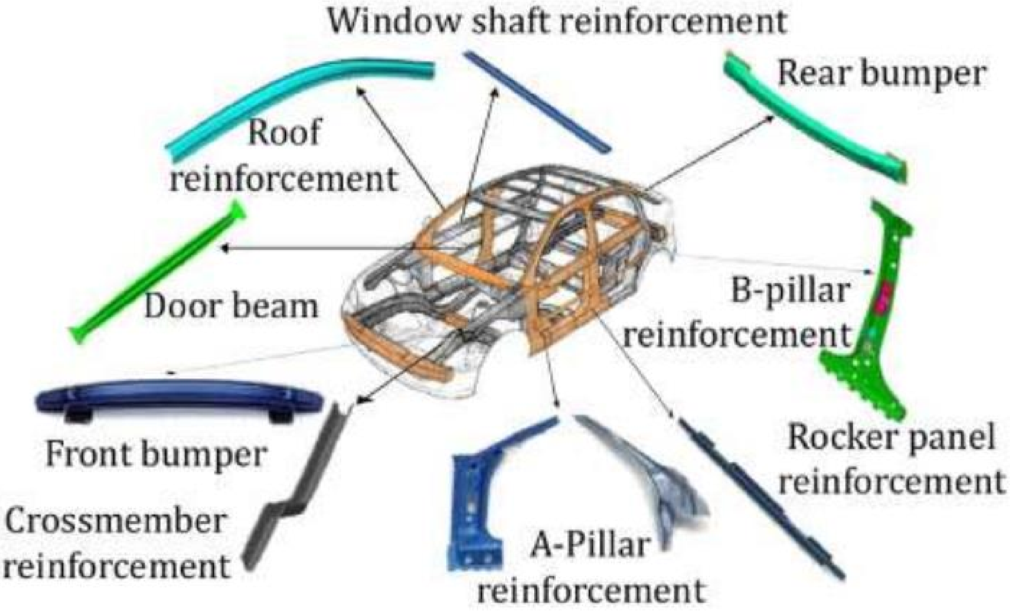

Fig. 7: Hot stamped parts produced by *Benteler Automotive* (courtesy of *Benteler Automotive*). [6]

The global market was monopolised by *SSAB HardTech*, which exclusively sold its products to the carmakers, up until the mid-1990s, when the patent expired.

This fact allowed other tier 1 supplier to compete with *SSAB HardTech* to provide the OEMs with the hot stamped Boron-steel parts, by producing them on their own.

A tier 1 supplier is a society that directly supplies the OEMs. In this case, *SSAB HardTech* is a tier 1 supplier which provides carmakers with hot stamped Boron-steel parts to be used to produce vehicles. Tier 2 societies supply tier 1 societies.

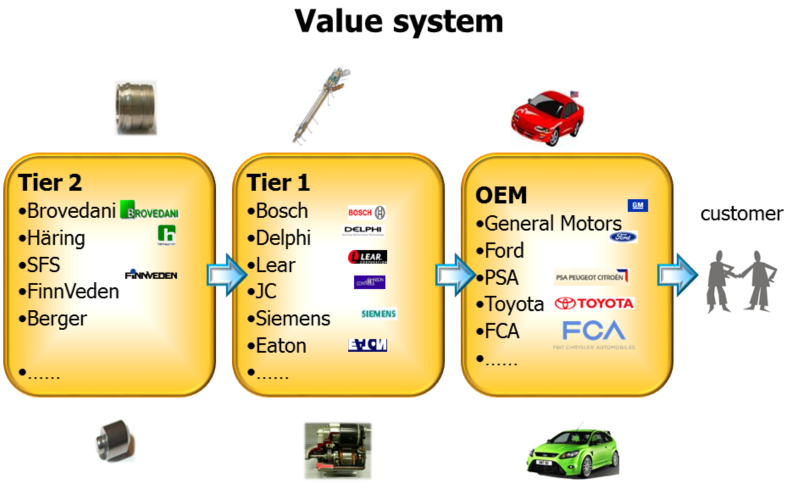

Fig. 8: The value system in the automotive industry.

As a consequence of the expiration of the patent owned by *SSAB HardTech*, then, press hardening technology for Boron-steel parts became more and more used and popular worldwide; it was also due to the fact that in the late 1990s this technology had become significantly more efficient and less expensive.

The demand from automotive industry of hot stamped Boron-steel parts became so high that in 1996 *SSAB HardTech* only dedicated its production to the automotive field, renouncing to other applications like the agricultural one.

By the early 2000s the number of hot stamped Boron-steel parts per vehicle increased dramatically.

The *2004 VW Passat* was the first ever passenger vehicle showing an integrated hot stamped Boron-steel safety cell, with hot stamped Boron-steel parts representing almost the 15% of the body-in-white.

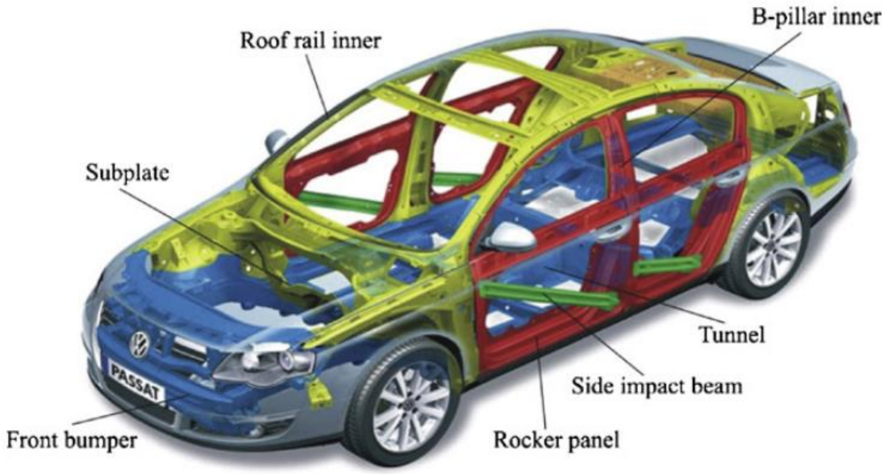

Fig. 9: 2004 Volkswagen *Passat*: it was the first production passenger vehicle to exhibit an integrated hot stamped Boron-steel safety cell. The hot stamped Boron steel accounted for nearly 15% of the BIW.

The first generation of hot stamped Boron-steel parts were uncoated, and several coating technologies were developed over years, giving rise to new generations of hot stamped sheet-steel parts.

The first hot-dip-aluminised Boron steel for hot stamping was developed and patented by *ArcelorMittal* in 1999, and its first commercial application took place in 2007.

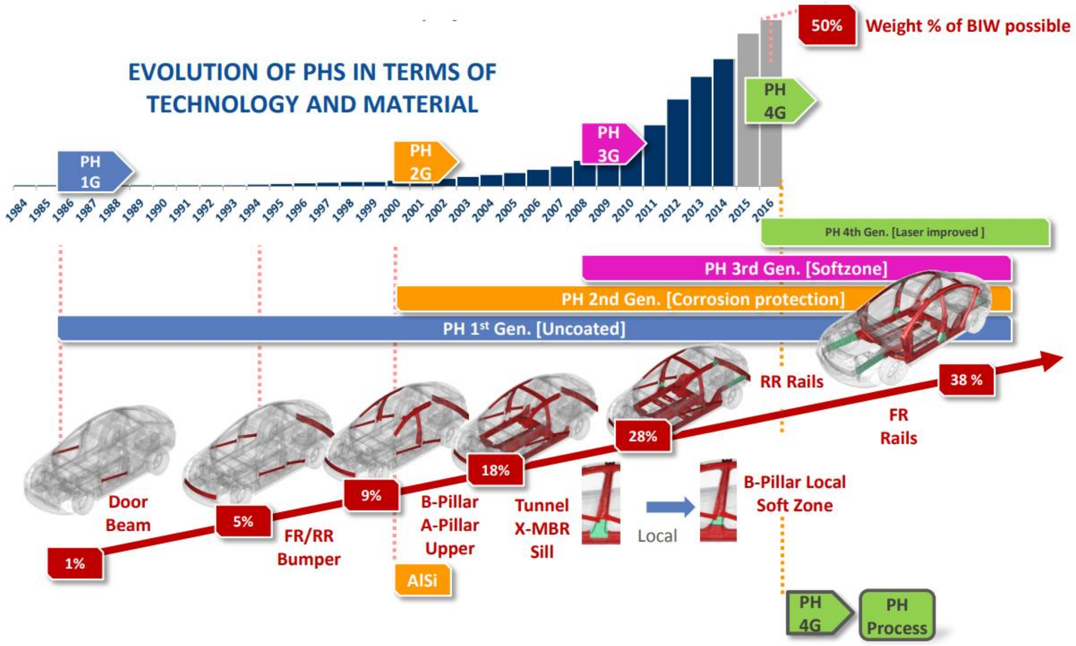

Fig. 10: Increasing application over years of hot stamped sheet-steel parts to the body-in-white, with the development of new generations of hot stamped products.

1.3 - A quick overview of press hardening

Press hardening is a process that combines three characteristics typical of other manufacturing processes: the fabrication of metal sheets (since the material used is a sheet steel), the hot forging (by means of the pressing of hot sheet steels) and the injection moulding (where it is present a cooling system directly in the mould, like in press hardening).

The most commonly used material in press hardening is the Boron steel 22MnB5.

Press hardening consists in several steps. Usually, the sheet steel which is going to undergo press hardening shows a ferrite-pearlite microstructure and a tensile strength of approximately 500-600 MPa at room temperature.

The main steps are the **austenitization** treatment into the furnace, the **transfer** of the piece from the furnace to the press, the **pressing** and the **final finishing** by trimming and piercing.

The sheet is brought at the temperature of 900-950 °C and maintained at that temperature for at least five minutes into a furnace. The result is the soak austenitization, which means the achievement of the FCC structure.

Then the piece is quickly put into the mould maintained at room temperature, where the final shape is given and the quenching takes place by means of liquid media flowing through the channels present in the mould structure (cooling rate of at least 27 K s^{-1} for 5÷30 seconds, in order to have only Austenite-to-Martensite transformation, preventing the formation of Bainite and/or Ferrite).

When the piece reaches the temperature of approximately 428 °C, the martensitic transformation starts. It finishes at more or less 280 °C.

Finally, the component is hardened in full Martensite distribution. At this point the shape is given and it cannot spring back anymore.

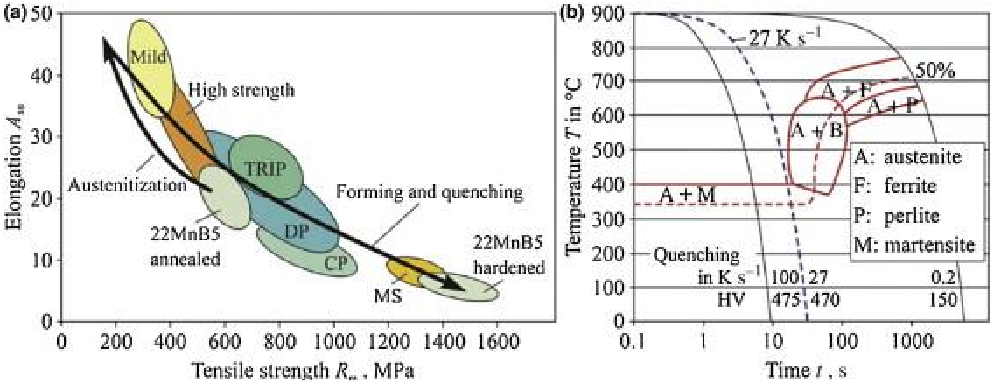

a) b)

Fig. 11: a) Change in Tensile Strength during press hardening; b) Continues Cooling Transformation curves relative to press hardening. [7], [8]

A typical hot stamping line is made up by the following parts: a **heating device**, a **material handling system**, a **press**, a **mould set**, an **exit line** and **trimming or piercing systems**.

Usually, in order to heat up, roller hearth furnaces are used: they are between 30 and 60 meters long and heated by means of gas or electricity.

For material handling it is possible to use both manual feeding (for prototyping production only, since there is heat loss during the transfer) and robots or linear feeders (for mass production), which allow to move the pieces more quickly without losing too much heat by radiation.

The type of presses usually used in press hardening are the hydraulic presses. The main requirement is not a high force but a high speed, in order to close quickly the mould when the piece placed inside the mould is still in the austenitic form. The high-force and low-speed condition is instead preferable at the end of the stroke.

The mould set has a double purpose: forming the piece and driving the heat away from it. In order to reach the critical cooling rate (27 K s^{-1} as mentioned above), it is necessary to extract a heat energy of 17.5 kW/kg.

There are several ways which could allow the mould cooling: the use of drilled cooling channels inside the mould, the use of shell cooling and also the use of cooling tubes inside the mould (see **Fig.12**).

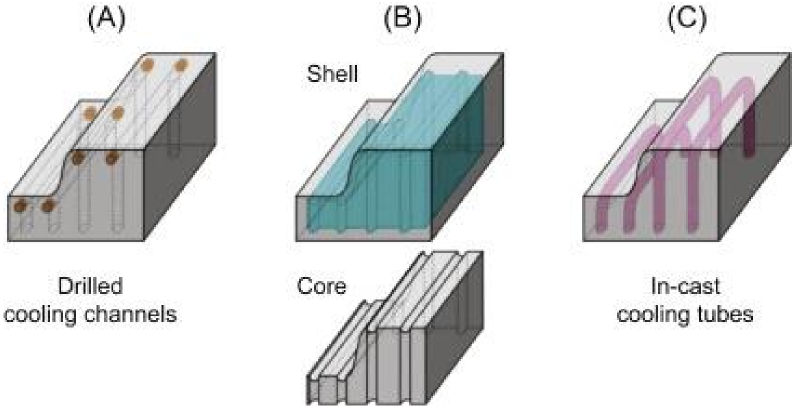

Fig. 12: Types of cooling systems.

In the end there is the need for trimming and piercing the piece. To do that it is used the laser cutting instead of conventional cutting, since conventional cutting can generate high stresses.

It is also possible to properly change the shape of the piece, so as not to require any or partial trimming. The piece could also be trimmed or pierced while it is still hot and then soft and more shapeable.

1.4 - Typical material for press hardening

The typical material used for press hardening is a **Boron-alloyed steel**, in particular the **22MnB5** steel grade. Not all the Boron steels achieve a fully martensitic microstructure after having been hot stamped. It is the case of the 8MnCrB3 steel grade, for instance.

It is possible to note, indeed, that the 8MnCrB3 steel grade results in much inferior mechanical properties (see **Table 1**) after the hot stamping operation, if compared to the steel grades which completely have their microstructure transformed into Martensite after press hardening.

These steel grades, like 22MnB5, 27MnCrB5 or 37MnB4, show a great enhancement of their mechanical properties after hot stamping.

Steel	Al	B	C	Cr	Mn	N	Ni	Si	Ti
20MnB5	0.04	0.001	0.16	0.23	1.05	-	0.01	0.40	0.034
22MnB5	0.03	0.002	0.23	0.16	1.18	0.005	0.12	0.22	0.040
8MnCrB3	0.05	0.002	0.07	0.37	0.75	0.006	0.01	0.21	0.048
27MnCrB5	0.03	0.002	0.25	0.34	1.24	0.004	0.01	0.21	0.042
37MnB4	0.03	0.001	0.33	0.19	0.81	0.006	0.02	0.31	0.046

Table 1: Chemical composition in wt.% of some Boron-steel grades. [9]

Steel	Martensite Start Tempereture [°C]	Critical Cooling Rate [K/s]	Yield Stress [MPa]		Tensile Strength [MPa]	
			As delivered	*Hot stamped*	*As delivered*	*Hot stamped*
20MnB5	450	30	505	967	637	1354
22MnB5	410	27	457	1010	608	1478
8MnCrB3	-*	-*	447	751	520	882
27MnCrB5	400	20	478	1097	638	1611
37MnB4	350	14	580	1378	810	2040

*There is no possibility to have fully martensitic microstructure.

Table 2: Mechanical properties of some Boron-steel grades. [9]

The most widely used steel grade for hot stamping is the 22MnB5, since it became the benchmark steel grade for press hardening among the steel manufacturers, through cooperation agreements between the tier 1 part manufacturers and the OEMs.

In the as-delivered form (i.e. before being hot stamped) it has a ferritic-pearlitic microstructure, with 73-77 wt.% of ferrite (in bright grey in the **Fig. 13**) and 23-27 wt.% of Pearlite (in dark grey in the **Fig. 13**).

According to ASTM, the typical grain size of a ferritic-pearlitic microstructure is > 9.

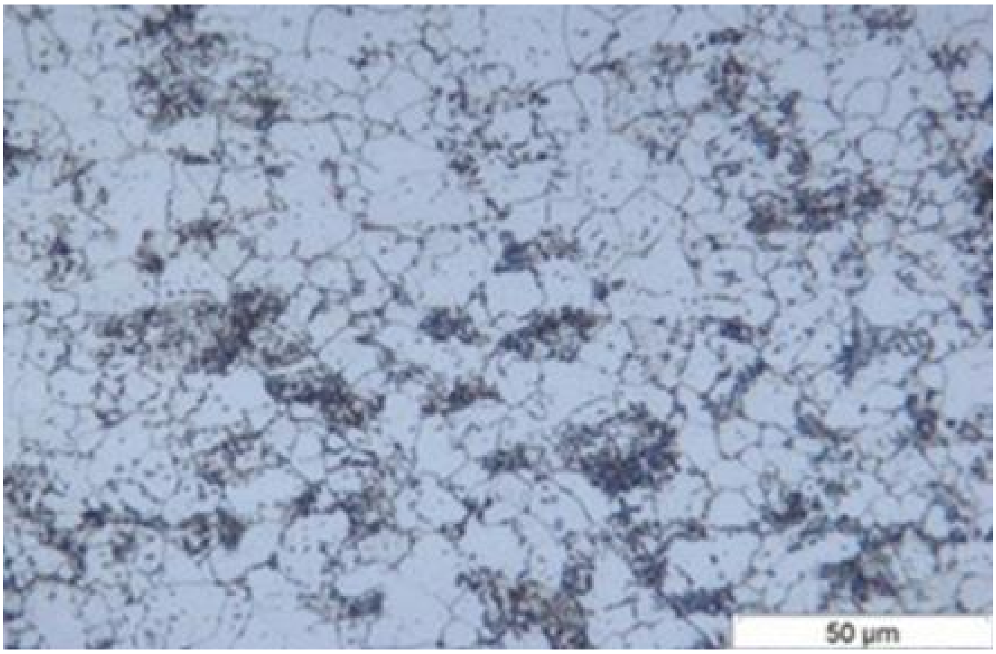

Fig. 13: Microstructure of 22MnB5 Boron steel.

Some steel manufacturers apply a registered product-trade name to the 22MnB5 steel, implying a certain composition. For instance, the commercial name of the 22MnB5 steel produced by *ArcelorMittal* is “Usibor1500” (see **Table 3**).

Manufacturer	Product	C	Mn	Si	Cr	Ti	B
ArcelorMittal	**Usibor 1500**	0.20-0.25	1.10-1.40	0.15-0.35	0.15-0.35	0.02-0.05	0.002-0.005
Swedish Steel AB	**DocolPHS1500**	0.20-0.25	1.00-1.35	0.20-0.35	0.14-0.26	-	0.002-0.005
ThyssenKrupp Steel AG	**MBW1500**	0.20-0.25	1.00-1.40	0.20-0.40	0.20-0.50	0.02-0.05	0.002-0.005
Tata Steel	**HQ1500**	0.20-0.23	1.10-1.30	0.20-0.30	0.10-0.30	0.02-0.04	0.002-0.004
Nippon Steel & Sumitomo Metal Corp.	**NS25CTB**	0.22-0.28	0.90-1.20	≤ 0.35	0.10-0.40	≤ 0.03	0.001-0.003

Table 3: Different chemical composition ranges (in wt.%) for the major elements of 22MnB5 products, depending on steel manufacturers (obtained from the respective steel manufacturer website). [10]

There are not any international standards for 22MnB5, while there are for 20MnB5, like the European Standard EN10083 (Steel for Quenching and Tempering); there exist also other equivalent non-European standards referred to this steel.

The 20MnB5 is the closest standardised steel to 22MnB5, but instead of just referring to a standardised steel grade, tier 1 manufacturers and OEMs prefer to impose determined mechanical properties specifications of as-delivered sheet steels on the steel manufacturers, including their own unique chemistry.

Always considering the 22MnB5 steel grade, while the various chemical specifications used by steel manufacturers are similar (as it is possible to observe in the **Table 3**), the mechanical properties specifications could be pretty different from manufacturer to manufacturer (see **Table 4**).

Manufacturer	**Condition**	**Proof Strength-Rp0.2 [MPa]**	**Ultimate Tensile Strength-Rm [MPa]**	**Total Elongation-A80 (%)**
General Motors	Hot rolled, cold rolled and aluminised	≥ 300	≥ 500	≥ 14
General Motors	Hot stamped	≥ 1170	≥ 1475	≥ 4.5
Renault	Hot rolled and cold rolled	280-360	≥ 450	≥ 20
Renault	Aluminised	≤ 550	≤ 700	N/A
Renault	Hot stamped	1000-1250	1300-1650	≥ 4.5

Table 4: Proof Strength, Ultimate Tensile Strength and Total Elongation specifications, by *General Motors* [11] and *Renault* [12].

The main alloying elements which are present in the 22MnB5 steel grade are Manganese, Carbon, Silicon, Chromium, Nickel, Titanium, Aluminium and Boron.

As seen before, the wt.% content of each element can slightly vary from the various type of 22MnB5 steels, depending on the steel manufacturer. Here there are for example the compositional ranges given by *ArcelorMIttal* for its Usibor1500.

22MnB5 steel	**C**	**Mn**	**Si**	**Cr**	**Ti**	**B**
Usibor 1500	0.20-0.25	1.10-1.40	0.15-0.35	0.15-0.35	0.02-0.05	0.002-0.005

Table 5: Chemical composition of Usibor1500, the 22MnB5 steel grade produced by *ArcelorMittal*. [10]

1.4.1 - The route to as-delivered 22MnB5 sheet steels: a quick overview

The as-delivered 22MnB5 sheet steels can come from continuous casting: after having been continuously cast, the sheet steel is hot rolled and then cold rolled.

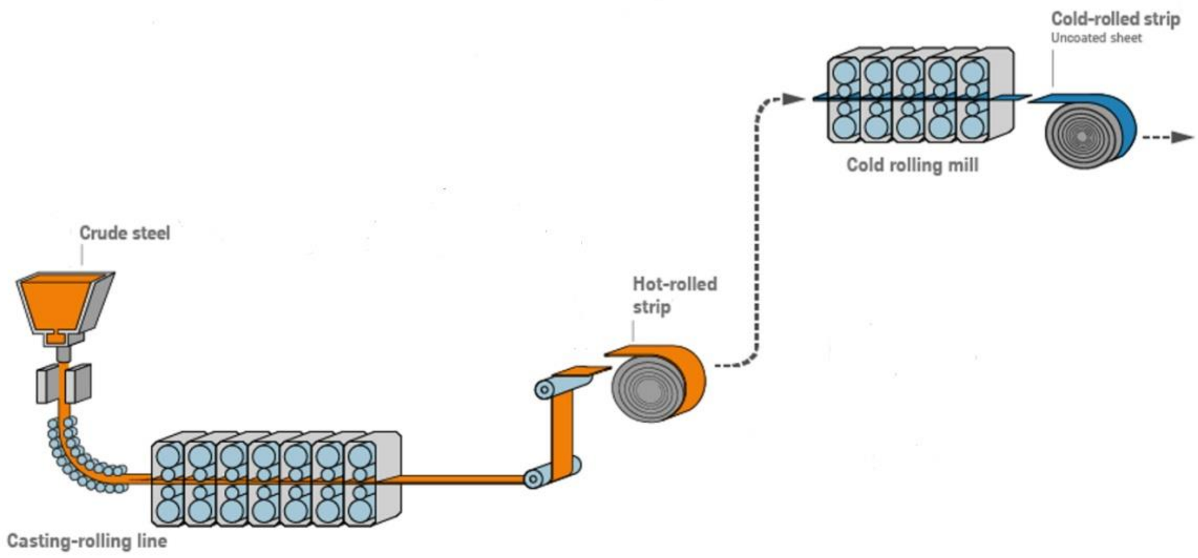

Fig. 14: Continuous casting followed by hot rolling and cold rolling. [56]

The cold rolled sheets are then annealed, either via the continuous annealing route or via the batch annealing route.

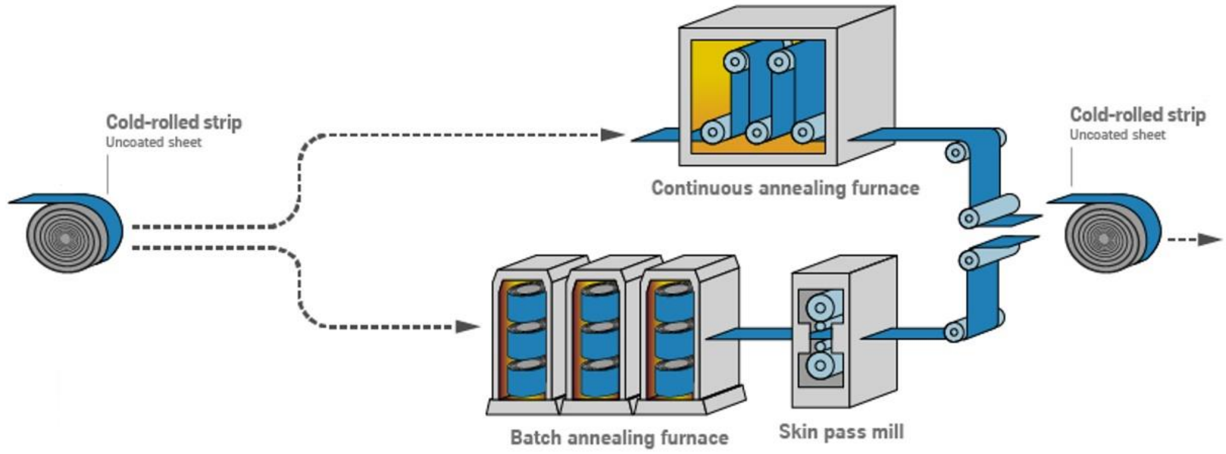

Fig. 15: Two possibilities after cold rolling: continuous annealing route and batch annealing route. [13]

Nowadays the cold rolled 22MnB5 steel is mostly produced by means of continuous annealing rather than batch annealing.

The sheet steels can also have an Aluminium coating in order to avoid surface oxidation that could happen during the hot stamping process, when the piece comes in contact with the air.

Hence, the continuous annealing process can be followed by a hot-dip coating line, that allows to aluminise the sheet steel.

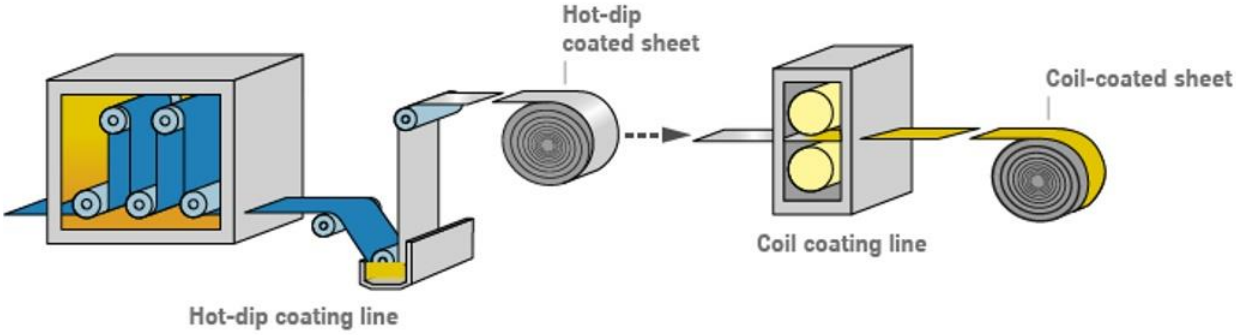

Fig. 16: Hot-dip aluminising process after continuous annealing. [13]

Mechanical properties of as-delivered steels, before being hot stamped, are about 390 MPa for Yield Strength, 600 MPa for Tensile Strength and 24,5% of Elongation.

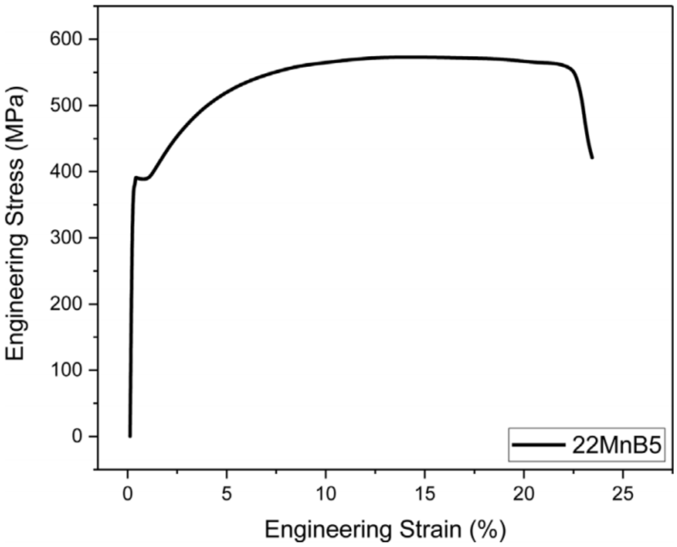

Fig. 17: As-fabricated 22MnB5 Stress-Strain curve.

As-delivered sheet steels should be soft and ductile enough, in order to make the blanking operations easier and, also, a possible pre-forming operation in case of indirect hot stamping method, as it is shown further.

Mechanical properties of the as-received steel have almost no influence on the mechanical properties during hot stamping and on the final mechanical properties, after the press hardening process.

Then the intention is to have a good formability before press hardening, and ultra-high-strength properties after the heat treatment of hot stamping.

1.4.2 - Alloying elements in 22MnB5

There are several alloying elements in the 22MnB5 steel used for press hardening, plus other undesired elements like Sulphur and Phosphorous, that cannot be avoided at all, but only reduced.

Among the alloying elements there is of course the **Carbon**, which has the major effect on the final properties. In fact, it is responsible for steel hardenability, i.e. the ability of the steel to form Martensite in depth during quenching.

It also contributes to steel hardness, that is the ability of resisting to a deformation when applying a load, by means of the solid solution strengthening mechanism: as the Carbon content increases, hardness and tensile strength increase as well (tensile strength starts to slightly decrease when Carbon is more than 0,85 wt.%), while ductility, weldability and elongation are reduced.

Another alloying element that improves steel hardness by substitutional solid solution strengthening, even though less than Carbon, is the **Manganese**. Like for Carbon, the increase of Manganese content reduces ductility, weldability and elongation, but to a lesser extent if compared to Carbon, indeed. On the other hand, the impact on steel hardenability enhancement is greater than Carbon.

Chromium content improves hardenability and provides substitutional solid solution strengthening.

Silicon improves hardenability and substitutional solid solution strengthening as well. Nevertheless, it is not much appreciated since it tends to oxidate.

It is in fact a deoxidising agent in steelmaking. This is explainable by means of Ellingham diagram, which reports on the y-axe the free energy of formation of metal oxide, and on the x-axe the temperature.

Roughly speaking, the several curves show the reaction of a certain metal with the oxygen, at a certain temperature. The more the curve is low in the diagram, the more stable is the oxide relative to that metal.

So, the fact that the curve referred to Silicon is pretty low in the diagram means that Silicon tends to reduce into the metal form the metal oxides that show a curve which is situated above the silicon curve in the Ellingham diagram.

Then, Silicon tends to form oxide and hence its content is minimised, in order to avoid the formation of Silicon oxide bonded to the surface, that would increase rolling loads during steel manufacturing, and would also affect the adherence of possible metallic coatings, like the Aluminium coating.

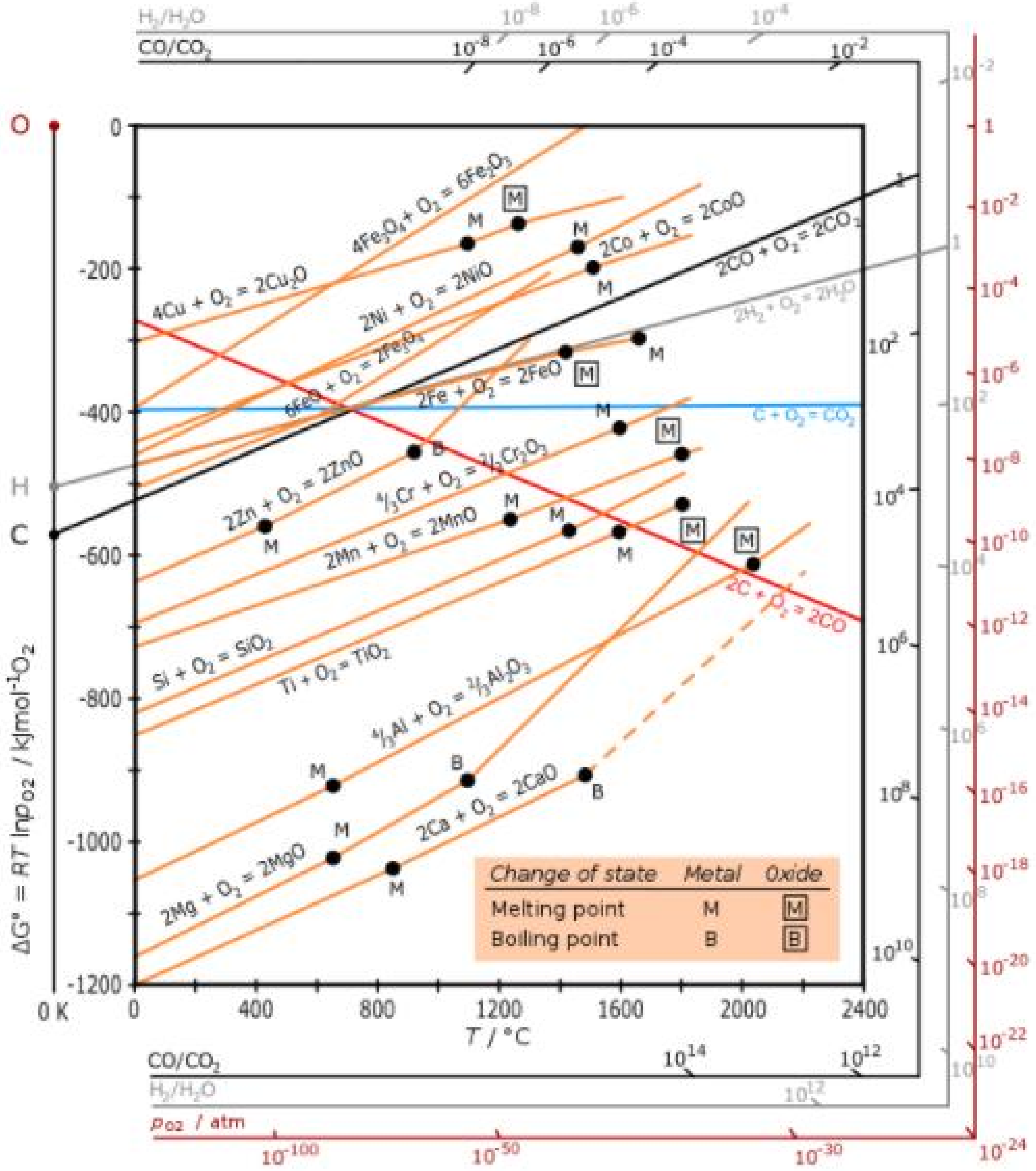

Fig. 18: Ellingham diagram. [14]

Other undesired elements are **Phosphorous** and **Sulphur**.

They both reduce steel ductility, toughness and notch impact toughness. It is not possible to remove them at all during steel fabrication, but it is only possible to reduce them, by means of ladle pre-treatment, for instance.

1.4.3 - The role of Boron

Boron is one of the microalloying elements (i.e. elements whose content in wt.% is less than 0.15%) that are present in the 22MnB5 steel grade. Other important microalloying elements in 22MnB5 are Vanadium, Niobium and Titanium. Their role is going to be analysed further.

A very small amount of Boron (typically between 0.001 and 0.005 wt.%, depending on the types of 22MnB5 specifications) strongly influences hardenability: in fact, it tends to segregate to prior-Austenite grain boundaries, limiting the formation of Ferrite, Bainite and Pearlite, while promoting the martensitic transformation during the quenching in the press hardening.

Boron is indeed the alloying element that mostly influences hardenability; hence, a Boron steel can boast mechanical properties (like tensile strength) which are comparable to the ones of steels with a superior content of Carbon or other alloying elements. TTT diagrams move to the right and the hardenability increases.

The reason why the Boron dissolved in an Austenite solid solution promotes the martensitic transformation and delays the formation of Ferrite, Bainite and Pearlite, inhibiting them, comes from classic Thermodynamics.

Indeed, the ferritic transformation is a reconstructive transformation, while the martensitic transformation is a displacive transformation that distorts the lattice (see **Fig. 19**, b).

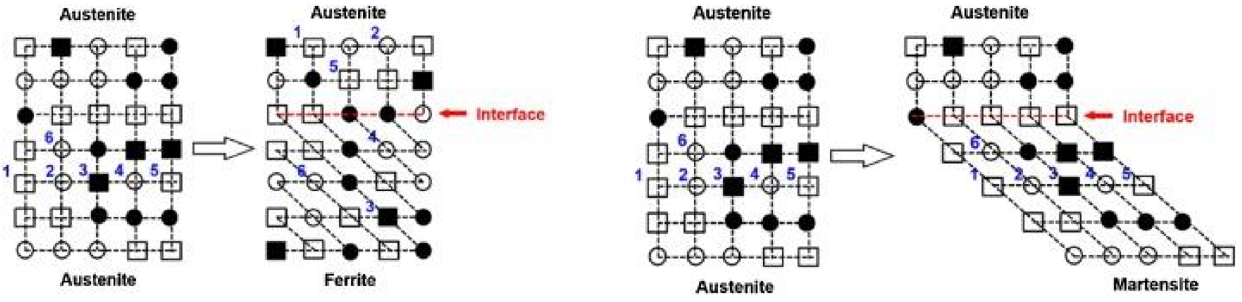

(a) Reconstructive transformation (b) Displacive transformation

Fig. 19: Difference between the two transformations. a) Reconstructive ferritic transformation; b) Martensitic displacive transformation. [15], [16]

Then, by segregating to Austenite grain boundaries, Boron increases the grain boundary surface energy and the activation energy (see **Fig. 21**) for a reconstructive phase transformation (like the ferritic one), while reducing the thermodynamic driving force of such a transformation.

This leads to a delay of the ferritic transformation and to an increase of possibilities of having a displacive transformation, like the martensitic one, thus increasing the hardenability [17].

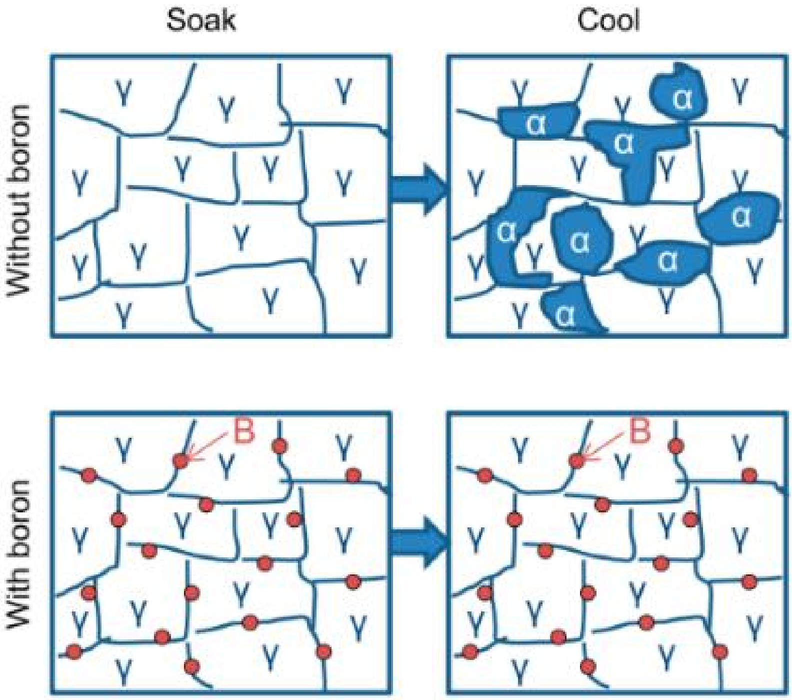

Fig. 20: Prevention from the formation of Ferrite (α) actuated by Boron, located at the Austenite (γ) grain boundaries. [18]

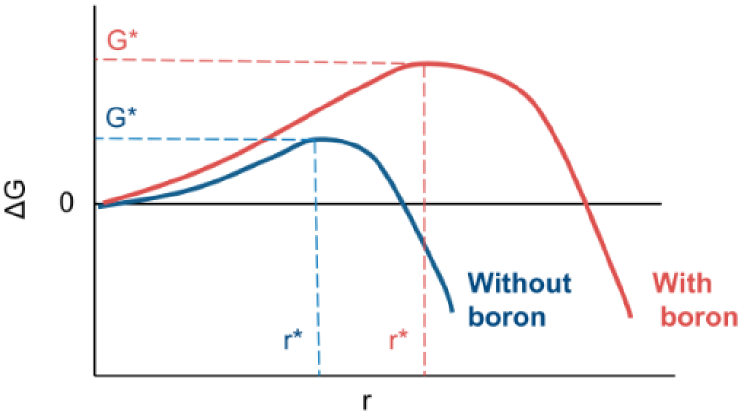

Fig. 21: Increase of ferritic transformation activation energy provided by Boron. [18]

The activation free energy of nucleation (G^*) in the graph above is driven by the following equation.

$$G^* = \frac{16\pi\sigma^3}{3[\Delta H_f(T_e - T)/T_e]^2}$$

G^*: Activation free energy of nucleation (related to the critical atomic radius r^*);

σ: Surface free energy;

ΔH_f: Latent heat of fusion;

T_e: Equilibrium transformation temperature;

T: Absolute temperature;

r: Size of the atomic radius.

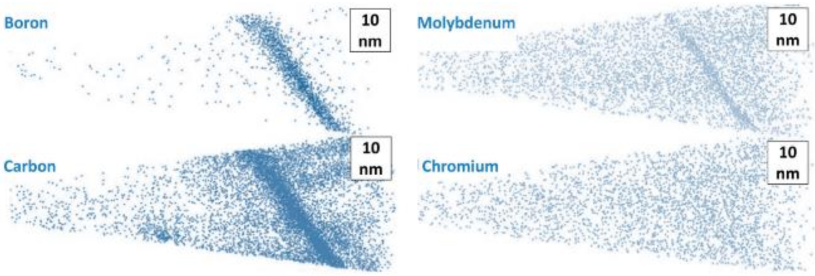

Fig. 22: APT (Atom Probe Tomography) analysis of the 22MnMoB5 (chemical composition in wt.%: 0.19 C, 1.20 Mn, 0.20 Cr, 0.50 Mo, 0.001 B), showing how the segregation of Boron atoms takes place almost completely in correspondence of Austenite grain boundaries. [18]

In **Fig. 22** it is highlighted, by means of Atom Probe Tomography, how the alloying elements arrange into the austenitized steel. It is evident how Boron atoms segregate at the grain boundaries, unlike the Chromium atoms, that are more homogeneously dispersed into the Austenite grain.

Even though Boron enhances hardenability, it is important to mention that the more Carbon is present in the steel, the less the Boron is able to do that.

For that reason, the benefits provided by the addition of Boron are more relevant for low-Carbon steels (i.e. steels with a content of Carbon inferior to 0.3 wt.%), and are reduced as the Carbon content increases. For steels whose Carbon content reaches the 0,8 wt.%, the hardenability effect is almost null.

The reduction in the hardenability effect as the Carbon content iscreases is due to the fact that the Carbon tends to cause the precipitation of borocarbides at the grain boundaries. These borocarbides promote the formation of proeutectioid Cementite and Pearlite, which cause a reduction of hardenability.

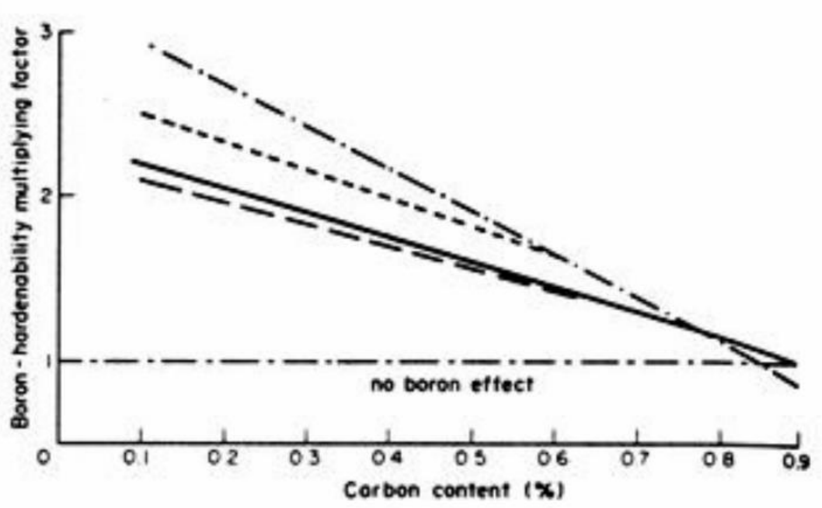

Fig. 23: Variation of the Boron hardenability effect with Carbon content in plain Carbon and low–alloy steels. [19]

Another thing that influences the hardenability is the austenitizing temperature. In fact, since there is a competition between the Boron concentration at the grain boundaries and the Boron concentration into the solid solution, the higher is the austenitizing temperature, the more Boron into the solid solution is going to be present, and the hardenability will be reduced.

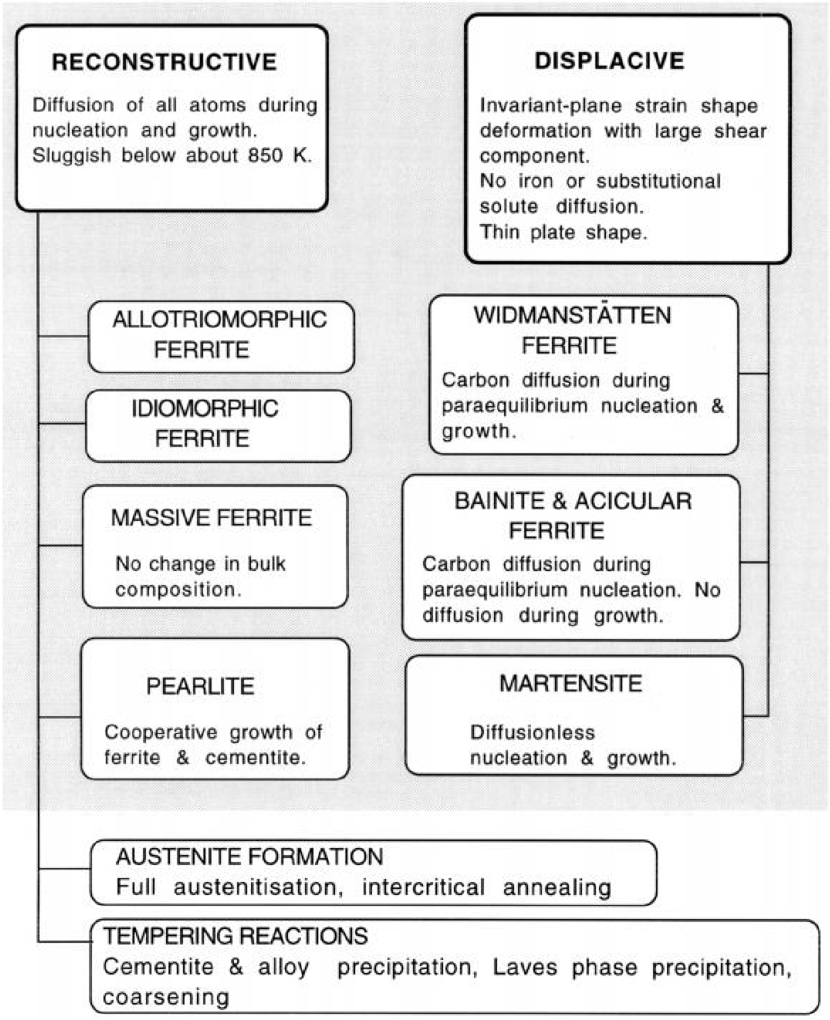

Fig. 24: Flowchart showing the two families of steel transformations and their characteristics. [20]

1.4.4 - Aluminium coating

It is possible to apply an Aluminium coating at the surface in order to protect the pressed piece from the oxidation, that can happen both when the piece is into the oven and during its life.

The Aluminium coating is applied through an aluminising liquid bath, which is at a temperature of about 630-640 °C after the annealing process, where Niobium carbides precipitate (see chapter 2.3.1).

The sheet steel is hot rolled, then cold rolled and annealed, after which it is aluminised. When the sheet steel exits the aluminising bath, it is cooled down and ready to be press hardened.

Unfortunately, Aluminium acts as a Hydrogen catalyser: that means that if in the oven is present some Hydrogen, it goes at the surface where enters the material by means of a reaction. Hydrogen presence into the material is bad since it causes Hydrogen embrittlement.

1.5 - The press hardening process

There are two types of press hardening process: **direct** and **indirect**.

The difference is that in the direct press hardening process the piece is mould-formed only after having been heated, while in the indirect process the piece is mould-formed at the beginning of the process, before being heated up to the austenitizing temperature (when the part is still cold), and then hardened in another mould after having been austenitized in the furnace.

In the indirect method, the initial cold drawing make the piece reach about the 90-95% of its final shape.

The additional step present in the indirect method is useful to be able to obtain even more complex geometries, which would not be obtainable with the direct process if the formability of the material is not so much good at high temperatures.

On the other hand, this additional step represents a higher expense, given by the cost of the cold forming tools and by the running costs of the process. Hence, indirect press hardening comprises the additional capital and running costs of a cold-forming tool and it presents the same limitations of the conventional cold forming.

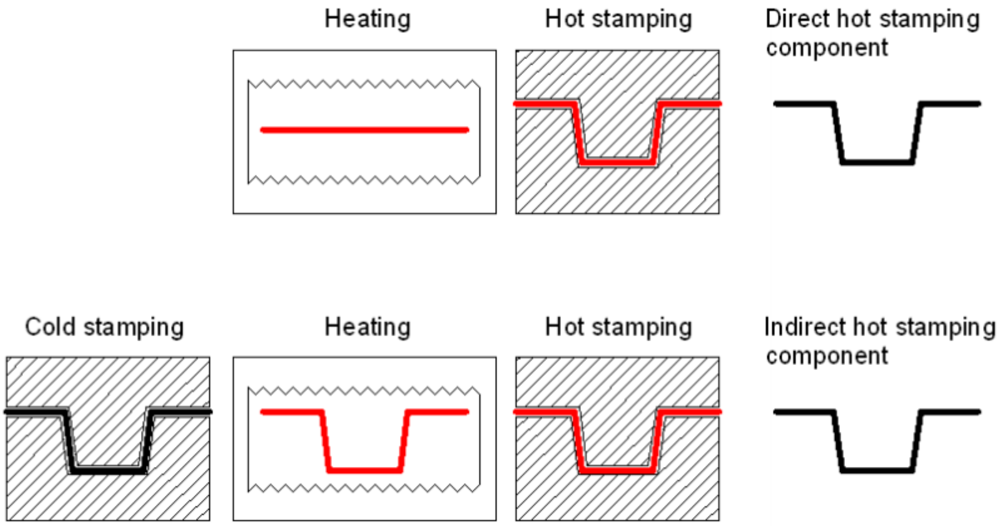

Fig. 25: Schematic differences between direct and indirect press hardening process.

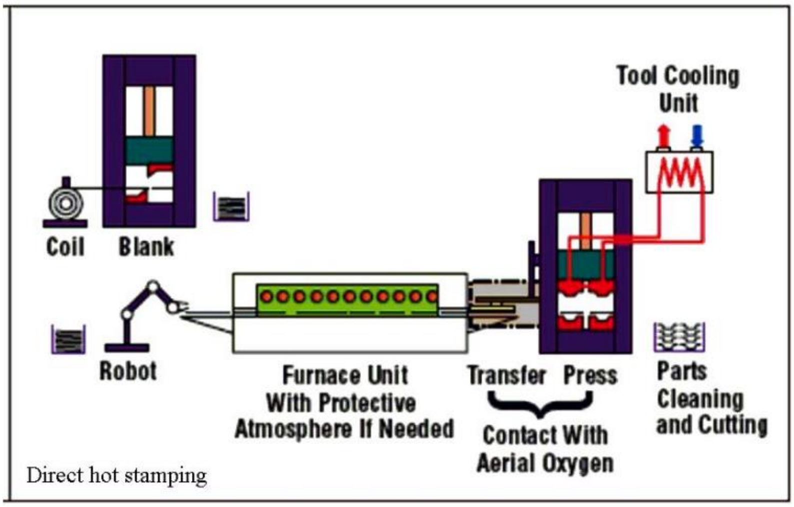

Fig. 26: Particulars of direct press hardening process.

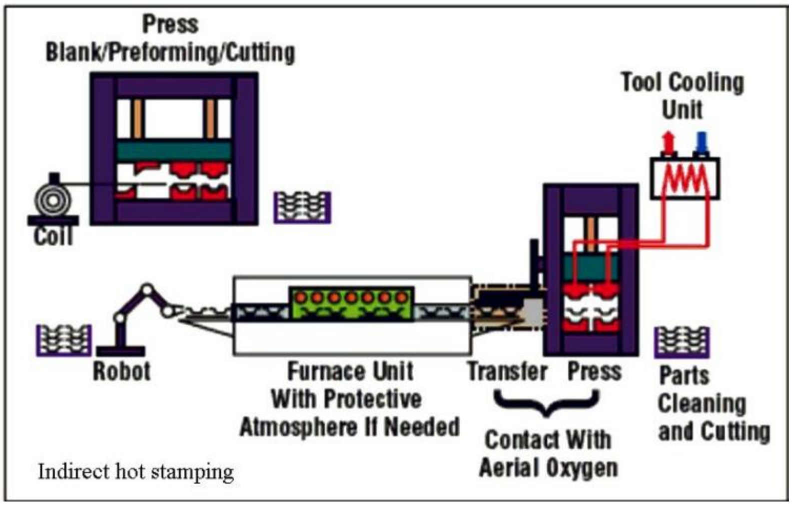

Fig. 27: Particulars of indirect press hardening process.

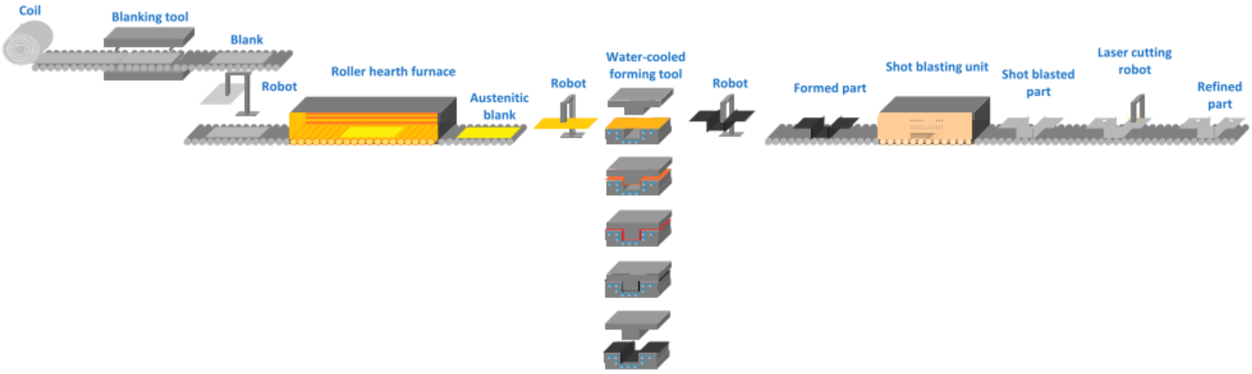

Fig. 28: Direct press hardening process line.

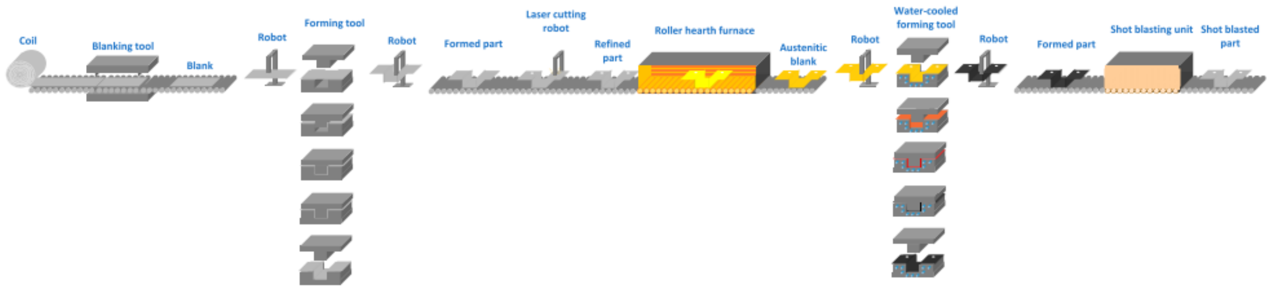

Fig. 29: Indirect press hardening process line.

1.5.1 - Blanking

Generally speaking, in the blanking operation a piece of sheet steel is removed from a larger piece of stock. This removed piece, called "blank", is not scrap, but the useful part, which is flat and of proper geometry. On the other hand, the scrap is the original sheet from which the piece was removed.

To create the blank, a hot or cold rolled coil of sheet steel continuously feeds the system and is cut by means of a blanking press. The blanking cut takes place at room temperature: indeed, it is a cold shearing operation where it is necessary to apply a sufficient shearing force.

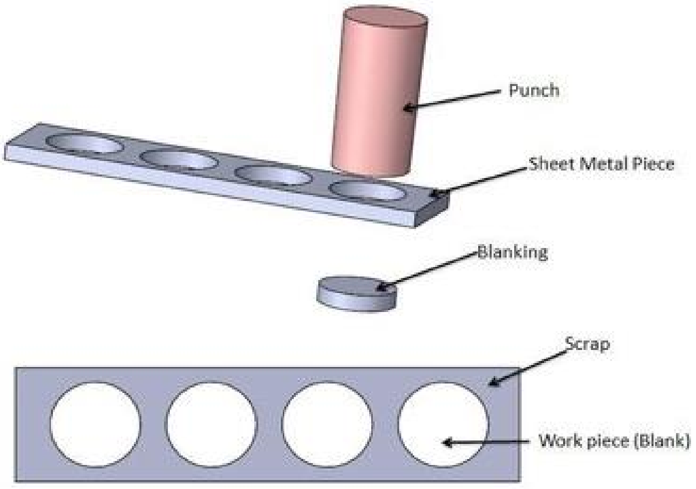

Fig 30: Sheet-steel blanking concept.

The most relevant parts of the blanking press are the punch and the die. The die is placed below the sheet, while the punch is placed above it.

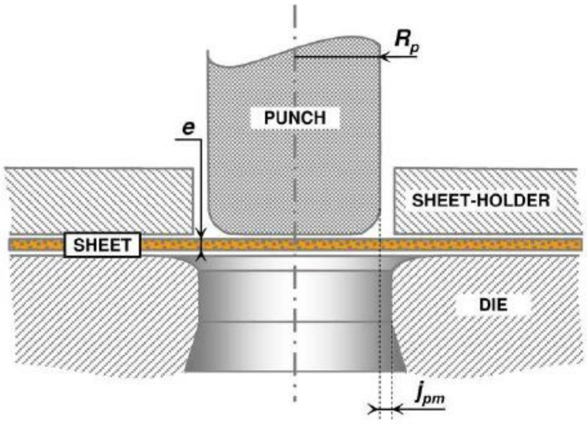

Fig. 31: Blanking test configuration.

The punch and the die have the geometry required for the blank, and show a clearance of 10-20% sheet gauge.

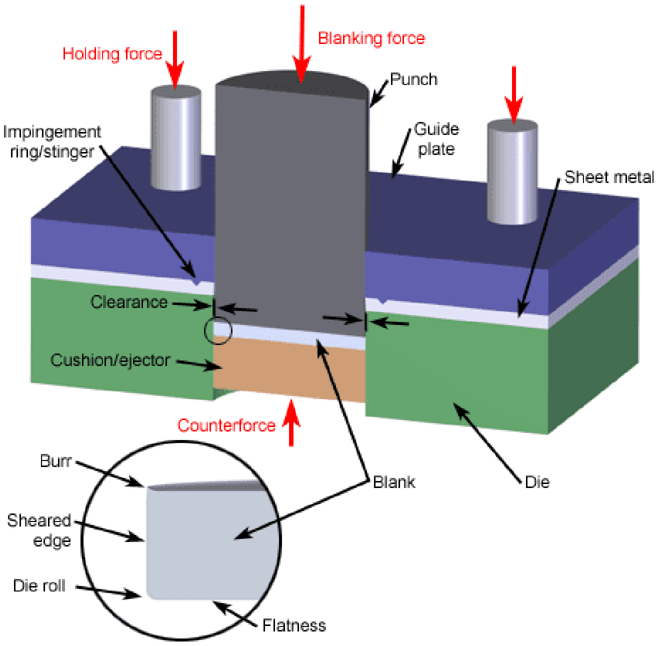

Fig. 32: Blanking press.

Then the blank obtained is ready to go to the furnace, where it is going to be hot formed.

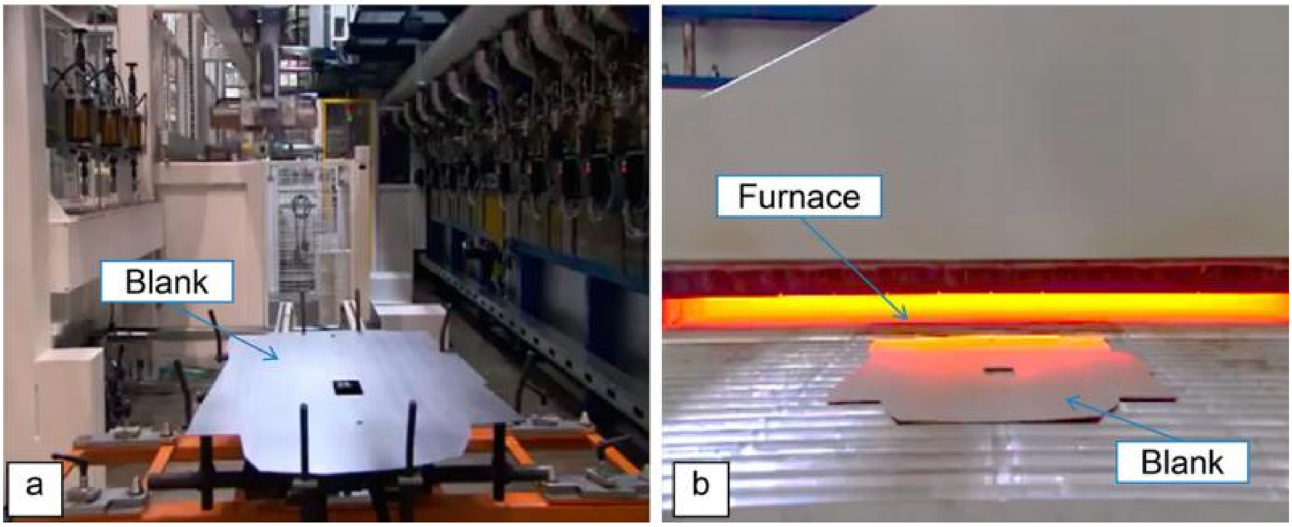

Fig. 33: Referring to direct method: a) Blank after blanking operation; b) Blank led into the furnace to be hot formed.

1.5.2 - Pre-forming

In the indirect method it is also present the pre-forming operation. Here, once the blank is obtained, it is cold formed before entering the furnace, by means of a press with a ram, a punch, a die and a blank holder. The geometry reached after the pre-forming operation corresponds approximately to the 95% of the final geometry. Then the pre-formed piece is led to the furnace, where it is going to be austenitized.

1.5.3 - Austenitization

From now on we refer to “the piece” to indicate both the blank (if the direct method is used) and the pre-formed part (if the indirect method is used).

To make the piece reach the austenitization it is possible to use several heating systems. These are the following ones:

- **Roller hearth furnace** (the conventional method used in Hot Stamping):it is an electric-fuelled or gas-fuelled furnace which generates heat by radiation and convection.
- **Infrared heating**: the sheet steels are heated up by radiation.
- **Induction heating**: the path of the piece is surrounded by a coil in which flows the electric current. The current flowing into the coil generates an electromagnetic field, which produces the heating of the pieces by passing inside them.
- **Resistance heating**: the piece that has to be heated is positioned between two electrodes, and the heating of the sheet is directly generated by the passage of the current through it; it

requires few seconds. This method is useful when there is the necessity of partially heating the blank, for instance when tailoring is required: it is achievable for example using a copper bypass.

- **Contact heating**: the piece is manually put between two heated plates and clamped. The heating is not uniform, since the purpose is to achieve just a partial heating of the blank.

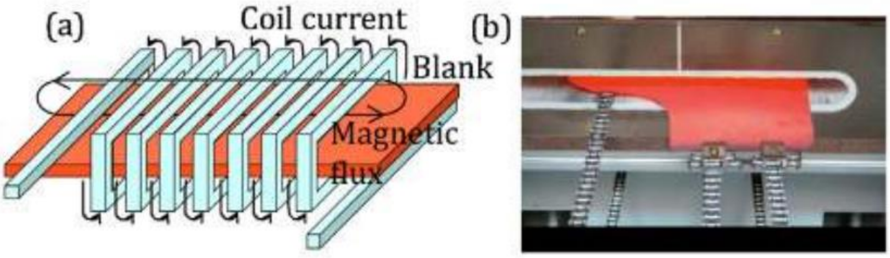

Fig. 34: a) Principle of induction heating; b) Induction-heated blank for press hardening.

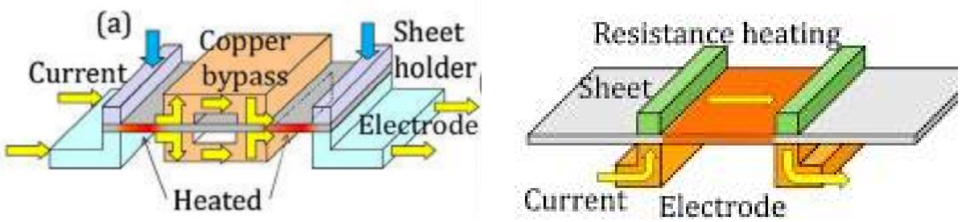

a)

b)

Fig. 35: a) Resistance heating involving a copper bypass to customise the heating; **b)** Resistance heating in general.

Fig. 36: Two operators handling the piece in order to partially heat it by clamping it between heated plates.

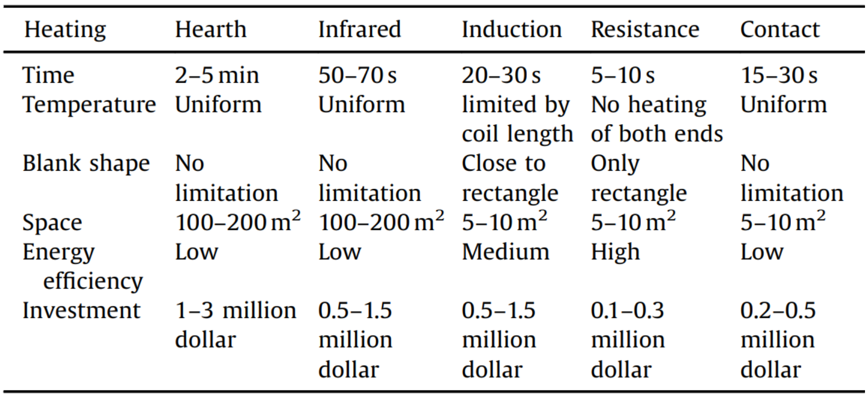

Heating	Hearth	Infrared	Induction	Resistance	Contact
Time	2–5 min	50–70 s	20–30 s	5–10 s	15–30 s
Temperature	Uniform	Uniform	limited by coil length	No heating of both ends	Uniform
Blank shape	No limitation	No limitation	Close to rectangle	Only rectangle	No limitation
Space	100–200 m^2	100–200 m^2	5–10 m^2	5–10 m^2	5–10 m^2
Energy efficiency	Low	Low	Medium	High	Low
Investment	1–3 million dollar	0.5–1.5 million dollar	0.5–1.5 million dollar	0.1–0.3 million dollar	0.2–0.5 million dollar

Table 6: Quick overview of the features of heating approaches used for press hardening.

We are now considering the conventional method, i.e. the one involving the roller hearth furnace.

Once the piece is ready, it is put into a roller-hearth furnace in order to austenitize the steel structure. A typical 1300-1500 mm wide sheet steel of 22MnB5 has, at this point, a microstructure of proeutectoid Ferrite and Pearlite, with the following characteristics:

- Proof Strength < 500 MPa;
- Ultimate Tensile Strength < 600 Mpa;
- Total Elongation > 20%.

The piece is brought to the austenitizing temperature of about 900-950 °C and left at that temperature for several minutes (usually for 3-10 minutes), depending on the thickness of the piece: then it becomes extremely ductile, which allows to shape the piece itself with a press and reaches complex shapes.

The Proof Strength and the Ultimate Tensile Stress descends to about < 200 MPa, while the Total Elongation becomes > 60%.

The austenitization takes place by means of radiant heating and convection heating, inside a roller hearth furnace.

At the end of the heating, complete and homogeneous austenitization and sufficient grain growth (for hardenability) must be ensured. In case of coated parts, it is also necessary to guarantee the inter-layer alloying between the coating and the substrate.

The piece is brought inside the furnace by means of many rotating rollers, which extend for about 30 meters or more, depending on the productivity of the hot stamping operations. The rollers have different speeds depending on the area of the furnace where they are collocated. In the heating area the rollers rotate at a relatively high speed, while in the soaking area their speed is much slower or even null, so as reach the proper soaking time. Usually, the total time of this operation of heating and soaking takes less than ten minutes.

Roller-hearth furnaces are suitable for continuous uniform heating of sheet steel and for easy handling of the workpieces.

Fig. 37: Austenitized pieces coming out of the furnace sliding on the rollers.

It is possible to use an inert atmosphere by using Nitrogen, Hydrogen and Argon, so as to avoid oxidation and decarburisation of the sheet steels, particularly when there is no coating present.

If oxidation happens, it is necessary to operate a subsequent mechanical treatment (like the shot blasting) to remove the oxide scales.

1.5.4 - Transfer to the hot blank

In this step the piece is moved from the furnace to the mould by means of a robot.

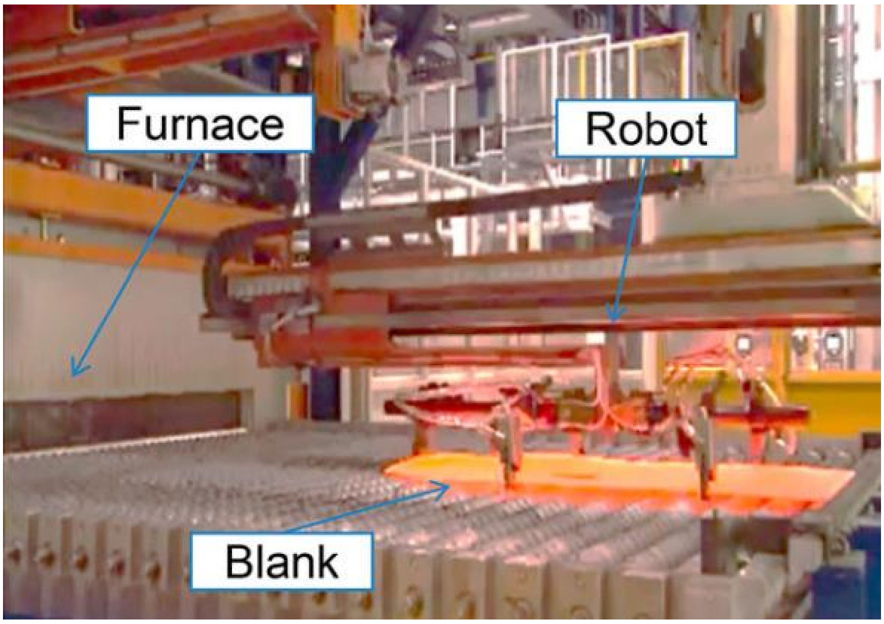

Fig. 38: Transfer of the blank from the furnace to the mould.

The piece comes out of the furnace at a temperature of about 900-950 °C.

It is necessary that the piece is moved from the furnace exit into the mould in less than 10 seconds, in order not to make the temperature of the piece decrease too much in the meanwhile: it must remain above 780 °C before the beginning of the quenching in the mould, to prevent the formation of some Bainite and/or proeutectoid Ferrite in the austenitized structure of the piece.

The formation of Bainite and Ferrite before quenching would affect the martensitic transformation, indeed not all microstructures would turn into Martensite, but only the still austenitized parts. Then the microstructure would partially harden to Martensite during quenching.

Moreover, this fact would also compromise the hot formability.

So, the microstructure must be entirely austenitic (stable or metastable) when hot stamping and mould quenching begin, in order to obtain a whole martensitic microstructure with the required mechanical properties, according to the CCT diagrams.

Another reason that makes necessary to make the moving time as short as possible is the avoidance of oxidation and decarburisation of the uncoated pieces when exposed to the atmosphere at high temperatures, during the transfer from the furnace to the mould.

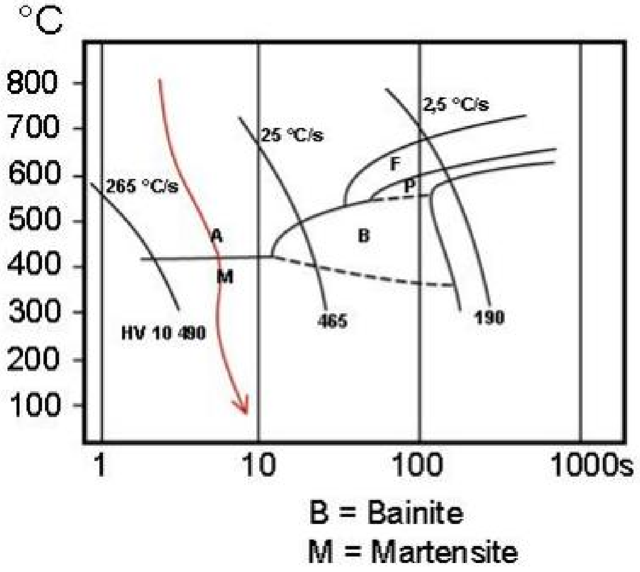

Fig. 39: CCT Curves.

Thus, coated sheet steels are favourable even with the utilisation of a furnace operating in an inert gas atmosphere.

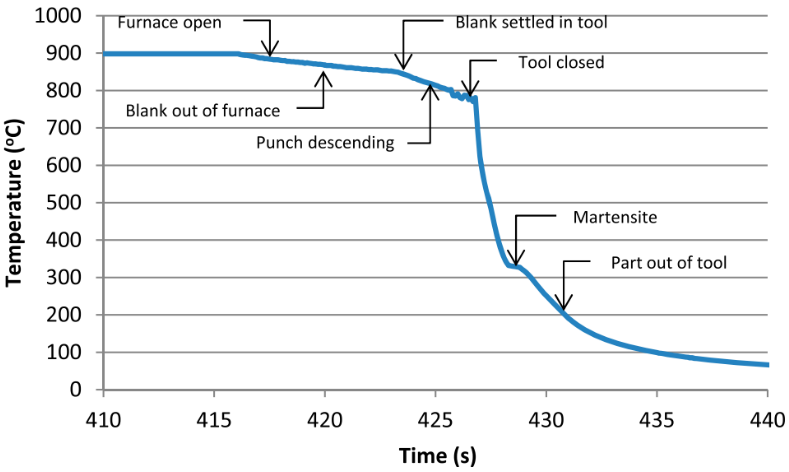

Fig. 40: Transfer, hot stamping and die quenching stages of the thermal cycle obtained from physical simulation of the direct press hardening process with 22MnB5 steel.

1.5.5 - Hot stamping and die quenching

As said, during the transfer from the furnace to the hot-forming press, which lasts less than 10 seconds, the piece cools down from about 900-950 °C to a temperature 780-850 °C.

Then the piece enters the mould with a temperature in this last range.

The first step is the hot stamping: it provides the piece with the final geometry by means of a hydraulic hot-forming press. The press is made by a ram, a punch, a mould and a blank holder.

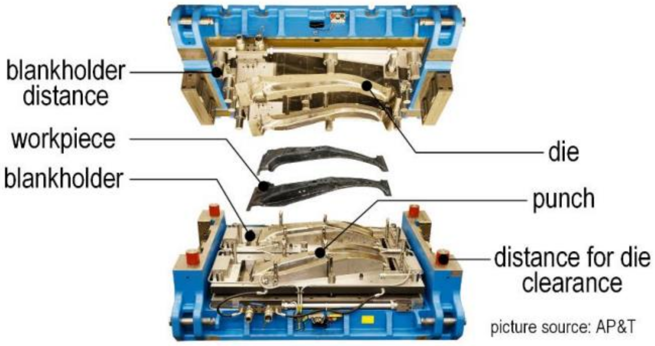

Fig. 41: Die-casting hydraulic-press set.

After the piece has been placed into the press, the mould closes in about 6 seconds: the piece is constrained in the blank holder, between the punch and the die, and the final shape is given by applying pressure.

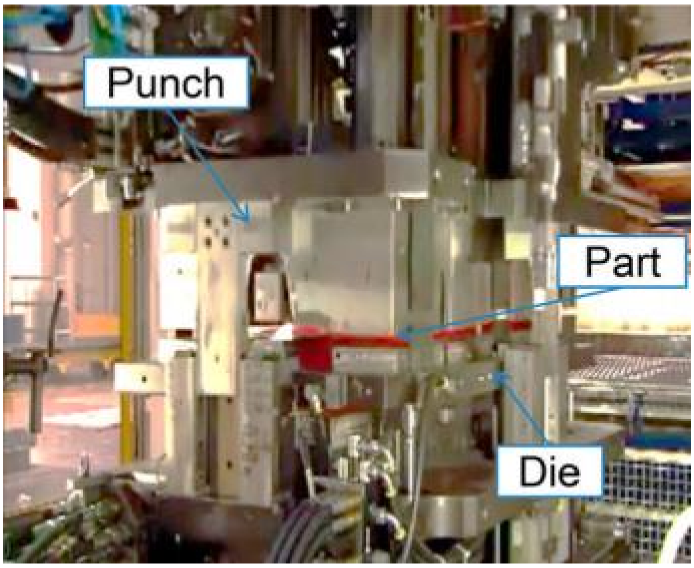

Fig. 42: Hot stamping operation.

Since the material placed into the mould starts cooling by conduction (cooling rate of 50-80 $°C/s$) by simply being in contact with the mould walls, at the end of the hot-stamping step the temperature has further gone down, to about 600-650 °C.

Once the mould is completely closed, with the piece fully in contact with the punch and the die (which perfectly match), the die quenching starts to take place, by making circulate cool water (at a temperature of 10 °C) inside channels placed into the mould.

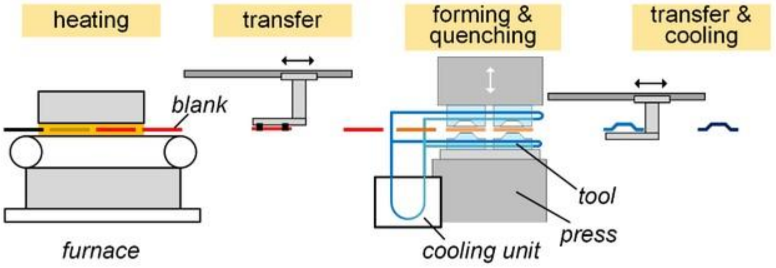

Fig. 43: A quick overview of some steps of direct press hardening process, including the forming (or "hot stamping") step and the die quenching step.

The aim of the quenching is to make the austenitized microstructure of the piece become martensitic, gaining better mechanical properties indeed.

Theoretically speaking, the quenching starts immediately when the piece is put into the mould, touching the punch and the die, even before that the mould is totally closed and the press has provided the piece with its proper final geometry. This happens by means of conduction, and this cooling effect becomes greater and greater as the punch descends and the pressure inside the mould increases.

The actual quenching starts when the mould is completely closed, after the hot stamping stage.

An intricate inner system of cooling channels makes the water circulate inside the punch and the die, 5 mm below the surface.

Water is cooled by a chilling system; the circulation of cool water inside the press is really high, something about hundreds of litres per second for each die set: it makes the quenching possible, driving away the heat by the piece by means of conduction heat transfer: the heat flows from the piece to the water-cooled tooling.

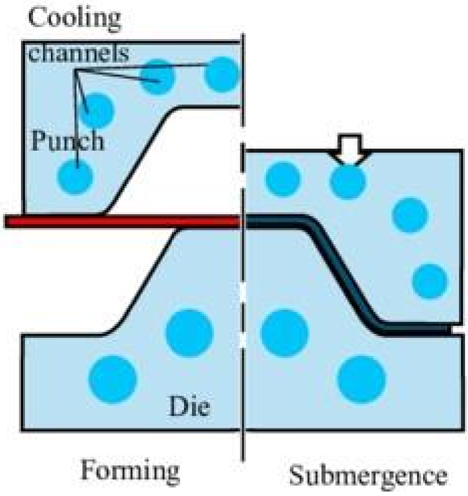

Fig. 44: Geometry of the cooling system, with water channels placed inside the punch and inside the die.

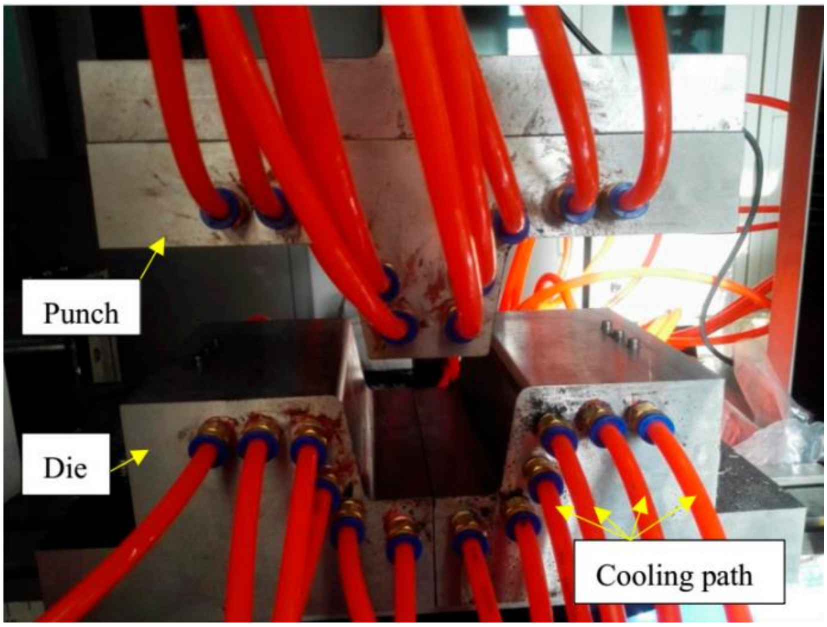

Fig. 45: Hot-stamping mould.

In the meanwhile, the pressure is maintained for a quenching time of about 15 seconds, before expelling the quenched piece.

At the end of the quenching operation the piece is released by the press and ejected at temperature of about 200 °C (which is below the temperature of martensitic finish transformation, i.e. 230 °C for 22MnB5) and let cooling down in the air at room temperature.

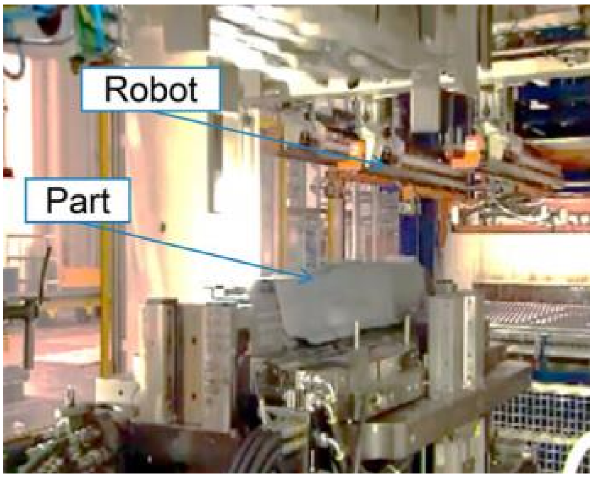

Fig. 46: Piece cooling in the air after having been ejected by the press, at the end of the die-quenching operation.

The piece results completely quenched and shows a fully martensitic microstructure, apart from a little volume fraction lower than 5%, due to inter-lath retained Austenite, which did not manage to become Martensite.

For 22MnB5, the critical temperatures are:

- Martensite start (M_s): 410 °C: temperature at which the martensitic transformation begins;
- Martensite finish (M_f): 230 °C: temperature at which the martensitic transformation ends.

The critical cooling rate is typically 25°C/s.

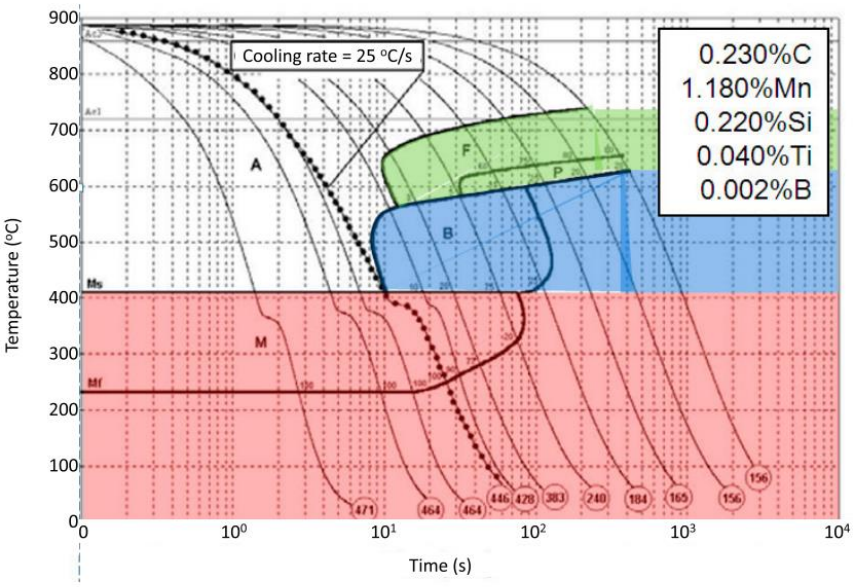

Fig. 47: Continuous cooling transformation diagram of 22MnB5 steel, with the critical cooling rate of 25°C/s showed.

The coloured areas in **Fig. 47** represent the kinds of microstructures that are going to appear during the cooling operation, depending on the cooling rate adopted.

The green area represents the time-temperature conditions for having the formation of Ferrite or of Ferrite-Perlite, the blue area is about the formation of Bainite, and the red area represents the conditions where the Martensite can exist.

The curves represent the cooling rates.

The final microstructure will be made up of the microstructures relating to the fields of existence that the cooling-rate curve crossed during the cooling operation.

So, for instance, if the cooling operation takes much time, its cooling-rate curve will be kind of delayed, crossing for instance the fields of existence of Ferrite, Bainite and Martensite. It will result in a final microstructure made by these three phases.

On the other hand, if the cooling is fast enough, the cooling-rate curve will only cross the field of existence of the Martensite, and the final structure will be wholly martensitic.

Said that, the higher cooling rate which allows to obtain a completely martensitic structure is 25°C/s. This cooling rate is called *critical cooling rate*, and above it the final microstructure will have also other phases like Bainite or Ferrite, and not just Martensite.

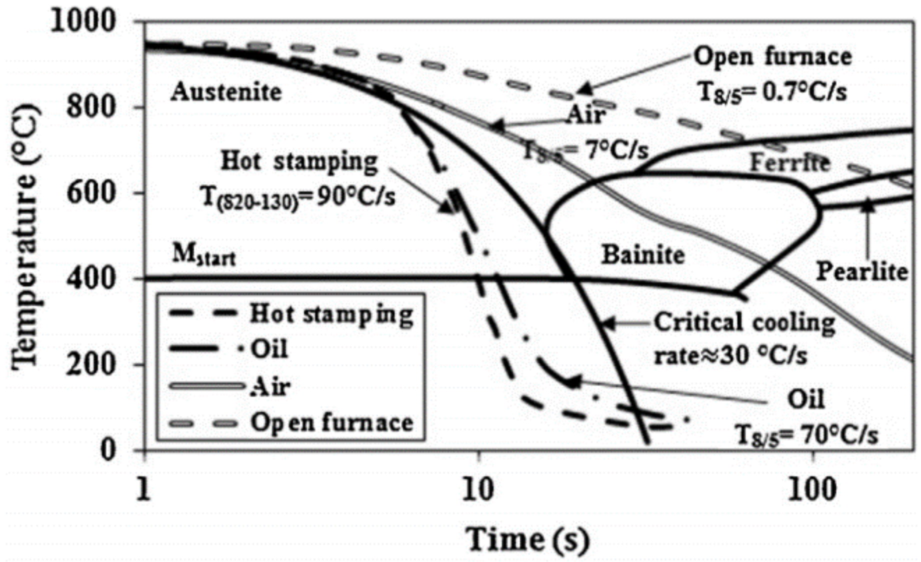

Fig. 48: Different cooling rates depending on the cooling process and/or media.

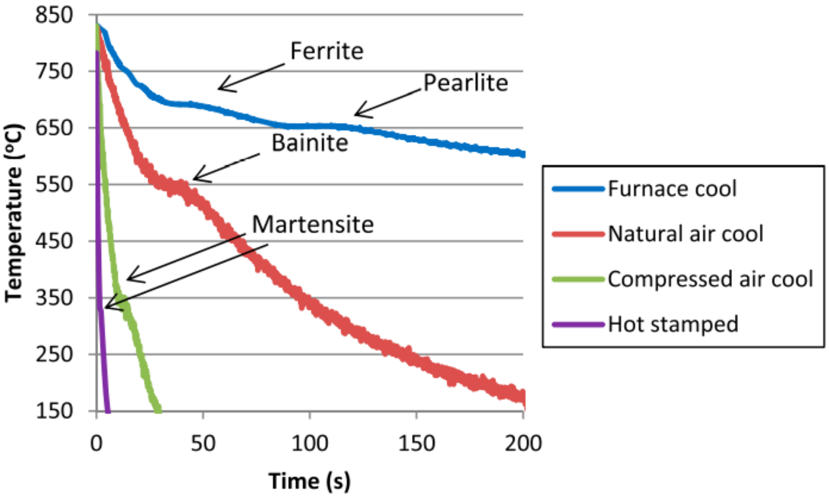

Fig. 49: Influence of cooling rate on phase transformations in 22MnB5 steel.

The properties of the 22MnB5 steel material change during the whole process as follow:

1) Blank/pre-formed part shows a Proof Strength of about 500 MPa, an Ultimate Tensile Strength (also "UTS") at most of 600 MPa, and a Total Elongation of 20%;
2) The austenitized piece has a Proof Strength between 150 and 300 MPa, an UTS of 200 MPa and a Total Elongation between 40 and 60%;
3) The hot stamped piece achieves a Proof Strength of 1000-1250 MPa, an UTS of 1400-1700 MPa and a Total Elongation of 4-8%.

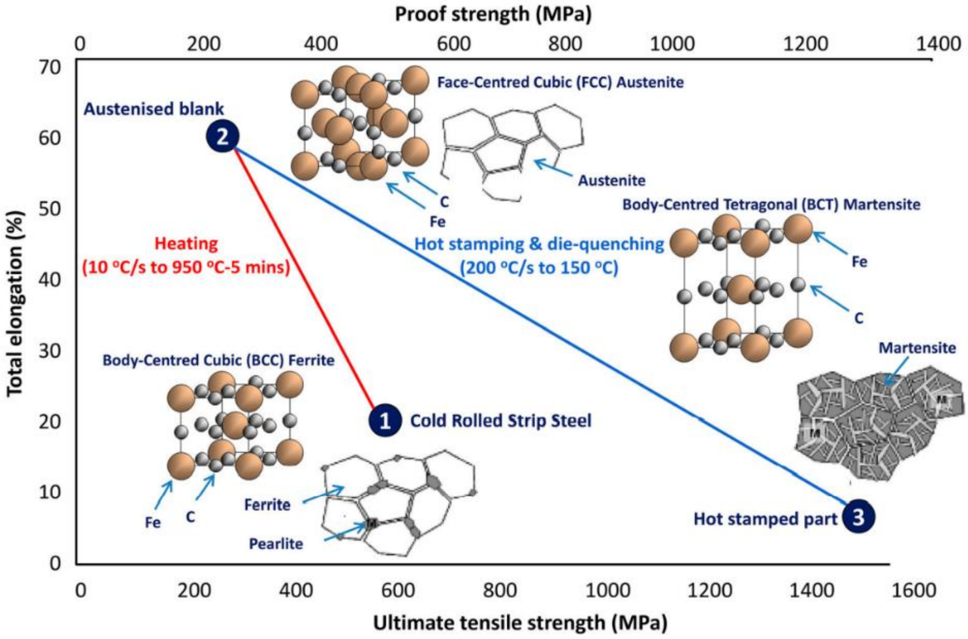

Fig. 50: Evolution of the 22MnB5's properties from the blank/cold pressed piece to the hot stamped and quenched final piece.

1.5.6 - Post processing

At the end of the hot-stamping process the piece is not ready yet and needs some further operations in order to be usable.

If no Aluminium coating is present, by the contact of the piece with the air during the final cooling some oxide scales can form on the steel surface. Hence, they must be removed. It can be done by means of shot blasting, which consists in forcing a stream of abrasive material against the surface to be treated, by using high-pressure air through a nozzle. In this way, the welding operations and the paint adhesion are improved.

Then, to refine the shape and the geometry, it is possible to do the machining. It includes several kinds of operations like cutting, trimming and piercing. They allow for instance the flange removal and the addition of welding points.

Usually laser machining is preferred to mechanical machining simply performed by a mechanical press, since the martensitic microstructure shows a ultra-high strength and then it is more difficult to be worked.

When indirect hot stamping is practised, it is also possible to refine the piece after the cold forming operation, before entering the austenitizing furnace. In this way the piece still shows a ferritic-pearlitic microstructure and it is softer, more malleable and more workable.

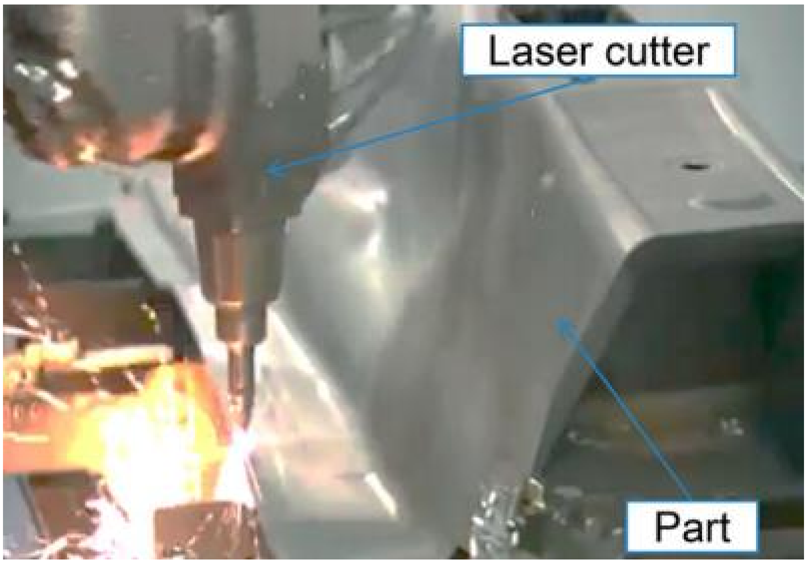

Fig. 51: Laser-cutting operation: addition of welding points.

1.6 - Press hardening drawbacks

Despite the advantages of being able to obtain springback-free steel parts with a ultra-high strength, hot stamping also shows several issues.

Some of these drawbacks are shown in the following picture.

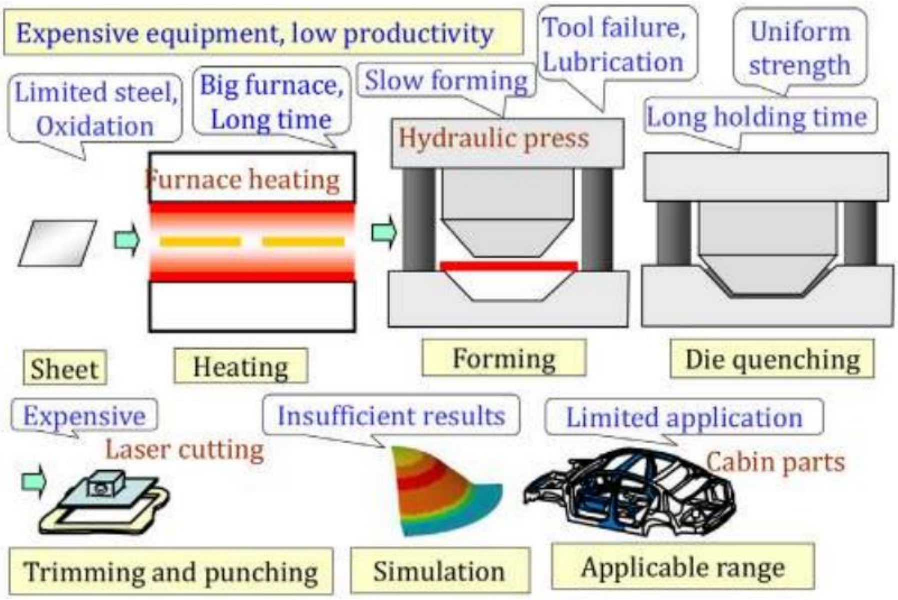

Fig. 52: Some press hardening drawbacks.

The investment cost results to be important, due to the necessary equipment such as the furnace, the press and the laser cutting machine.

Moreover this equipment requires much space and the furnace has a low efficiency.

Another issue is related to the productivity, which cannot be high: in fact, the piece must be held into the press in order to be quenched.

The oxidation of the heated steel parts is another problem, but it is faced by means of the use of Aluminium coatings. On the other hand, the coatings are expensive, and it represents another sort of general disadvantage, because it contributes to increase the cost of the process.

It could be difficult to properly lubricate the tools at elevated temperatures, so they may be affected by failure.

The applicable range of hot stamping is limited to the production of cabin parts of body-in-white for protecting passengers against automobile collisions because of insufficient energy absorption.

But one of the most critical problems of the high-strength steels (steel above 1000 MPa of tensile strength) is that they are affected by Hydrogen embrittlement.

1.6.1 - Hydrogen embrittlement

It is also possible to refer to Hydrogen embrittlement as “Hydrogen induced cracking” or “Hydrogen attack”.

What happens is that the Hydrogen, having a small mass and a low atomic size, is able to penetrate into the crystal lattice of metals.

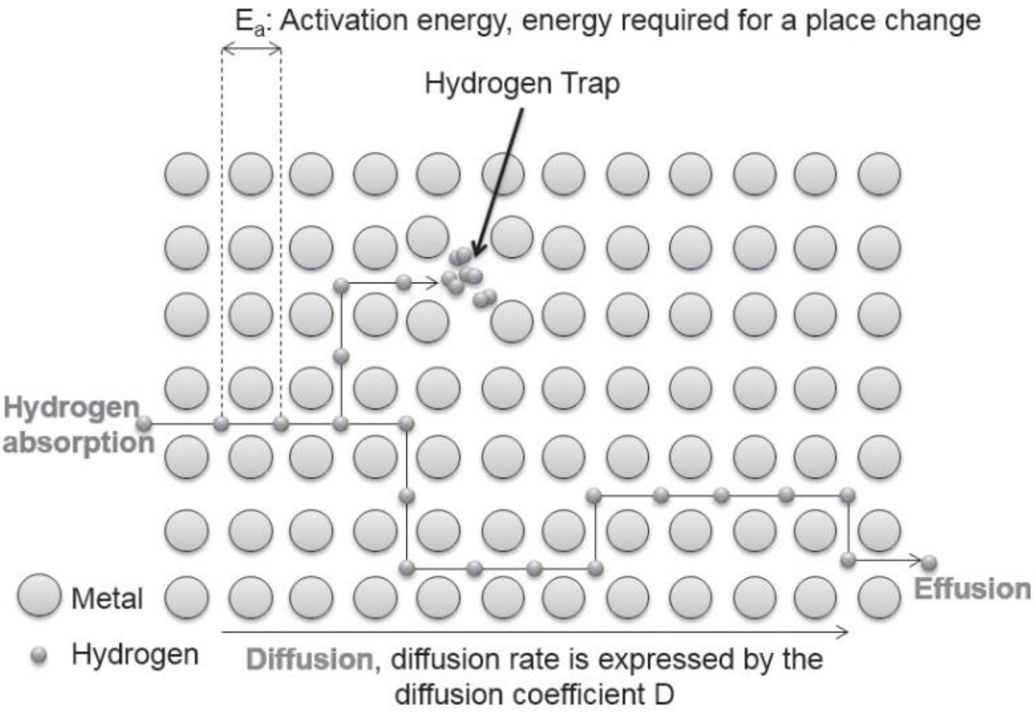

Fig. 53: Schematic representation of Hydrogen transport in metals.

The Hydrogen penetration could take place in every step of the production of car body.

The Hydrogen that penetrates is monoatomic and it is called “diffusible Hydrogen”. This monoatomic Hydrogen is unstable: it moves into the lattice and, since it is unstable, when meeting another monoatomic Hydrogen it combines with it, forming the H_2 molecule or other molecular forms, such as methane.

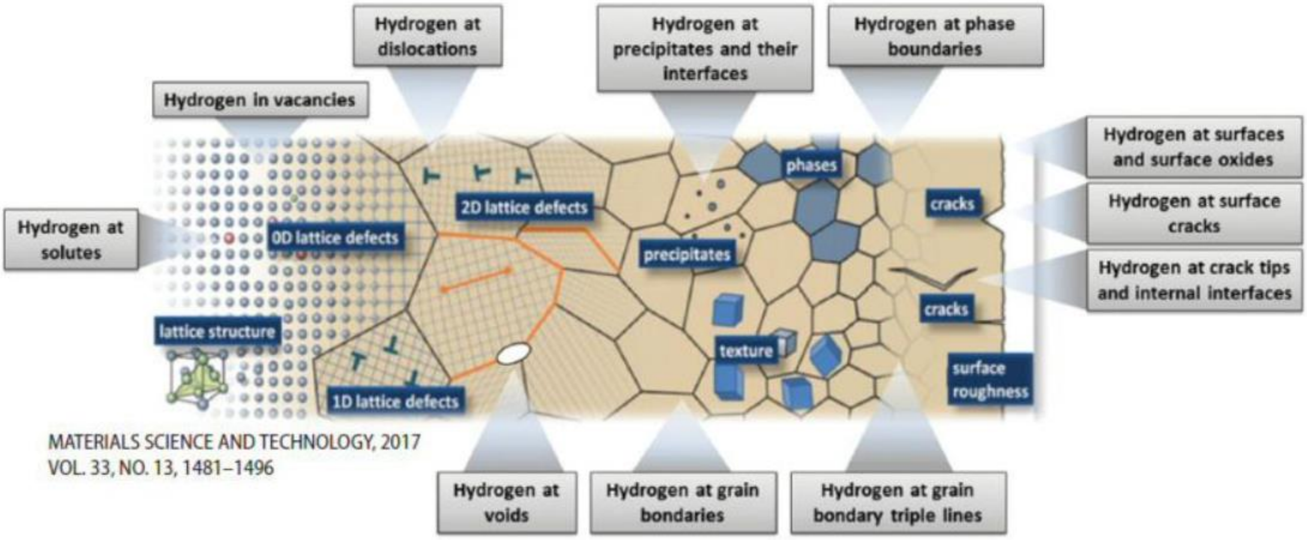

Fig. 54: Hydrogen traps, i.e. places where monoatomic Hydrogen could accumulate, originating cracks. [21], [22]

The monoatomic Hydrogen can accumulate in correspondence of Hydrogen traps, which can be defects and different phases; for instance, there could be a growing presence of Hydrogen into the vacancies, at solutes, at dislocations. Also, at voids, at the interface of second phases or of precipitates present into the lattice, at the grain boundary.

In proper conditions it may also leave the lattice, diffusing out of the steel, but it is more improbable.

The H_2 molecule is not as little as the diffusible Hydrogen: hence, it does not find space into the lattice except by creating distortions.

Every distortion generates an internal stress, which creates spaces inside the lattice. Other diffusible Hydrogens will go into these spaces, combining in turn, as well.

This is a self-enhancing phenomenon, and when the internal stress exceeds the material resistance, there is a crack formation that drives the material to failure.

The subsequent failure does not happen immediately, but it takes time, from 12 to 48 hours: hence, it is called “delayed failure”.

For this reason, it is such a critical failure: indeed, a quenched steel piece at the end of the hot stamping process is not broken yet, but it is perfect.

After the hot stamping process, the piece is sent to the bodywork, a phase where the various components are assembled by welding. The welding operations creates external stresses which cause distortions, that can be seen as energy.

If diffusible Hydrogen is present into the metal, the energy provided by the distortions makes the monoatomic Hydrogen movement possible. These movements of monoatomic Hydrogens result in Hydrogens combination, that creates internal stresses that are going to bring the material to failure.

Therefore, it can happen that the piece looks intact when assembled into the vehicle, and that it fails maybe the next day: of course, it is a problem, since the piece is already part of the vehicle.

Moreover, the rupture is brittle, catastrophic, unexpected and unpredictable, and it is able to damage the piece permanently.

This kind of problem is a big one, since a martensitic steel is not reparable because if it were welded, it would lose all its characteristics, and the unique solution would be to throw all the body away, for instance. It is clear that this would be an important damage for the vehicle production, in terms of costs and time waste.

Another factor that can lead to Hydrogen generation during the component life and hence to delayed rupture is the stress corrosion cracking, which is the combination of corrosion, stress and presence of Hydrogen.

In general, the embrittlement is a phenomenon that causes a decrease of ductility in the material, so that it becomes brittle.

The main factors that cause delayed fracture due to Hydrogen embrittlement are:

- The kind of **material**, which may differ by crystal structure, substructural conditions, second phases, phase stability; it could be monocrystalline or polycrystalline; the Hydrogen diffusivity and solubility vary from material to material.
  As said, high-strength steels are susceptible to Hydrogen embrittlement.

- The type of **stress** the material is subjected to. There can be a mechanical stress applied from the outside (generated for example by welding operation), or residual internal stresses. These stresses make the monoatomic Hydrogen move through the material.

- The **environment**, which can be more or less corrosive, facilitating the Hydrogen adsorption and the subsequent absorption into the material.

Failure is possible with at least two of these three factors.

It may also happen that Hydrogen diffuses out of the steel (see the “effusion” in **Fig. 53**).

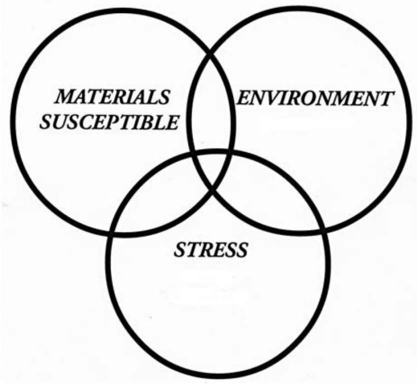

Fig. 55: Main factors that cause Hydrogen embrittlement.

1.6.1.1 - Hydrogen embrittlement mechanism

The Hydrogen adsorption can take place both in a gas phase and in a liquid phase, since Hydrogen is contained in the air and into H_2O water molecules.

In the hot stamping operation the relevant one is the Hydrogen absorption by the liquid phase.

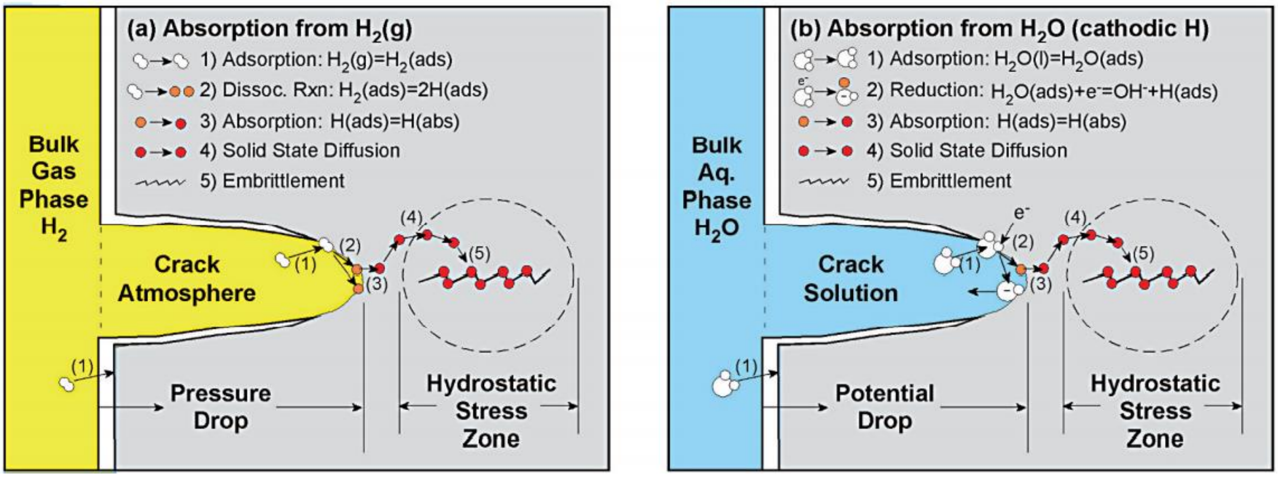

Fig. 56: Hydrogen absorption mechanism in two different environmental conditions: a) Hydrogen absorption by gas phase; b) Hydrogen absorption from liquid phase.

Considering the adsorption in the gas phase, the Hydrogen molecule is adsorbed on the metal surface: there, the molecule splits giving the dissociation into two monoatomic Hydrogens, which are absorbed by the metal. At this point the diffusion of the monoatomic Hydrogen into the metal starts to take place. As seen before, since the diffusible Hydrogen is unstable, it tends to combine with other monoatomic Hydrogens, originating the molecule of Hydrogen or molecular forms, like methane.

These molecules are too much large, so they are impeded from keeping diffusing through the material. In particular, the Hydrogen molecules get stuck in correspondence of the defects present in the material, such as the crystallographic ones (vacancies and dislocations) or like voids, inclusions and interfaces, which represent a discontinuity into the lattice.

Hence, the stuck molecules give rise to a pressure which originates small cracks, that make the metal more and more brittle, becoming less ductile and tough.

The exact mechanism of Hydrogen embrittlement is actually unknown.

In general, Hydrogen penetration can take place both at room temperature and at elevated temperature, when the metal is in contact with some kind of Hydrogen (monoatomic or molecular, for instance). At room temperature, Hydrogen embrittlement is more relevant. Usually it may happen during manufacturing operations or during assembly, or even when the piece is already in service.

Moreover, even if Hydrogen is not present when the piece in put in service, there could be a subsequent Hydrogen penetration as well, as a consequence of phenomena like corrosion, acid attacks on the metal and chemical reactions of the metal with other chemicals.

1.6.1.2 - Types of damages due to Hydrogen embrittlement

A broken piece may present damages like **internal cracks** or **blistering**. The difference between them is that the cracking takes place more deeply in the material, while the blistering happens at the surface. The blistering effect is visible, as different types of bubbles or blisters appear on the surface.

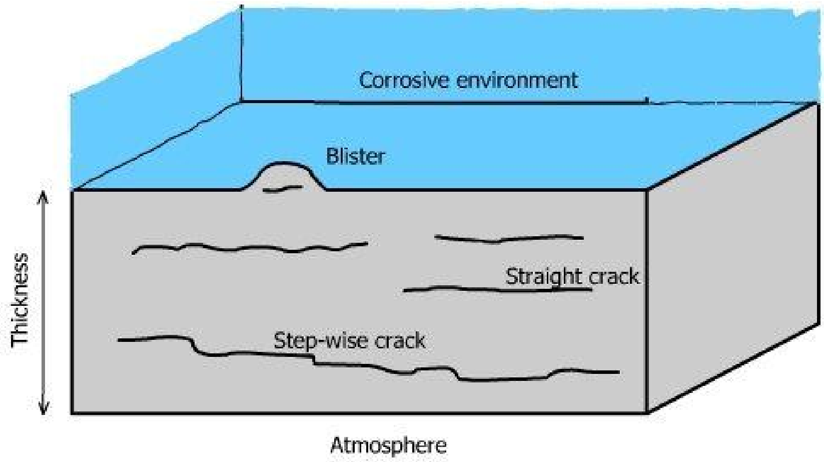

Fig. 57: The difference between blistering (crack present at the surface) and common cracking (crack present in the bulk). [23]

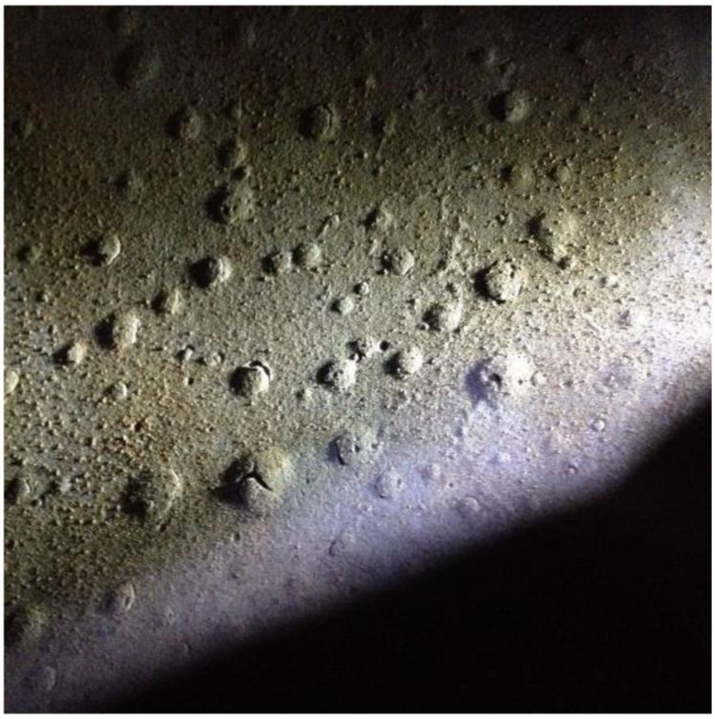

Fig. 58: Blistering effect given by Hydrogen embrittlement.

The greater the steel strength is, the higher is its susceptibility to the embrittlement given by the presence of Hydrogen. That is the reason why Hydrogen embrittlement is one the most critical issues of press hardened steels, which are ultra-high strength steels indeed.

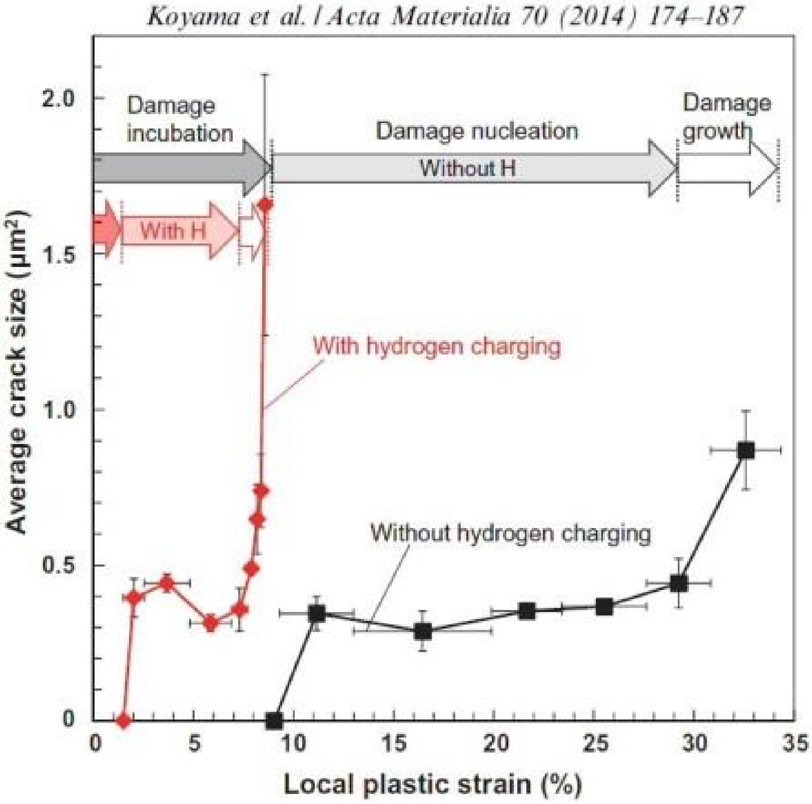

Fig. 59: Damage evolution plotted against local plastic strain with and without Hydrogen. [24]

In **Fig.59** it is shown the dramatic effect of the presence of Hydrogen on the plastic strain of the piece. In presence of Hydrogen, the damage incubation dramatically decreases, the crack nucleation is pretty short and the final damage growth is tremendously fast, leading quickly to a brittle rupture, as seen before.

A relevant source of Hydrogen in press hardening is the operating atmosphere.

1.7 - Microalloying elements in 22MnB5

The purpose of the microalloying elements is to increase the strength of the steel and also to face the problem of Hydrogen embrittlement. In particular, they make possible to increase the steel strength reducing at the same tame the Carbon content, making feasible the high strength steels fabrication.

They are called “microalloying elements” since they are added in extremely small quantities, usually smaller than 0.10 wt.%. Despite the small amount involved, their effect on the steel is much relevant.

The most common microalloyers are **Vanadium**, **Niobium** and **Titanium**.

These microalloyers increase the steel resistance by precipitating at the grain boundaries in the form of carbides. This gives rise to the pinning effect, which takes place since the precipitates act as an obstacle to the dislocations movement, and hence to the advancement of the cracks.

The precipitated carbides at the grain boundaries prevent the grains from overgrowing, so that there is grain refinement. This provides strengthening. Moreover, unlike the strengthening caused by Carbon enrichment, the ductility will be improved and the energy absorbed during an impact will be greater (i.e. better resilience).

Otherwise, by conventionally strengthening with Carbon addition, increasing the resistance means to reduce the ductility.

Niobium is a better grain refiner than Vanadium: due to the fact that it has a better effectiveness, it is possible to achieve the same effects obtainable with more Vanadium.

2 – Niobium

2.1 - History of the element Niobium

Niobium is a chemical element, located in the V group and second period in the Periodic Table of Elements. Its atomic number is 41 and its atomic weight is 92.91. It does not have stable isotopes.

The history of the effective discovery of this element is not simple and, at the same time, it is extremely interesting and deserves to be mentioned. It took many years in order to recognise the effective presence of Niobium and to obtain it in the pure form.

Everything started in **1801**, when the English chemist and mineralogist **Charles Hatchett** found the presence of this element into a heavy black mineral from the British Museum.

This mineral was discovered in North America around 1634 by John Winthrop the Younger, the early governor of the Connecticut Colony, who was a scientist and a rock collector. He called this mineral “Columbite”, after the name “Columbia”, the poetic name of North America. Winthrop’s grandson sent it to the British Museum in 1753 in order to have the mineral displayed and analysed. Just out of curiosity, this sample still exists nowadays.

Hence Hatchett, who was working at the British Museum, tried to analyse the constitution of this ore.

Fig. 60: Fragment of the mineral Columbite-Tantalite, also called “Coltan”, 6 centimetres long. [25]

Hatchett came to the conclusion that in the Columbite there was an unknown element, that he named “Columbium”, from the name of the mineral Columbite where he found it. Actually, as we are seeing later on, unbeknownst to Hatchett in the Columbite there were two elements that were unknown hitherto: Niobium and Tantalum (which was discovered the following year by Ekeberg).

Fig. 61: Charles Hatchett (1765-1847), Lithograph by W. Drummond, 1836, after T. Phillips. [26]

Then, as said, one year later, in **1802**, the Swedish chemist **Anders Gustav Ekeberg** discovered a new element in a mineral coming from Skogsböle, in the island of Kimito, in Finland.

Ekeberg called this element “Tantalum”, referring to the Greek mythology. In fact, Ekeberg observed that the oxide of this new element was insoluble and could not be dissolved in acids: therefore, this fact reminded him the legend of Tantalus, king of Lydia, who as a punishment for his crimes was condemned by the Gods to be immersed into the water up to his chin without ever being able to satiate his thirst.

Fig. 62: The torture of Tantalus in 'Tableaux du temple des muses' (1655) by Michel de Marolles (1600 - 1681). [27], [28]

It was then in 1809 that the dispute began: in fact, the English chemist and physicist William Hyde Wollaston, known today for the discovery of the elements Palladium and Rhodium, contested the discovery of Tantalum, stating that Tantalum actually consisted in the already discovered Columbium, and that the two elements were identical.

Due to this fact, people used to refer to the new element identified by Hatchett in different ways. Some called it “Columbium”, as Hatchett did; this name was particularly used in the Anglo-Saxon countries, like Great Britain and United States. Others preferred to call it “Tantalum”, especially in Europe, due to the fact that the Swedish chemist Jöns Jacob Berzelius considered this name more suitable, since it conveyed the fact that the element was insoluble in acid.

Anyway, the chemists were not convinced at all about the fact that Columbium and Tantalum were the same element, since the minerals from which they came from (i.e. Columbite and the so called Tantalite from Finland, respectively) showed different densities: 5.918 g/cm^3 for the American Columbite and 7.953 g/cm^3 for the Finnish Tantalite.

Hence, several suspicions remained up until the 1840s, when the German chemist **Heinrich Rose** accurately investigated the issue.

This happened because in **1844**, thirty-five years after the wrong report made by Wollaston in 1809, Heinrich Rose was convinced by the German mineralogist Gustav Rose to try to shed light on this old matter, availing of the new techniques available at that time.

Note that the mineral that was analysed by Heinrich Rose was not the American Columbite from Connecticut, but another type of Columbite coming from Bodenmais, a German region located in Bavaria.

After having analysed a portion of the American Columbite, Rose came to the conclusion that the two minerals were identical, apart from a slight difference in their specific gravity. For that reason, during his work, he used to refer to the mineral from Bodenmais as “Columbite” as well.

In fact, over the years there had been discovered new sources in several places for the high-density Tantalite and the low-density Columbite: the first one could be found in Sweden and Finland, while the Columbite, as said, in Connecticut and in Germany.

So in 1844 Rose declared that the Tantalite was composed of one metal, the Tantalum, while the Columbite was composed of two metals: the Tantalum and another unknown element that Rose called “Niobium”, also referring to mythology used by Ekeberg, where Niobe was the daughter of Tantalus.

The difference between Tantalum and Niobium lied in their chlorides, prepared by Rose by making react the oxides with charcoal and gaseous chlorine. The chlorides were different in colour and in melting behaviour: in fact, Tantalum chloride was yellow and could be easily melted; moreover, it was volatile. On the other hand, Niobium chloride was white, infusible and was not volatile.

Rose also thought of having discovered a third element, to whom he gave the name “Pelopium”, since in mythology Pelops was the son of Tantalus and the brother of Niobe. But when he tried to separate the “three” elements, i.e. Tantalum, Niobium and Pelopium, he eventually found out that Pelopium was just Niobium in a different oxidation state.

Other presumed new elements were found, but many years later they all ended up being mixtures of Tantalum and Niobium, also with other impurities.

Nevertheless, in about twenty years Rose never managed to separate Tantalum and Niobium. His two-decades long research is reported in the Poggendorff’s Annalen (*Annalen der Physik und Chemie*).

It was due to the Swiss chemist **Jean-Charles Galissard Marignac** from Genève and the Swedish mineralogist and chemist **Christian Wilhelm Blomstrand** that, around **1866**, it was possible to prove that the only metals actually existing in that minerals were Tantalum and Niobium, and that all the other presumed metals found early on (such as Pelopium, Decinium and Ilmenium) consisted in simple mixtures of Tantalum and Niobium in different proportions or in mixtures of Tantalum and Niobium with other impurities like Tungsten, Titanium or Iron. The two chemists worked independently, and their conclusions were supported by the studies of their French colleague, the chemist Henri Sainte-Claire Deville.

Marignac developed a separation procedure that allowed him to separate and characterise the double fluoride salts of Tantalum and Niobium: with his method, the Tantalum salt precipitated out of the solution, while the Niobate salt remained dissolved into the solution. The way of industrial production of Tantalum and Niobium relied on this separation method up until the middle 20th century.

Marignac's purifications schemes allowed the preparation of the two pure elements: Blomstrand managed to obtain the first pure sample of Niobium, while the first pure sample of Tantalum was prepared by the German chemist and materials scientist Werner von Bolton, in 1903.

To sum up, **Hatchett** analysed a mineral coming from Connecticut and discovered the Columbium in 1801, while Ekeberg discovered Tantalum in 1802 in a mineral similar to the American one but with different density. These two new elements were so similar that they were assumed to be the same one by Wollaston, who in 1809 claimed that Tantalum was none other than Columbium. In 1844 **Rose**, analysing a mineral coming from Germany which was pretty the same of the one from Connecticut studied by Hatchett years before, recognised that the elements were more than one (not just the Columbium, as Wollaston thought): one of these elements was the already known Tantalum, but in addition to it Rose discovered and recognised the presence of Niobium as an isolated element. What he missed was to understand that Tantalum and Niobium were the only elements present in the mineral: in fact, he was convinced that other presumed elements were present, like Pelopium. In 1866 **Marignac** and **Blomstrand** came to the conclusion that the only element present in the mineral were Tantalum and Niobium, while the other presumed elements turned out to be mixtures between Tantalum and Niobium and between them and other metallic impurities. Finally, Blomstrand managed to isolate Niobium and to prepare the first sample of pure Niobium, as von Bolton did with Tantalum in 1903 as well.

Hence we can say that the element Niobium was indirectly discovered by Hatchett in 1801 with the name of Columbium, was re-discovered by Rose in 1844 with the current name ("Niobium") and was at last isolated in its pure form by Blomstrand, in 1866.

The German chemist and mineralogist **Karl Friedrich Rammelsberg**, who had been a student of Heinrich Rose at the University of Berlin and that took his place as a professor in the same Faculty, said these things relative to the discovery of Niobium:

"*The discovery of a new element, niobium, was a splendid result of this great, laborious, and .... difficult investigtion, and history will forever attribute to it an honourable place in science*". [29]

2.1.1 - Nomenclature

Even after having discovered the effective presence of two elements, people used to refer to Niobium in two different ways: "Niobium" in Europe, as Rose had named it, and "Columbium" in the United States. In the United States, Niobium continued to be called "Columbium" also in the American Periodic Tables of Elements.

Finally in **1949**, during the 15th meeting of the IUPAC ("International Union of Pure and Applied Chemistry") which took place in Amsterdam, the name "Niobium" was officially and definitively assigned to the element. From then on, also the American Periodic Tables of Elements were updated and printed with the new official name "Niobium". But apart from that, in the United States sometimes it is still possible to come across the name "Columbium", in particular in engineering journals or in trade journals.

2.2 - Niobium in nature and the Araxá deposit

In the world there exist 85 available deposits, so it is not a rare mineral. But only three of these 85 deposits are explored, since Niobium metallurgy is a new type of metallurgy and therefore there is not so much global demand yet to explore new sites around the world.

The element Niobium, as said before, is not present in nature in its pure form, but it is contained in other minerals, such as Pyrochlore, whose formula is $(Na,Ca)_2Nb_2O_6(OH,F)$, rich in Niobium pentoxide Nb_2O_5.

The largest Niobium reserve known so far is in Araxá, a city located in the Brazilian state of Minas Gerais, where Pyrochlore is present in Carbonatite formations deposits.

Fig. 63: The location of the city of Araxá, belonging to the Minas Gerais state, in Brazil.

Alone it represents more than 70% of the current available reserves. It was discovered in 1954 by professor Djalma Guimarães, a Brazilian geochemist and geologist, while in 1965 the company **CBMM** (Companhia Brasileira de Metalurgia e Mineração) started to mine it.

The Araxá mine is an open pit mine: it consists in a great pit in the ground, whose terrain contains the 2.3% of Niobium pentoxide Nb_2O_5.

Fig. 64: Panoramic view of the Araxá mine.

The soil containing the mineral Pyrochlore is extracted from the mine, then it is deposited in the silos and the Pyrochlore is concentrated through physical separation. In this way the mineral is separated by the land and concentrated. By means of concentration it is possible to reach a concentration of 50% of Nb_2O_5, from the original 2.3%.

After that it is necessary to remove Sulphur and Phosphorus by means of desulphurization and dephosphorization, respectively.

Since Sulphur and Phosphorus represent about the 10% of the concentration, just by removing them it is possible to reach a concentration of 60% of Nb_2O_5.

Niobium pentoxide is then reduced by means of aluminothermic reduction and thus pure Niobium is obtained.

2.2.1 - Ferroniobium

In the field of steels, Niobium is not used in its pure form.

Therefore, after having obtained pure Niobium, it is mixed with Iron in order to obtain a FeNb mixture with 65 at.% of Niobium.

This particular percentage of Niobium is not casual, but it is chosen on purpose: in fact, it is the percentage corresponding to the eutectic point in the Fe-Nb diagram. The eutectic point has a lower melting point than the melting point of the pure element.

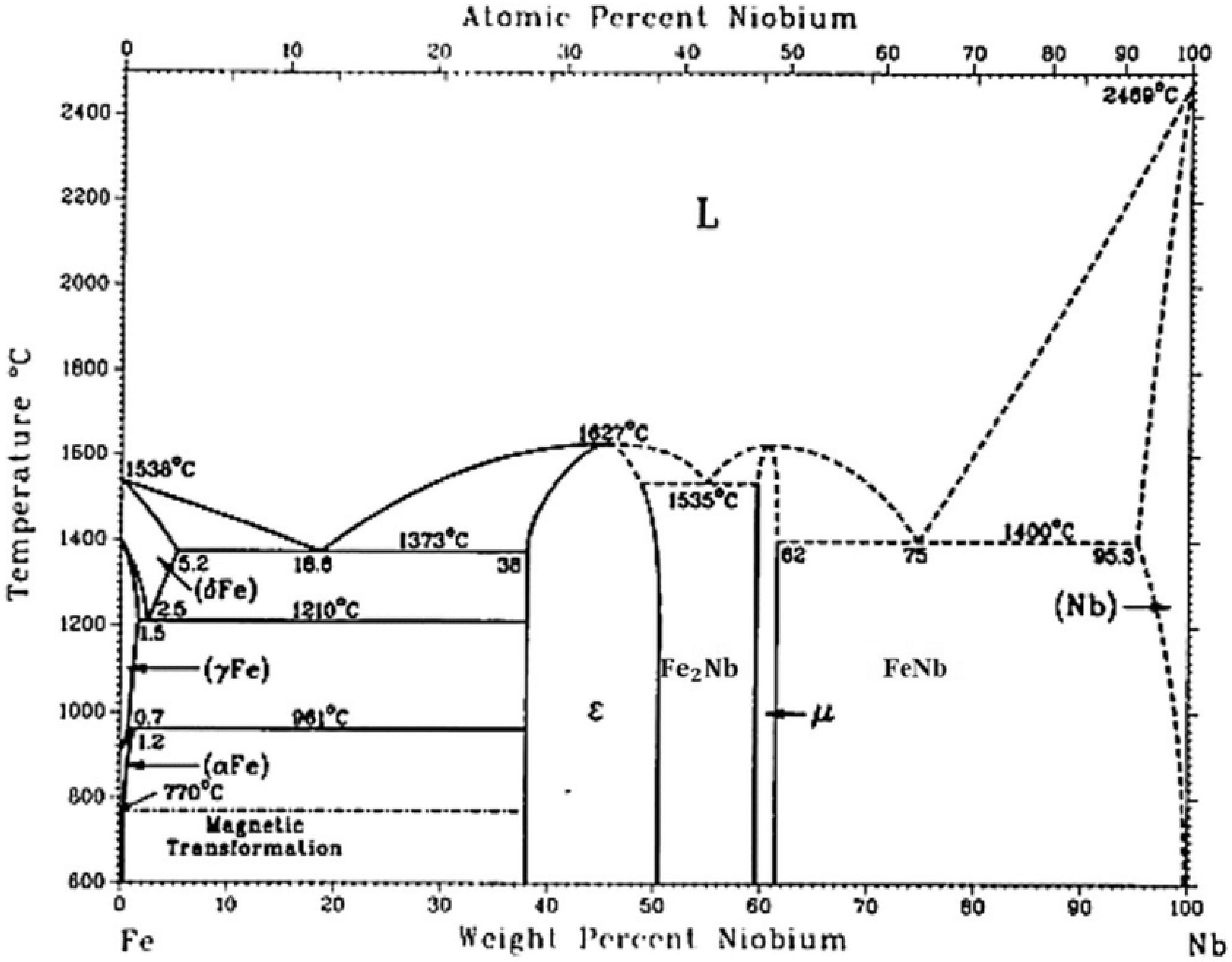

Fig. 65: Fe-Nb diagram. [30]

As it is shown in **Fig. 65**, there is an eutectic point for 65 at.% of Niobium that corresponds to a melting temperature of 1400 °C. Hence when the FeNb mixture is added to the ladle, which is at a temperature around 1600 °C, it immediately melts.

Otherwise, if pure Niobium was used, it would not be possible to have it melted when added to the ladle, since its melting temperature is 2477 °C (it can also be found to be 2468 °C, depending on the source), much higher than the 1600 °C reached into the ladle.

Fig. 66: FeNb storage, photography by Marcio Schimming. [31]

Actually, CBMM also produces pure Niobium, but not as a microalloying element for steels, for the reasons just seen.

Pure Niobium can be used for applications like MRI ("Magnetic Resonance Inductor"), in order to produce the wires, or in the field of Jewellery. In particular, when it has to be transformed into a wire, Niobium is sold in big ingots and drawn into a wire.

2.2.2 - Niobium applications

In general, nowadays Niobium (in its pure, oxide or alloyed form) is used in these three main sectors: Mobility, Energy and Structures.

In the field of Energy, it is used for instance in solar panels, wind turbines and batteries (creation of a Niobium-based anode). In particular, in the field of batteries, the objective is to switch from Lithium batteries to Lithium-Titanium oxide batteries and successively to Niobium-Titanium oxide (NTO) and Niobium-Tungsten oxide (NOW) batteries. This would allow to achieve an extremely fast charge, able to charge a vehicle in just 6 minutes. Moreover, such batteries would also be safer in terms of fireproof properties, being able to accumulate up to 30% more energy.

In the field of Structures it is used for reinforced concrete rods, profiles, cranes, bridges and constructions in general. It can be used to create smart windows based on electrochromic smart glasses, which become transparent or reflecting by making the electric current pass around the glass.

In the field of Mobility, Niobium is used for commercial vehicles, passenger transport, high-performance cars and also bicycles.

In the part relative to passenger transport, there can be Niobium applications related to exhaust, wheels, **body-in-white**, brake parts, powertrain components, transmissions and chassis.

Niobium is also used in its oxide form in the field of Electronics, for capacitors, inductors and sensors, and also for wireless charging.

2.2.3 - Global demand for Niobium

At the moment, global Niobium demand is not so high to justify an investment on another pole different from the one in Araxá.

In fact, in December 2020 the productive capacity of the company CBMM reached 150,000 tons, and in 2019 the pre-pandemic market demand was of 120,000 tons, whose 80% of the market share was held by CBMM. The remaining parts of the market share belonged to only two competitors, one Canadian and another one Chinese (but with its deposits in Brazil).

Therefore CBMM alone would be able to entirely cover the Niobium request, and Brazil owns a 200-years Niobium provisions.

So today CBMM almost represents a monopoly in the market of Niobium, which is constantly growing.

2.3 - Effect of Niobium on press hardened steels

Niobium has been added to the metal alloys (especially steels) since the 1970's in order to reinforce them.

The main disadvantages of press hardened steels are:

- **Low bendability**, which limits practical applications;
- **Hydrogen embrittlement**, which reduces the ultimate tensile strength;
- **Toughness**, which is hindered by grain coarsening;
- **Small process window**, that means that the piece cannot stay too long inside the furnace, otherwise the grains would become too much big and it would result in a reduction of toughness.

Niobium reinforces press hardened steels by means of precipitation strengthening, due to the precipitation of Niobium carbides NbC. It leads to grain refinement, Hydrogen trapping and improvement of bendability, with an overall strength and toughness improvement. Moreover, the process window becomes larger, which means that the pieces can withstand a longer period of permanence inside the furnace without showing grain coarsening.

All these improvements are extremely useful in enhancing the crash behaviour of the press hardened pieces destined to improve the vehicles safety.

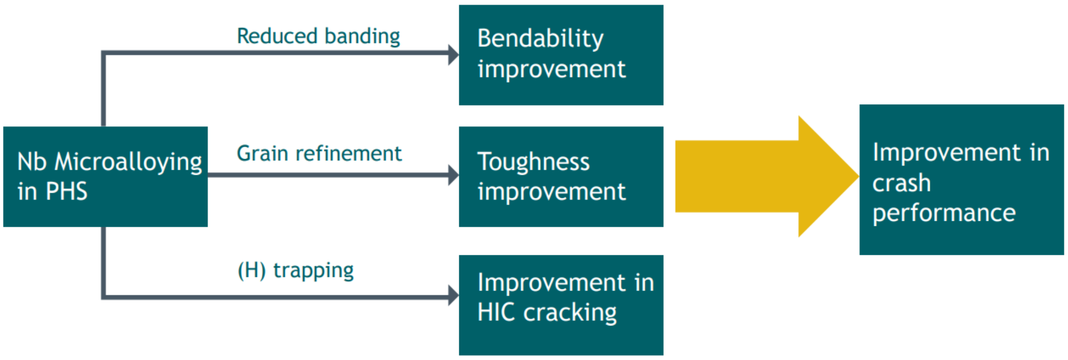

Fig. 67: Schematic view of how Niobium improves the properties of press hardened steels. [32]

There exist other microalloying elements able to precipitate at different temperatures, with also different sizes of atoms and precipitates. The most popular are Vanadium and Titanium.

The “reinforcement ratio” between Niobium and Vanadium is *1:1.5* (or even *1:2*) depending on the application: it means that in some steels it is possible to add about 50% Niobium less compared to Vanadium to obtain the same reinforcement effect, so it means that it is more effective.

This is one of the reasons why Niobium is more and more used to reinforce steels; it is alloyed to Carbon steels in very small amounts, normally not more than 1 Kg of Niobium per ton of steel.

2.3.1 - Niobium carbides precipitation

In order to be able to provide the steel with reinforcement properties, not only Niobium has to be present in the steel, but it also has to precipitate in the form of carbides.

Niobium carbides NbC have a size ranging between 5 and 10 nanometres, and they are usually observed by means of TEM (“Transmission Electron Microscopy”).

The dissolution of Niobium into the metal takes place at a temperature around 1300 °C, and it usually happens during the hot rolling of the sheet steel.

Then after hot rolling the sheet steel contains a supersaturated solid solution of Niobium. Niobium carbides must then precipitate, to confer the strengthening properties to the steel. The quantity of Niobium that precipitates in the form of NbC depends on the relation between time and temperature, according to the graph in **Fig. 68**.

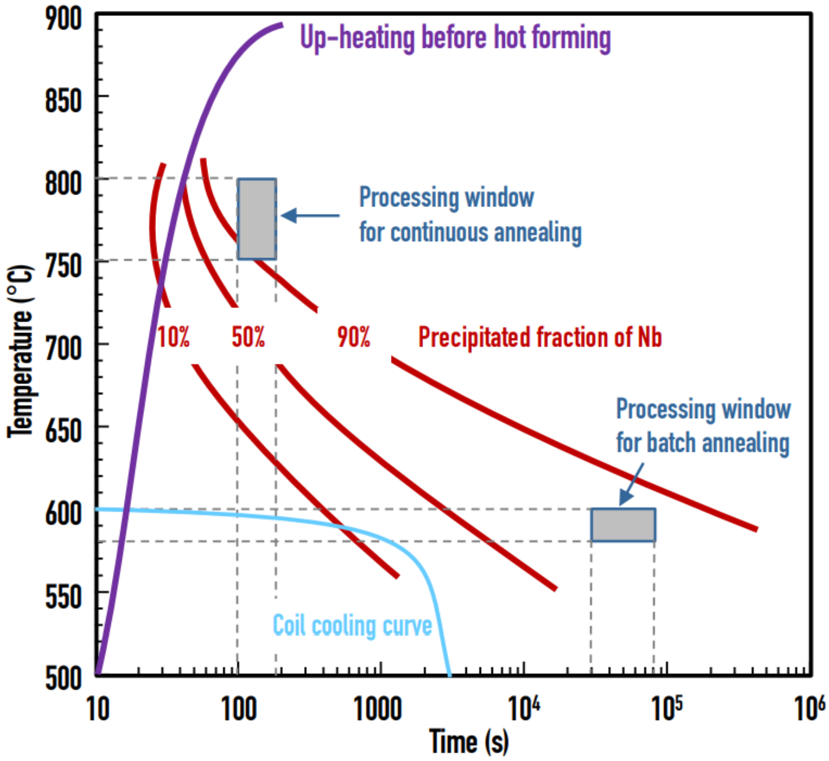

Fig. 68: Temperature-Time graph of Niobium carbides NbC precipitation.

As it is shown in **Fig. 68**, the coil cooling curve intersects the curve relative to a NbC precipitation of 10%. It means that the sheet steel is at a temperature of about 650 °C when the coiling operation begins, and that after some time during coiling a bit of precipitation of NbC takes place. In particular, about the 10% of the dissolved Niobium precipitates in the form of NbC, in this case. The NbC precipitation is not that consistent because the coiling operation is not much long and does not allow to make more Niobium precipitate. Thus, NbC precipitation through coiling operation is not effective, since only a very little amount of the Niobium present in the solid solution does precipitate as NbC.

To have a good precipitation of NbC, at least corresponding to the 90% of Niobium dissolved in the supersaturated solid solution, there are two possibilities:

- **Batch annealing**: the piece is kept into the oven at temperatures around 600 °C for a long time, even two days. The high duration of the process involves higher costs. Batch annealing is usually used for cold rolled press hardened steels.
- **Continuous annealing**: the piece is heated up to a much higher temperature, between 750 and 800 °C, but for a shorter period of time, in the order of seconds.

Once that Niobium carbides NbC have precipitated, it is possible to cool the sheet steel down both quickly and slowly. Usually, after annealing the cooling is slow.

Hence, after hot rolling it is necessary to do a up-heating in order to make NbC precipitation take place before hot stamping.

In this way, the sheet steel that is going to be press hardened has the Niobium almost completely precipitated in the form of NbC. Between hot rolling and continuous annealing it is also possible to have cold rolling, in order to obtain a lower thickness, of also 1 millimetre.

At this point, when the piece is austenitized in the press hardening process, Niobium does not dissolve anymore in solid solution, since the austenitizing temperature is of about 900 °C, not high enough to activate Niobium dissolution.

By remaining in the form of precipitate during the austenitizing stage of the hot stamping process, Niobium hinders grain coarsening in the austenitized sheet steel.

Note that Niobium carbides precipitation takes place **also** (and **not only**) during continuous annealing: in fact, it already happens during hot rolling! In this case, the subsequent cold rolling will be more difficult, since the steel was strengthened by means of NbC precipitation during the hot rolling.

That means that after hot rolling Niobium can precipitate if temperature-time precipitation conditions are present, regardless of the process! Niobium precipitation must therefore be controlled.

On the other hand, for a process involving for example a fast quenching after hot rolling at 1200 °C, Niobium will not have enough time to precipitate, and the resultant sheet steel will contain Niobium in solid solution, not precipitated. In this case it is necessary a subsequent thermal treatment, like annealing, in order to have Niobium precipitated in the form of Niobium carbides at the end of the process, otherwise Niobium would be irrelevant as a reinforcing agent if not precipitated.

To sum up, Niobium precipitates at a certain temperature, according to the curves showed in **Fig. 68**. This temperature can be reached during any process, and it must be ensured that the precipitation actually takes place in the desired process. **Fig. 69** shows the most common treatments performed to cause the NbC precipitation, indicated by the blue curves.

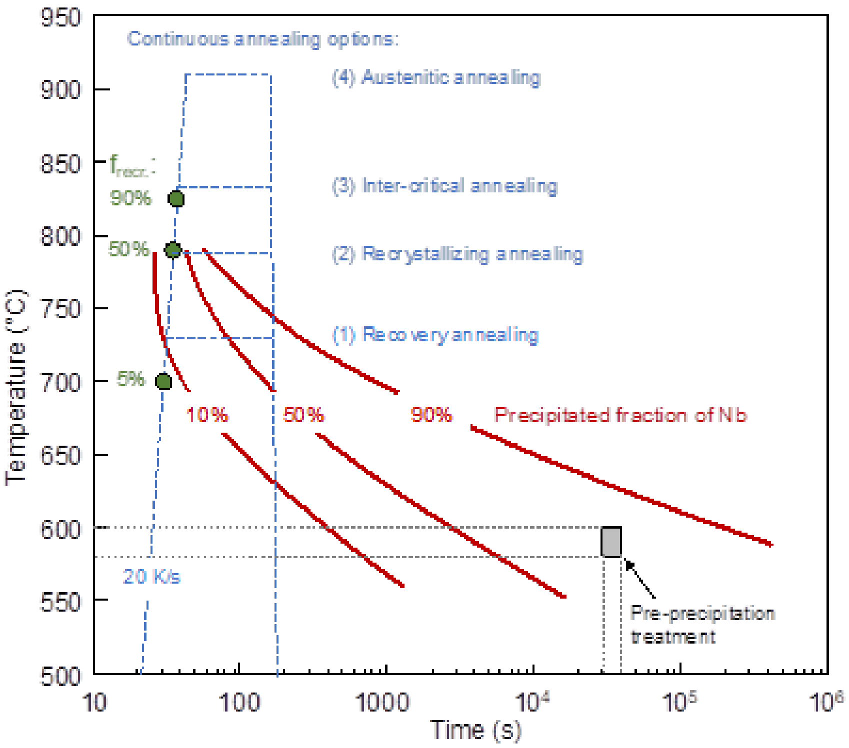

Fig. 69: Temperature-Time graph of NbC precipitation with blue curves showing the most common treatments performed to make the carbides precipitate.

Niobium carbides act as grain refiners and improve toughness by means of precipitation hardening. Moreover, being a hard phase, they enhance wear resistance.

Niobium carbide is one of the hardest technical compounds, with a hardness of about 2000 HV (see **Fig. 70**).

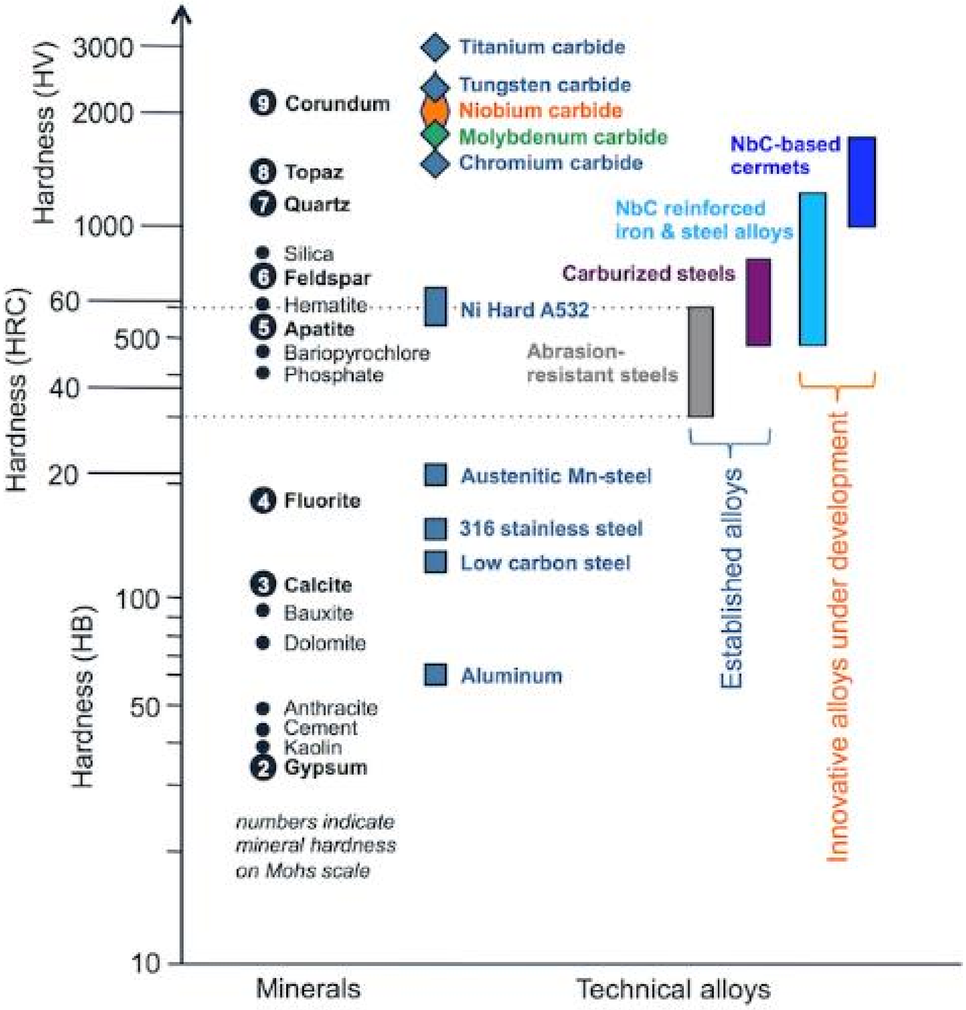

Fig. 70: Comparison between the hardness of several compounds. [33]

If compared to the Tungsten carbide WC, which has been the leading hard metal for decades and that is just above NbC in the Hardness scale, Niobium carbide shows several advantages in many applications:

- NbC has a lower density, therefore it is possible to purchase more volume per Kg if compared to WC;
- The fact that NbC has a lower density reduces the inertia in machining equipment or, in general, in dynamic applications where it is used instead of WC;
- Possibility of reducing the adhesive wear in tooling applications;
- Less friction in tribo-contacts compared to WC;

- Mechanical properties similar to the ones of Tungsten carbide WC (it is useful for the applications related to wear parts);
- Above 700 °C, similar or superior hot hardness of NbC compared to the one of WC (despite the fact that NbC hardness at room temperature is lower than the one of WC, as shown in **Fig. 70**);
- High chemical stability, due to the fact that Niobium has a low solubility in Iron: that reduces the need for the use of additional coatings in high-temperature applications;
- Niobium oxide is non-toxic, therefore potential tribo-oxidation products of NbC have a low environmental impact and do not constitute a risk for health (see **Table 7**).

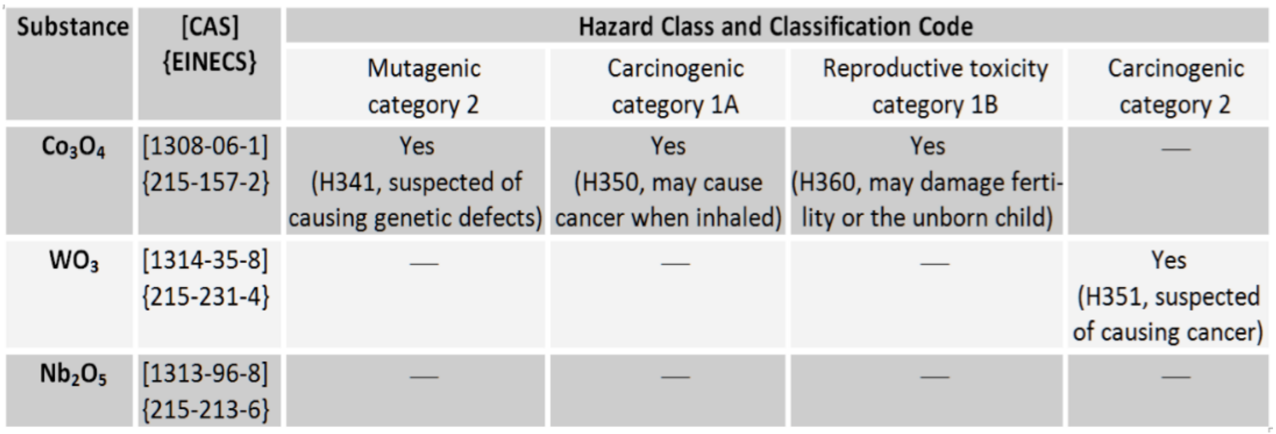

Substance	[CAS] {EINECS}	Hazard Class and Classification Code			
		Mutagenic category 2	Carcinogenic category 1A	Reproductive toxicity category 1B	Carcinogenic category 2
Co_3O_4	[1308-06-1] {215-157-2}	Yes (H341, suspected of causing genetic defects)	Yes (H350, may cause cancer when inhaled)	Yes (H360, may damage fertility or the unborn child)	—
WO_3	[1314-35-8] {215-231-4}	—	—	—	Yes (H351, suspected of causing cancer)
Nb_2O_5	[1313-96-8] {215-213-6}	—	—	—	—

Table 7: Summary of health&safety classifications, with labelling. [33]

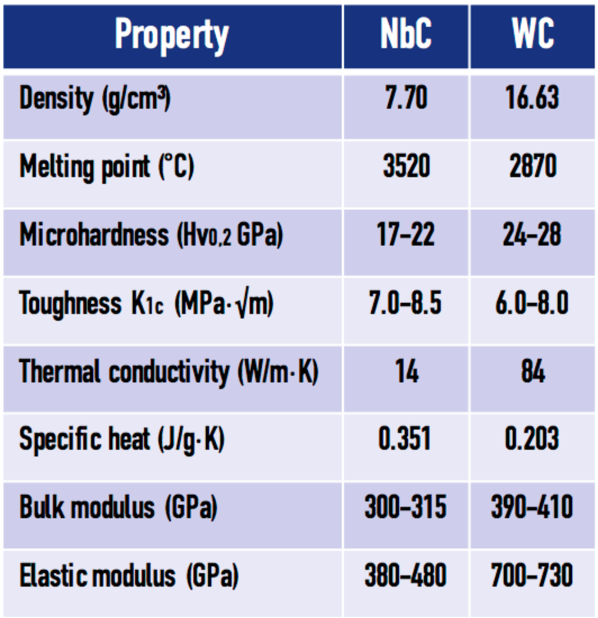

Property	NbC	WC
Density (g/cm³)	7.70	16.63
Melting point (°C)	3520	2870
Microhardness ($Hv_{0.2}$ GPa)	17-22	24-28
Toughness K_{1c} (MPa·√m)	7.0-8.5	6.0-8.0
Thermal conductivity (W/m·K)	14	84
Specific heat (J/g·K)	0.351	0.203
Bulk modulus (GPa)	300-315	390-410
Elastic modulus (GPa)	380-480	700-730

Table 8: Comparison between the main physical properties of Niobium carbide and Tungsten carbide. [33]

The structure of Niobium carbides is FCC. Niobium carbide particles firstly originate and precipitate at the Austenite (and Ferrite) grain boundaries, defects (like stacking faults) and dislocations, where Niobium has higher diffusivity.

In fact, since there is a pretty large difference between Niobium carbide and lattice of the metal matrix (Ferrite or Austenite), there is a higher probability of NbC nucleation nearby lattice defects, where strain energy is lower.

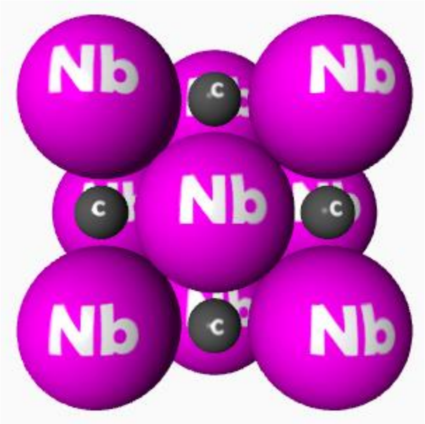

Fig. 71: FCC crystal structure of Niobium carbide NbC. [34]

When a nucleus of Niobium carbide nucleates at a grain boundary, what happens is that a small part of the boundary disappears, releasing energy and reducing the total energy concerning the nucleus formation.

Niobium carbide also precipitates due to the dislocations, since during their motion they contribute to cause the accumulation of solute atoms thus increasing solute concentration.

The strengthening effect given by precipitation hardening is described by the Hall-Petch equation:

$$\sigma_y = \sigma_0 + \frac{k}{\sqrt{d}}$$

σ_y: lower yield stress;

σ_0: friction stress;

d: Ferrite or Austenite grain diameter;

k: constant.

Both the friction stress σ_0 and the constant k do not vary with the content of Niobium.

The finer the grain, the higher the reinforcement.

2.3.2 - Grain refinement

When the grain is refined, the grain is smaller and more uniform. It confers better resistance, higher tenacity and higher energy absorption, since a crack would need more energy to proceed.

The reinforcement conferred by the grain refinement depends on the ductile-to-brittle transition temperature ("DBTT").

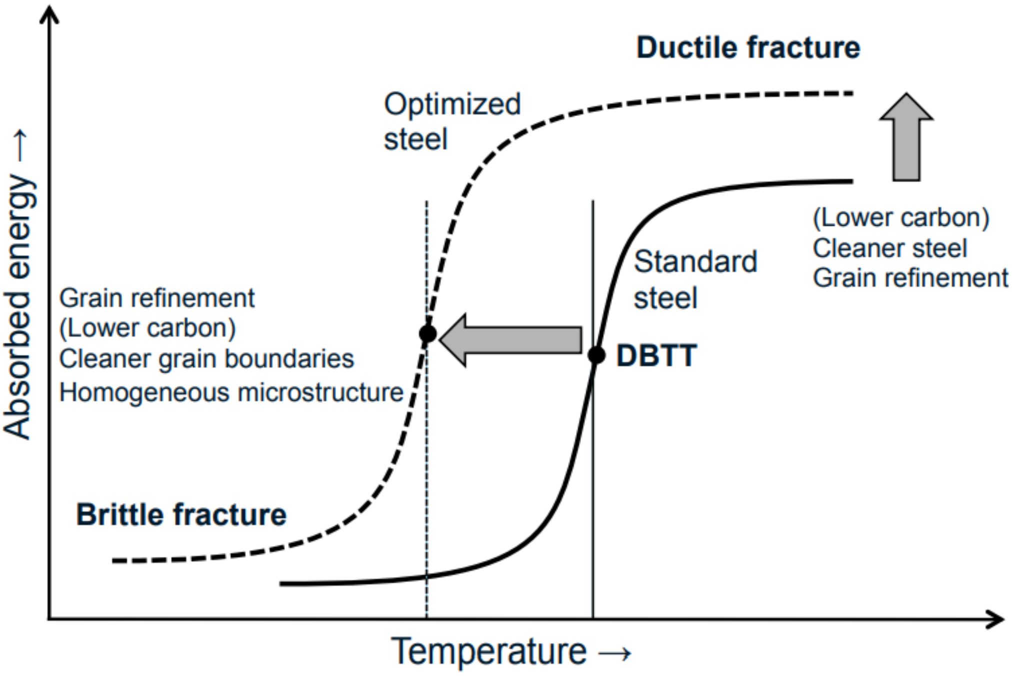

Fig. 72: DBTT curve.

In **Fig. 72** it is shown how the absorbed energy varies in function of the temperature. The ductile-to-brittle transition temperature is the temperature that separates the brittle behaviour of the piece from its ductile behaviour. The more ductile the behaviour, the greater the energy absorbed, and the stronger the piece. Ductile behaviour allows to avoid brittle fracture, which is catastrophic. Above the DBTT the piece will show a ductile fracture, while below the DBTT the fracture will be brittle. Out of curiosity, and to highlight the importance of the DBTT, in 1912 the famous transatlantic *Titanic* sank in such an easy way due to the fact that the steel used to fabricate its hull had a too much high DBTT. That means that in the cold waters of the Atlantic Ocean the steel had a brittle behaviour, and when the ship collided with the iceberg it could not help but break in a brittle and disastrous way, since the steel of the hull could absorb very little energy during the impact.

It is therefore important to reduce the DBTT, in order to have a ductile behaviour already at low temperatures, avoiding brittle fracture.

Having a higher absorbed energy during an impact is very important in the automotive sector, as previously seen.

With lower DBTT, the curve in **Fig. 72** is shifted to the left and up. As it was said before, it is possible to do that by means of grain refinement.

Grain refinement improves tenacity at low temperatures (even down to -30 °C), by reducing the DBTT.

Grain refinement raises the Stress-Temperature curve depicted in **Fig 73**, which corresponds to the ductile-to-brittle transition.

Martensite has a constant of 160*$\Delta d_{eff}{}^{-1/2}$ (where d_{eff} is the grain diameter and Δd_{eff} is the extent of grain refinement), so grain refinement has a great effect on Martensite, higher than on other materials with lower constant! The DBTT is lowered and the yield strength is much higher.

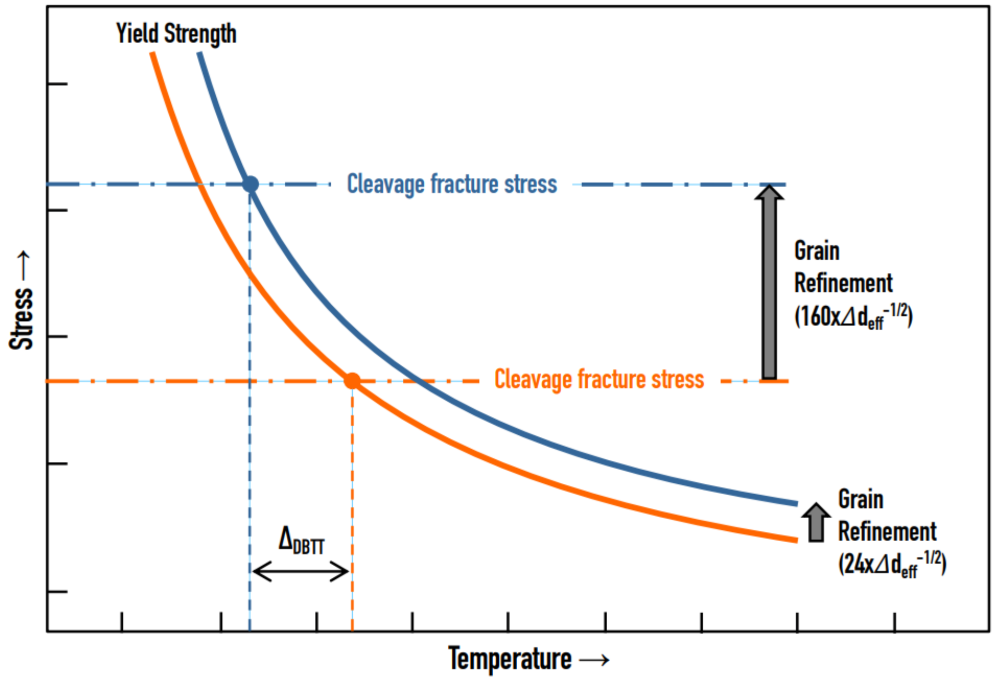

Fig. 73: Stress-Temperature curve with grain refinement effect depending on the particular constant of the material.

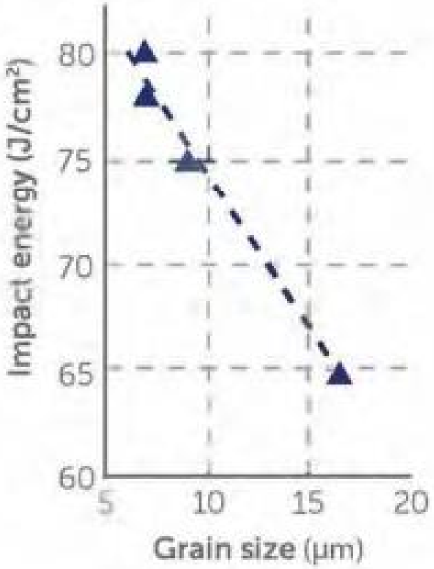

Fig. 74: Actual observed impact energy with finer prior-Austenite grain size.

Grain refinement can be achieved by means of Niobium carbides precipitation at the Austenite grain boundaries, that obstructs the Austenite grain growth, refining it before the quenching into Martensite. Niobium carbides refine the structure by means of pinning effect, hindering the movement of the dislocations and therefore the advancement of the cracks.

After the quenching the Martensite sub-structure develops within the prior-Austenite grain boundaries (abbreviated "PAGB"), which means that if the prior-Austenite grains are smaller, also martensitic grains will be smaller, with the beneficial effect of grain refinement.

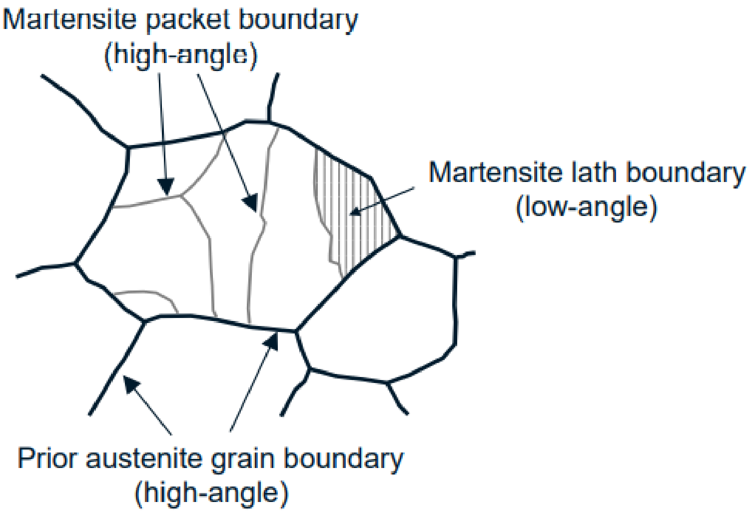

Fig. 75: Martensite grain boundaries and prior-Austenite grain boundaries.

The critical fracture stress is inversely proportional to the packet size, with the following relation:

$$\text{Critical fracture stress} = \frac{1}{\sqrt{Packet\ size}}$$

Grain refinement hinders the grain coarsening with the increase of temperature, as shown in **Fig.76**.

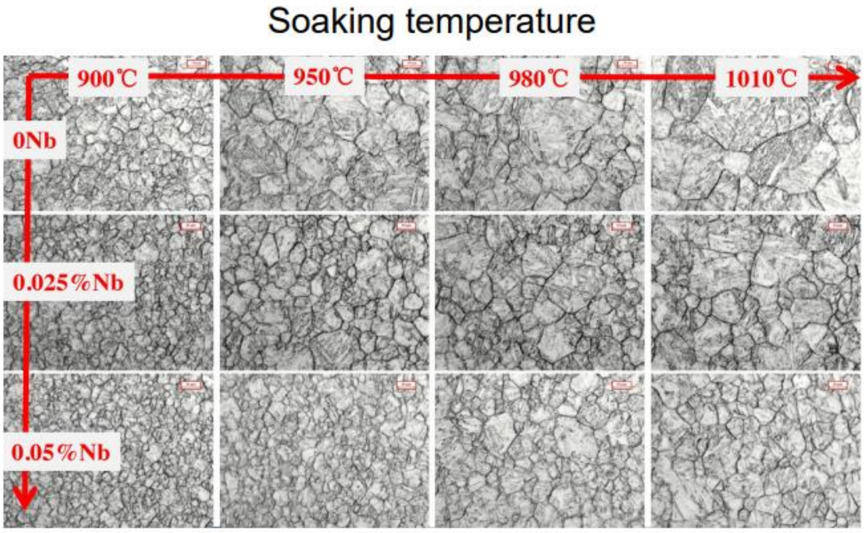

Fig. 76: Grain refinement improvement by means of Niobium addition.

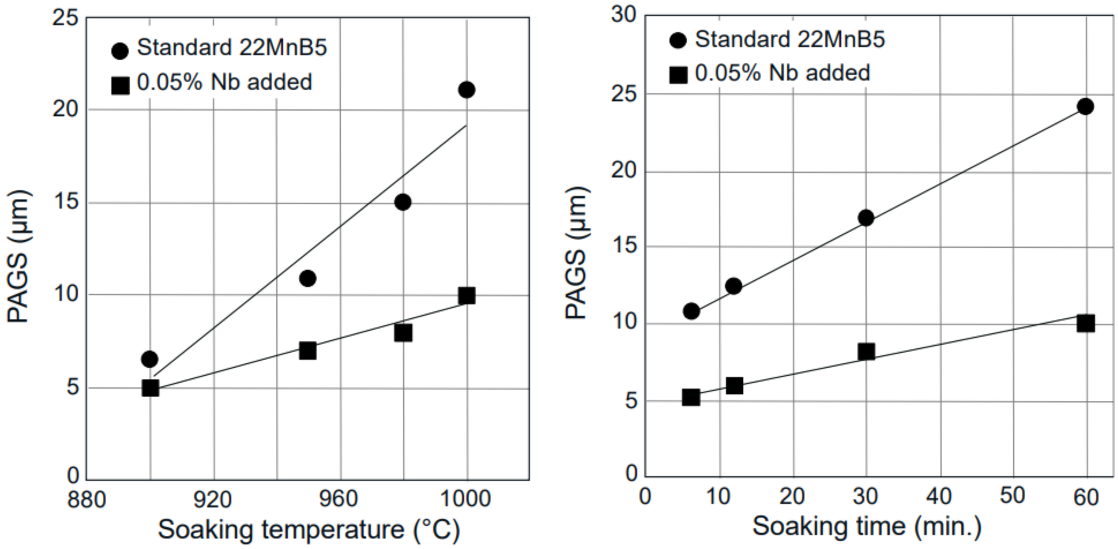

a) b)

Fig. 77: a) Relation between prior-Austenite grain boundaries size (“PAGS”) and soaking temperature; b) Relation between prior-Austenite grain boundaries size and soaking time. Standard 22MnB5 and 22MnB5 with 0.05 wt.% of Niobium are considered in both cases.

2.3.3 - Bendability

With the addition of 0.03-0.05 wt.% of Niobium there is an increase of the critical bending angle, thus improving the bendability. This is due to the fact that banding is reduced (see **Fig. 67**).

Banding consists in the aligning of the segregated alloying elements during hot working, such as hot rolling. This results in a banded microstructure, with an orientation parallel to the rolling direction.

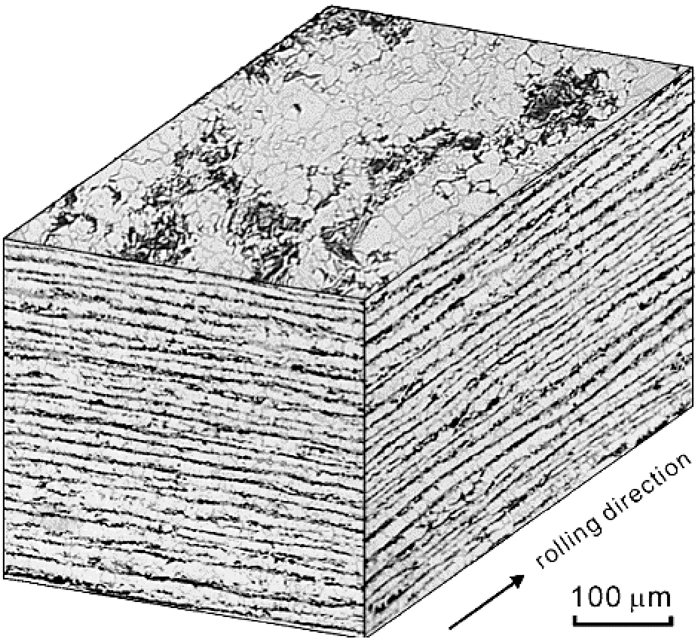

Fig. 78: Banding effect. [35]

If the grains are refined, there is a lower chance of inclusions and therefore of banding. In this way, there are less defects and the mechanical properties are higher, hence there is less possibility of crack initiation. This also leads to a better bendability.

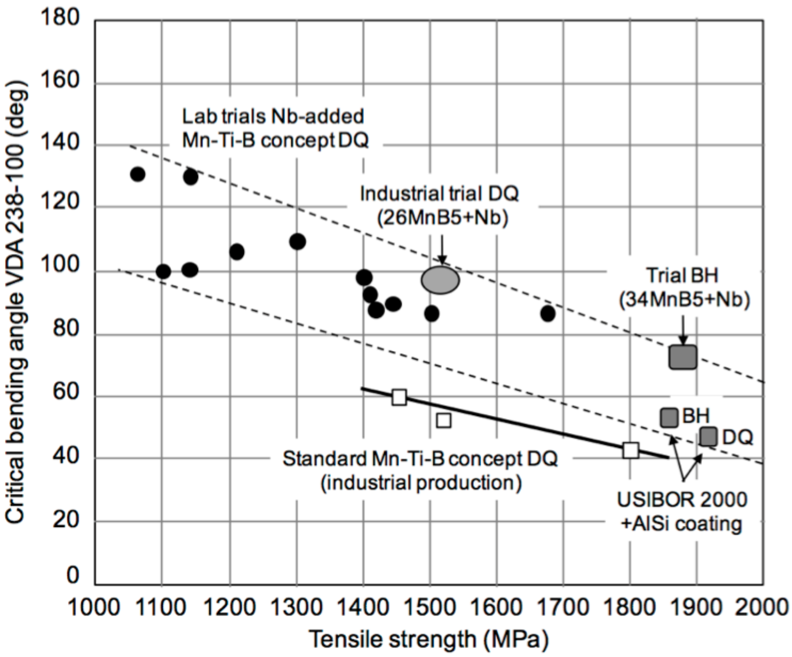

Fig. 79: Effect of Niobium micro alloying (filled symbols) on the critical bending angle of press hardened steels under VDA238-100 test conditions, in direct quenched (DQ) or bake-hardened (BH) condition. [36]

As shown in **Fig. 79**, in general the critical bending angle decreases with the increase of the tensile strength.

A larger critical bending angle means higher energy absorption, thus delayed failure.

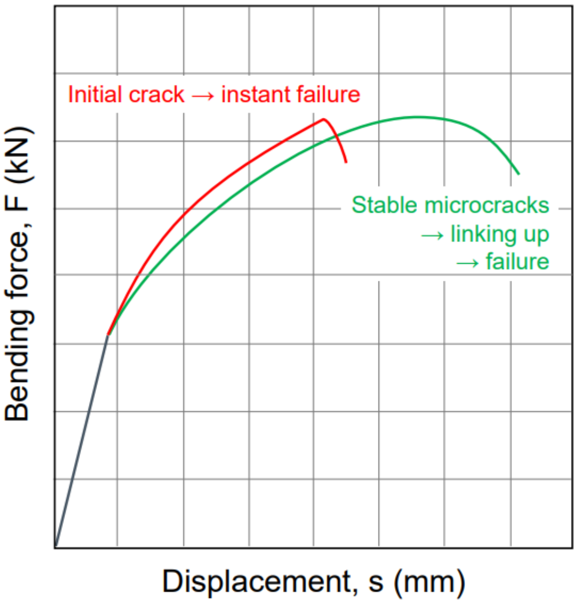

Fig. 80: Comparison between critical bending forces of a standard 22MnB5 steel grade (red curve) and of a 22MnB5 steel grade with a small addition of Niobium (green curve).

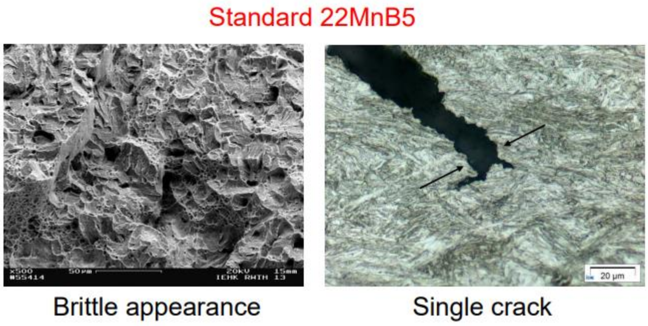

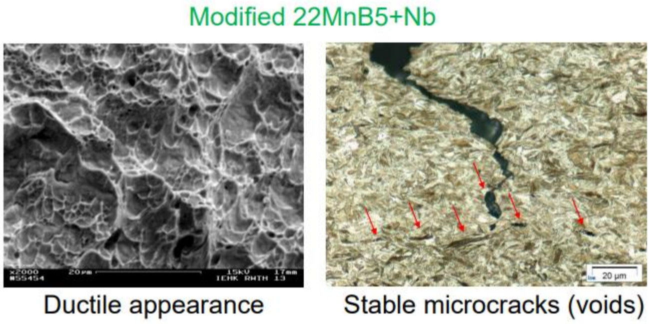

Fig. 81: Comparison between the way the standard 22MnB5 steel grade (more brittle) and the 22MnB5 steel grade with Niobium (more ductile) look and fail when a crack propagates.

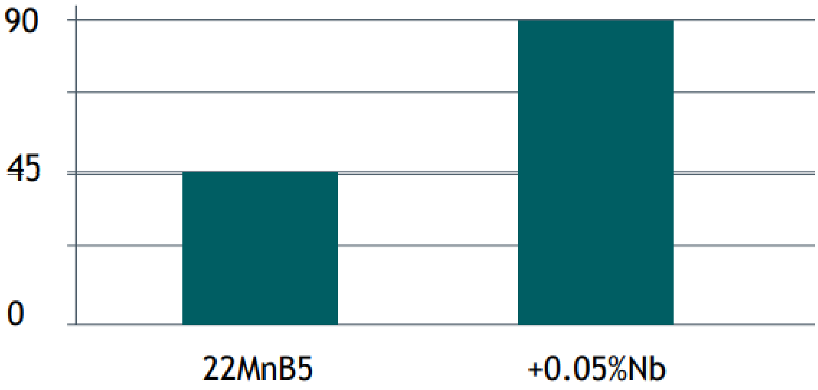

Fig. 82: Critical bending angle of a standard 22MnB5 steel grade and of a 22MnB5 steel grade with an addition of 0.05 wt.% of Niobium. [32]

2.3.4 - Hydrogen embrittlement

As already seen, press-hardening steels are subjected to Hydrogen embrittlement.

In these kinds of steels, Hydrogen embrittlement acts with three main mechanisms:

- Hydrogen-enhanced local plasticity (**HELP**): Hydrogen promotes dislocations motion and proliferation, things that lead to generation of microvoids, which cause fracture. There is a strong interaction between diffusible Hydrogen and dislocations at crack tips: this interaction facilitates the dislocations migration.

- Hydrogen-enhanced strain-induced vacancies (**HESIV**): there is a formation of clusters of vacancies (i.e. voids) at the crack tips, which promote crack propagation and thus fracture.

- Hydrogen-enhanced decohesion (**HEDE**): in this mechanism, Hydrogen segregates at grain boundaries and promotes decohesion between the metal atoms. It is an intergranular embrittlement.

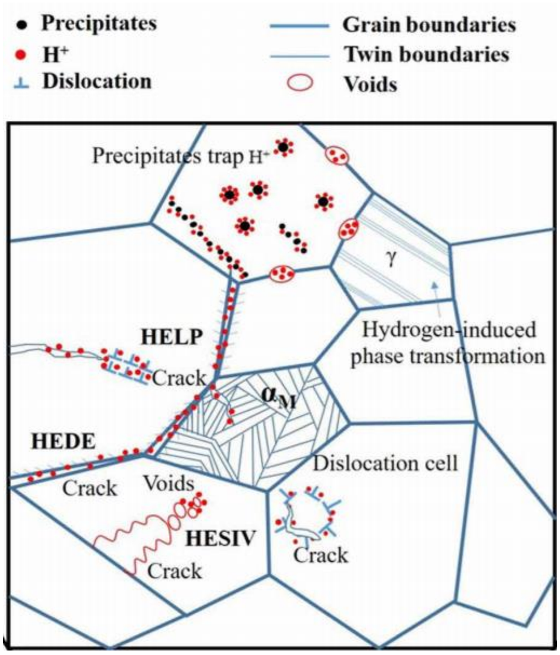

Fig. 83: Schematisation of HELP, HESIV, HEDE Hydrogen embrittlement mechanisms.

Regarding the reduction of Hydrogen embrittlement sensitivity of press hardened steels, Niobium acts by means of two main effects:

1) **Enhancement of the total large-angle grain boundary area**: it results in a lower specific Hydrogen concentration per grain boundary unit area, and it reduces the sensitivity for intergranular fracture;
2) **Hydrogen trapping**: it takes place by means of precipitation of ultrafine Niobium carbide, with diameter size inferior to 10 nm. In this way, diffusible Hydrogen is trapped and cannot move anymore; it means that it cannot diffuse to other sites and recombine with other diffusible Hydrogens, thus the sensitivity to delayed fracture is reduced and internal stresses and failure are avoided.

These two effects together considerably improve the resistance to Hydrogen embrittlement, by hindering it.

Absorbed energy is increased by increasing toughness.

2.3.5 - Process window

Another beneficial effect of the addition of Niobium is that the process window is longer, as previously mentioned: it means that it is possible to keep the piece into the oven for longer without compromising the piece's characteristics. It can happens for example due to an unexpected stop of the press line.

In fact, Niobium counteracts the grain growth. Hence, in the event that the piece is forced to remain into the oven longer than expected, due for example to some issues related to the mould that would make impossible to press the piece, it would not be necessary to throw the piece away after the thermal treatment, since the piece would not lose its properties indeed.

Then, after that the mould has been fixed, the pieces that were blocked into the oven can come out and can be pressed.

This is possible thanks to Niobium: without it, the grain growth would take place when the pieces remain stuck into the oven, and the final parts would not have the appropriated characteristics and properties.

3 - Experimental part

3.1 - Microstructure observation

The purpose of the experimental activities is to observe the microstructure of the steel before and after press hardening.

In particular, two companies provided us with two steel samples, consisting in two rectangular sheets of different thickness: steel A with a thickness of 1.4 mm, and steel B with a thickness of 1.2 mm.

These two samples are both made of 22MnB5 steel grade, but steel B also presents the 0.04 wt.% of Niobium.

Steel A sample is press hardened and does not contain Niobium, while steel B sample is just cold rolled but not press hardened. Both the samples are aluminised.

On sight they just differ by the colour, in fact the hot pressed sample is dark gray, while the cold rolled sample is silver.

With the benefit of an optical microscope we observed the microstructure of both samples, at different magnifications.

In particular, for steel A sample we observed a martensitic microstructure, since it was press hardened, as said. Steel B sample microstructure as received was pearlitic-ferritic.

Due to their small size, Niobium precipitates could not be detected by these techniques.

3.1.1 - Preparation of the samples

In order to be able to observe their microstructure at under the microscope, by means of an angle grinder we cut a small piece out of them and then we incorporated it into a resin polymeric matrix.

For each original sample we obtained two small pieces to be incorporated, in order to show both the face parallel to the rolling direction, and the face perpendicular to the rolling direction.

Once all the cut pieces were incorporated into the resin, for each piece it was necessary to polish the exposed face of the steel, to remove the scratches originated during cutting.

After having polished all the pieces, it was possible to observe the microstructures under the microscope and take some micrographs of them.

3.1.2 - Microstructures of the samples

The micrographs of the two samples are pretty similar if we do not realise a metallographic attack by means of acid. In particular, to perform chemical attacks we used Nital acid, which is a solution of alcohol and nitric acid. This solution is very useful to see the microstructure of Carbon steels, indeed. We immersed the incorporated samples into the solution and kept them there for a few seconds, 5 or 6 seconds in our case.

Only in that way it was possible to observe the microstructure, i.e. the ferritic and pearlitic grains in the case of steel B sample, and the martensitic grains in the case of steel A sample.

We could observe that the microstructure does not change relevantly regarding on the direction considered.

The micrographs were taken at 20x and 100x magnifications.

3.1.2.1 – Steel B sample (cold rolled)

This sample is the cold rolled one, not hot pressed, so the microstructure that we expected to observe was the ferritic-pearlitic one.

The following micrographs are taken before metallographic attack.

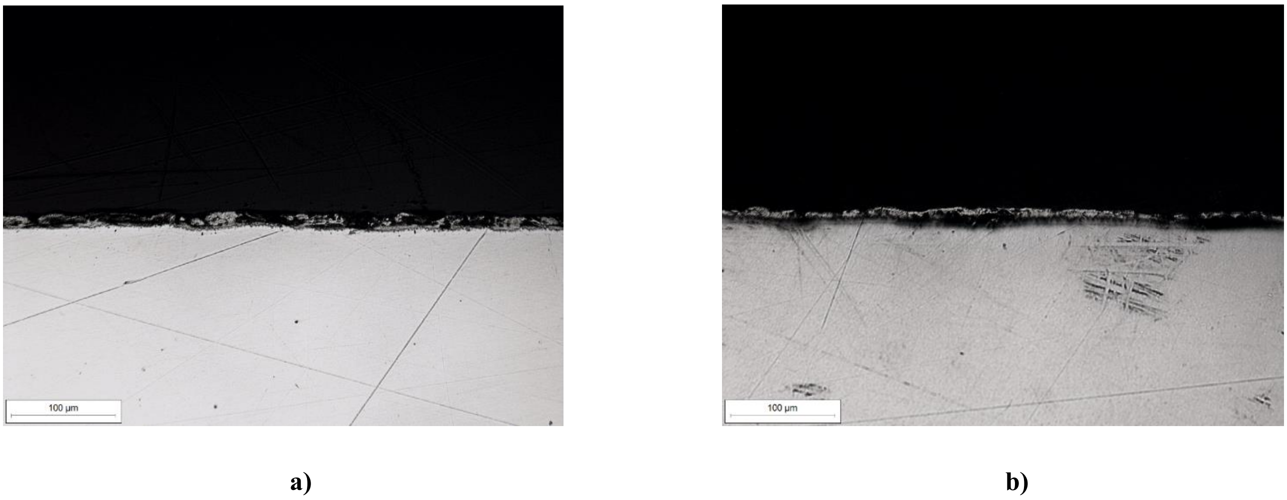

a) **b)**

Fig. 84: Micrographs taken at 20x1 magnification, before the metallographic attack. a) Side perpendicular to the lamination direction; b) Side parallel to the lamination direction.

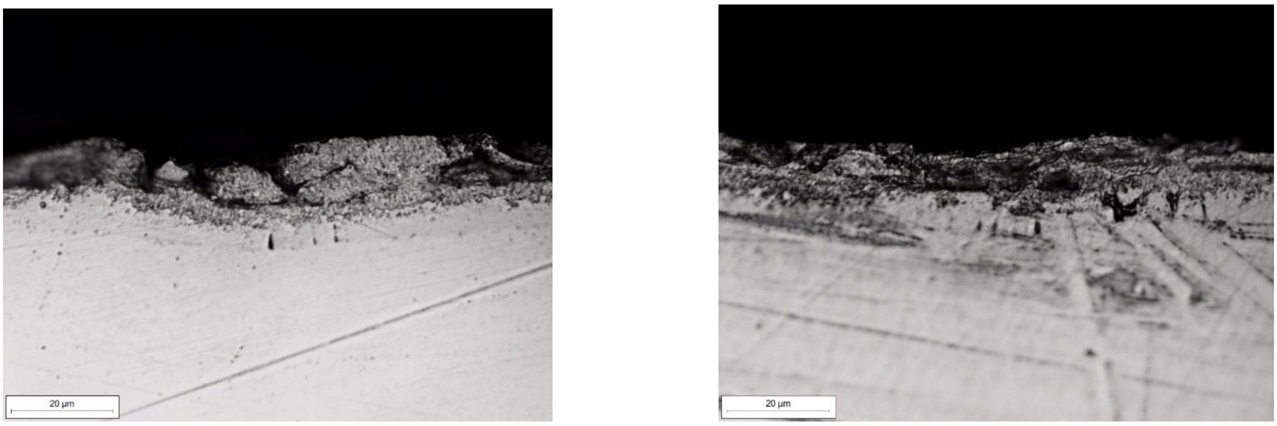

a) **b)**

Fig. 85: Micrographs taken at 100x1 magnification, before the metallographic attack. a) Side perpendicular to the lamination direction; b) Side parallel to the lamination direction.

By these micrographs it is clear that before the attack it is not possible to identify the ferritic-pearlitic microstructure expected.

Now here are the micrographs taken after the chemical attack.

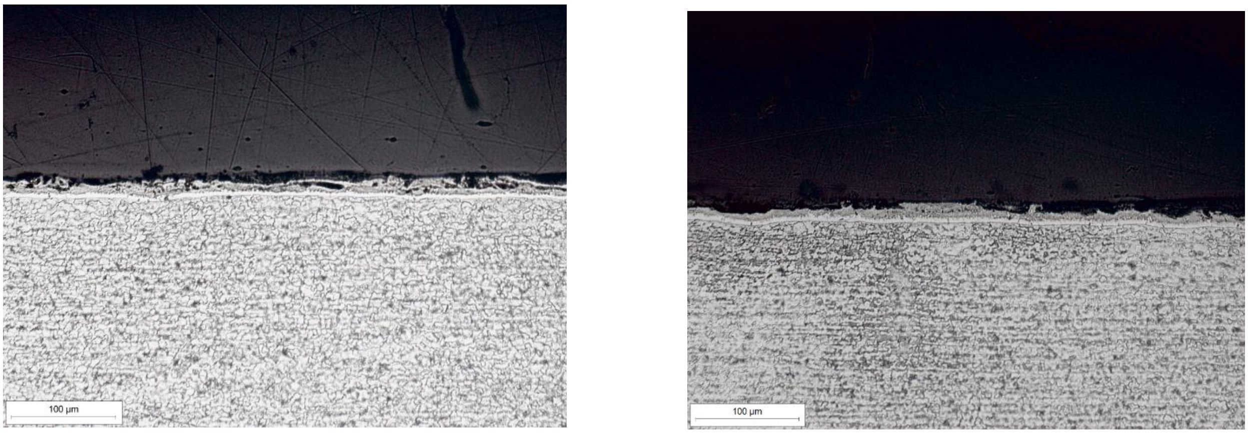

a) **b)**

Fig. 86: Micrographs taken at 20x1 magnification, after the metallographic attack. a) Side perpendicular to the lamination direction; b) Side parallel to the lamination direction.

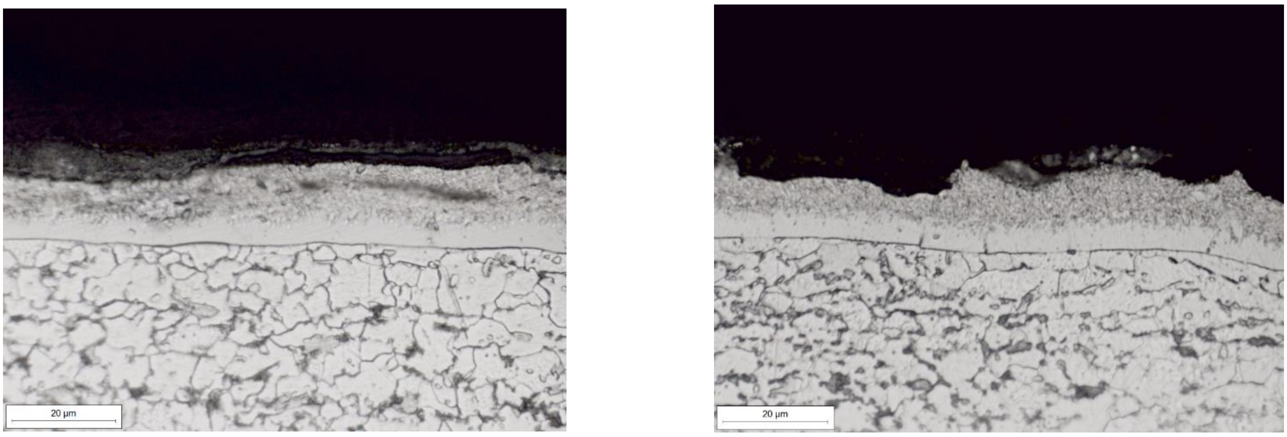

a) **b)**

Fig. 87: Micrographs taken at 100x1 magnification, after the metallographic attack. a) Side perpendicular to the lamination direction; b) Side parallel to the lamination direction.

By the micrographs taken after the metallographic attack it is possible to observe the ferritic-pearlitic microstructure, where the darker grains are the pearlitic ones while the brighter grains are that of Ferrite.

It is also evident that the shape of the grains does not have significant differences related to the rolling direction: considering the direction perpendicular or parallel to the direction of lamination, the situation does not change.

3.1.2.2 – Steel A (hot pressed)

This sample is the hot pressed one, hence we expected to observe a martensitic structure under the microscope.

From now on, since the steel microstructure is not visible before chemical attack, we do not report anymore micrographs taken before Nital attack. We also do not report micrographs for all directions, since whether it be perpendicular or parallel to the direction of lamination, the result is rather the same.

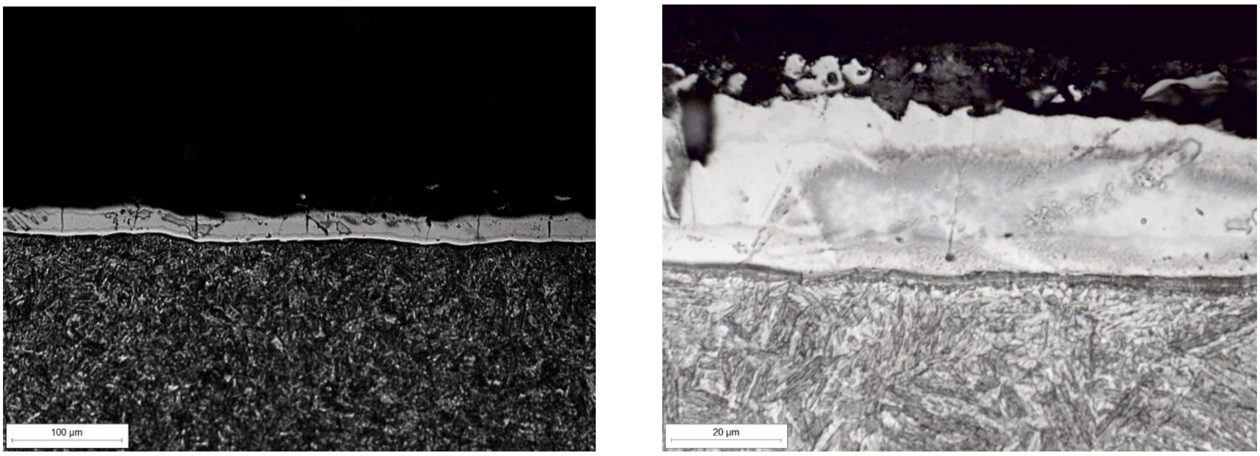

a) **b)**

Fig. 88: Micrographs of the side perpendicular to the direction of lamination taken after the metallographic attack. a) 20x1 magnification; b) 100x1 magnification.

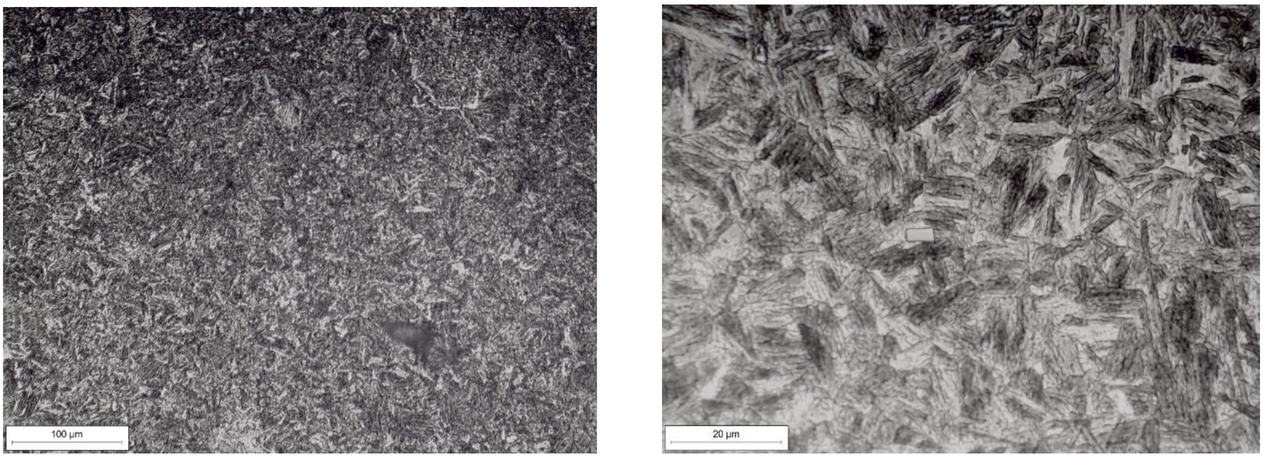

a) **b)**

Fig. 89: Other details of the microstructure of the sample showed in **Fig. 88**. **a)** 20x1 magnification; **b)** 100x1 magnification.

Here it is possible to observe the typical structure of the Martensite. It is also possible to see the Aluminium coating and its shape.

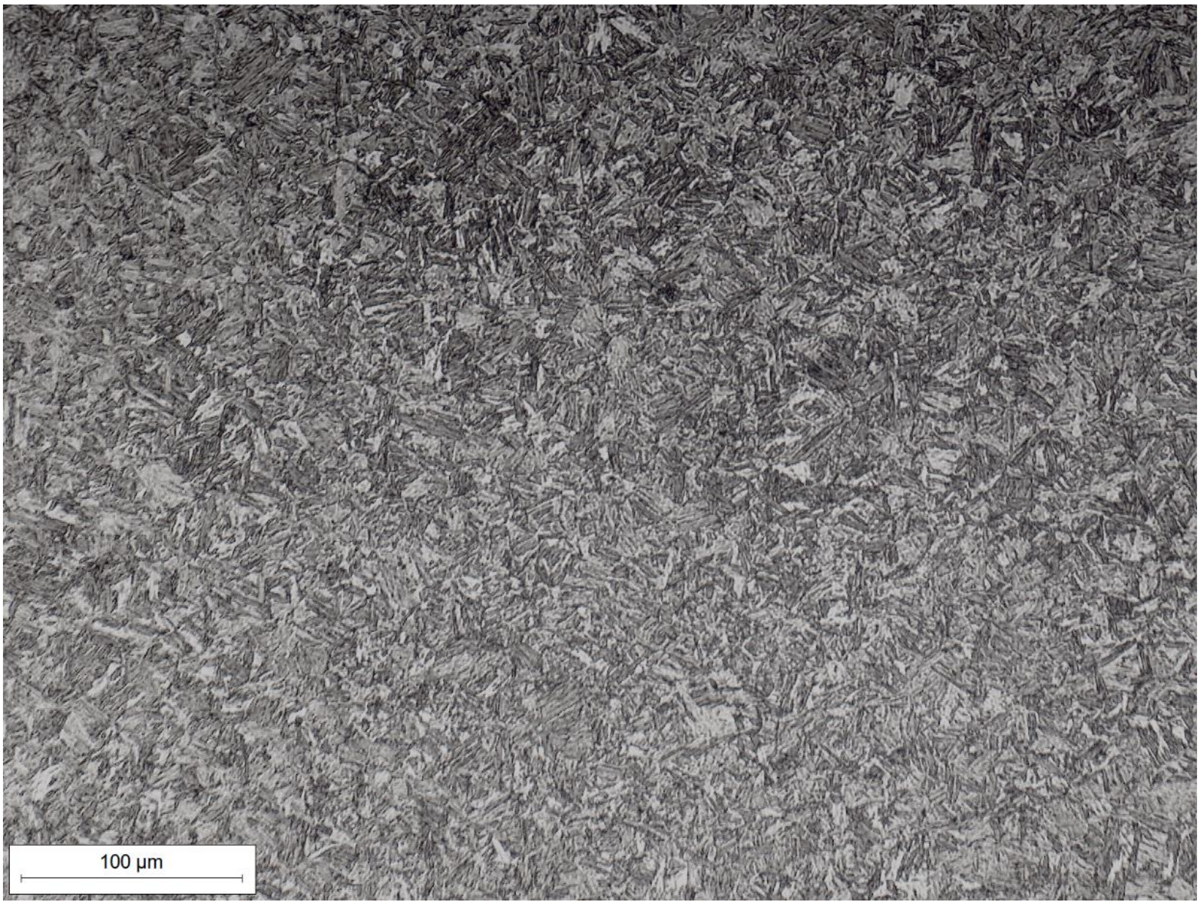

Fig. 90: Big detail of the martensitic microstructure, side parallel to the direction of lamination, 20x1 magnification.

3.2 - Chemical composition of the samples

By means of Spark AES technique (where “AES” stands for “Atomic Emission Spectroscopy”) we measured the chemical composition of both the cold rolled steel B sample and the hot stamped steel A sample.

In this way we could directly demonstrate that steel B contained a small amount of Niobium, while steel A not (or, better, that the amount contained is considerable irrelevant and therefore negligible).

The mode of operation of this technique is the following one: a series of electric sparks (or also an electric arc) are created, in order to generate a little plasma by removing atoms from the metal sample analysed. The removed atoms are excited at extremely high temperatures, so that they can emit photons according to their emission lines, which are determined by the quantum leaps of their electronic structure. These photon emissions are collected and analysed in function of their wavelength. It is possible to identify which atoms are present in the sample by comparing the emission lines obtained during the measurement with the tabulated emission lines known for the atoms.

The technique is destructive, since to remove the atoms to generate the plasma it is necessary to remove material from the sample, which will present a hole after the measurement.

Before performing this technique, we removed the external Aluminium coating, otherwise we would have measured the chemical composition of the external layer alone, and not the one of the underlying layers.

We removed the Aluminium coating by means of sandpaper. To do that, we scratched the sample with the sandpaper, measuring the thickness by means of a calliper from time to time. When we reached a thickness reduction of 0.1 mm, therefore a sample thickness of 1.3 mm for steel A and of 1.1 mm for steel B, we were sure that the Aluminium coating had been completely removed.

For each sample, the measurement was carried out several times, in order to make the average of the chemical composition of the elements of our interest and obtain a more precise value.

For each steel sample, a NB ring was used in the first four measurements. It is usually used for smaller samples, in order to have a little exposed area of the sample. The electric sparks pass through the hole of this ring to reach the sample. If the hole is little, there is the risk of removing not only material from the sample, but also a bit from the ring, with the result that the atoms removed from the ring are understood by the machine as being extracted from the sample, giving a wrong value of the actual chemical composition of the sample relative to the elements also extracted from the ring. For that reason, the rings are made of particular materials, like NB indeed.

So, since the ring that we used was made of NB, we were aware that in the resulting compositional analysis the values of Boron and Nitrogen could have been wrong.

On the other hand, the compositional values without the NB ring were expected to be more correct, but the holes made in the sample were bigger.

Element	**Steel A**		**Steel B**	
	***Mean** (over 7 measurements)*	***Standard deviation***	***Mean** (over 8 measurements)*	***Standard deviation***
C	0.225	0.0039	0.206	0.0044
Si	0.234	0.0066	0.238	0.0108
Mn	1.214	0.0129	1.233	0.0181
P	0.009	0.0007	0.012	0.0009
S	0.001	0	0.002	0
Cr	0.181	0.0033	0.170	0.0031
Mo	0.007	0.0011	0.008	0.0007
Ni	0.012	0.0005	0.009	0.0006
Al	0.035	0	0.045	0.0011
Cu	0.014	0	0.013	0.0007
Co	0.002	0	0.002	0
Nb	0.004	0.0005	0.038	0.0019
B	0.0022	0.0001	0.0024	0.0002
Bi	0.004	0.0004	0.004	0.0007
Ti	0.040	0.0007	0.034	0.0009
V	0.003	0	0.038	0.0005
W	0.018	0.0024	0.016	0.0023
Pb	0.0026	0.0002	0.0037	0.0002
Ca	0.0033	0.0001	0.0011	0.00008
Zn	<0.001	0	<0.001	0
Zr	0.002	0	0.002	0.0003
Fe	97.944	0.0229	97.905	0.0280
As	<0.002*	0*	0.003**	0.002*
N	0.0111*	0.0013*	0.0076**	0.0004**

[*] Value relative to measurements from the fifth to the seventh, carried out without the NB ring.

[**] Value relative to measurements from the fifth to the eighth, carried out without the NB ring.

Table 9: Mean values and standard deviations of the measurements of chemical compositions executed by means of Spark AES technique, both for press hardened steel A and for cold rolled steel B.

With the hot pressed **steel A** sample we performed seven measurements, whose first four were executed with the NB ring. For each component, the average value of the seven measurements is reported in **Table 9**.

The resulting chemical composition provided an average value of 0.00428 wt.% for Niobium. This quantity is irrelevant and negligible, and demonstrates that the steel A sample is not considerable microalloyed with Niobium, as we expected.

With the cold rolled **steel B** sample, we performed eight measurements, whose first four were executed with the NB ring. For each component, the average value of the eight measurements is reported in **Table 9**.

The resulting chemical composition provided an average value of 0.0376 wt.% for Niobium, which was what we expected since steel B does contain Niobium as a microalloying element.

In **Table 9**, for each chemical component it is reported the average value of its weight percentage, over seven measurements for steel A and over eight measurements for steel B.

In calculating the mean weight percentage and the standard deviation for the elements **As** and **N**, the values of the first four discharges (the ones carried out with the use of the NB ring) were not taken into account, since they looked to be altered: in fact, they resulted to be much higher than the values obtained without the use of the NB ring. Hence, the NB ring evidently influenced the values.

The reason why the values obtained for the element N were altered using the NB ring is obvious: in fact, the ring contains the element Nitrogen itself.

It is less clear the reason why also the values obtained for the element As were altered by using the NB ring: one possibility is that the NB ring was already contaminated with the element Arsenic.

3.3 - Hot pressing simulation

For the cold rolled steel B sample we performed a press hardening simulation.

We tried to reproduce the process from the entry of the sheet steel into the austenitization furnace to the quenching in the mould.

To do that, we availed ourselves of a small furnace, that simulated the industrial austenitization furnace, and of two big steel blocks, that were meant to act as a mould to reproduce the stamping operation of the austenitized sheet steel come out of the furnace.

The sample was a rectangular sheet steel of the steel B sample, the one containing Niobium.

We set the temperature inside the furnace at 930 °C. Once the temperature inside the furnace reached the one set at the beginning, we put the sample into the furnace and we kept it inside for 5 minutes.

Thereafter we extracted the sample from the furnace: we calculated that the time taken for the transfer, i.e. to move the sample from the furnace to the big steel blocks that reproduced the mould, was of 6 seconds, two of which to place the sample between the blocks and to “close” them.

We maintained the sample into the blocks for 8 seconds, thus simulating the stamping stage into the mould.

Fig. 91: Furnace utilized in the laboratory to reproduce the hot pressing process. On the ground, there are the two big steel blocks, used to simulate the mould.

In the end we obtained a press hardened sample, so we observed its new microstructure under the microscope.

3.3.1 – Microstructure of cold rolled hot pressed sample after hot pressing simulation

Also in this case, to observe the actual microstructure of the sheet steel it is necessary to perform a metallographic attack. We did that, using Nital again.

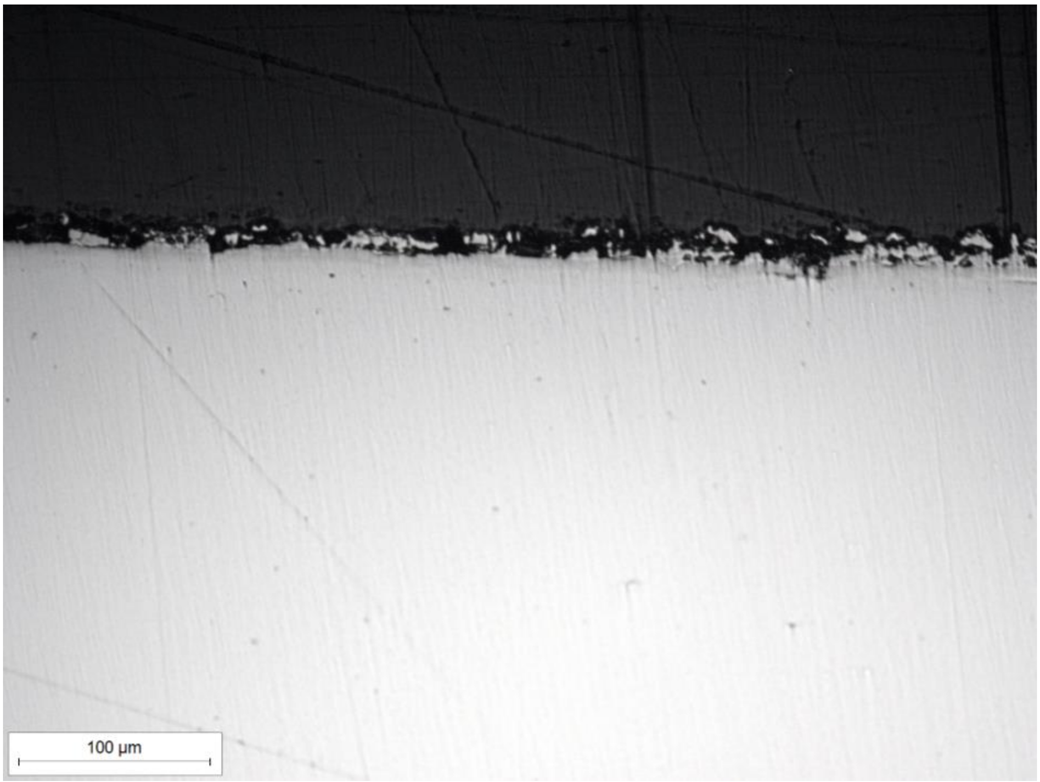

Fig. 92: Micrograph of the sample after hot pressing simulation, before chemical attack with Nital, at 20x1 magnification, side parallel to the direction of lamination.

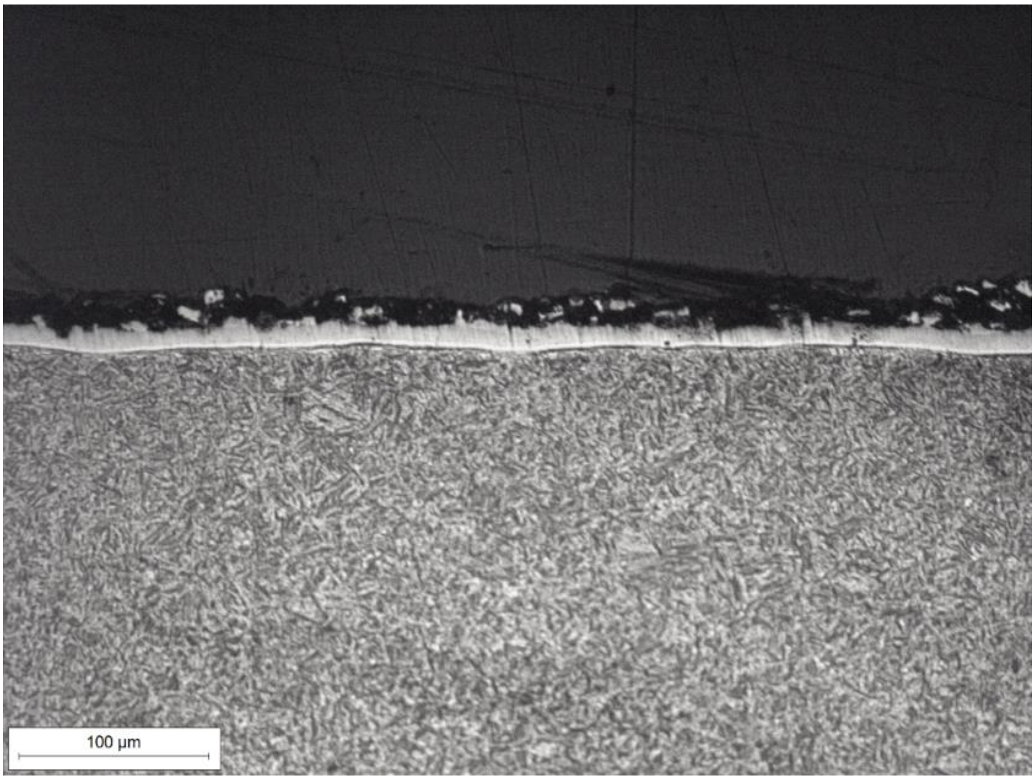

Fig. 93: Micrograph of the sample after hot pressing simulation and after the metallographic attack with Nital, at 20x1 magnification, side parallel to the direction of lamination.

It is possible to observe the formation of the Martensite, as expected.

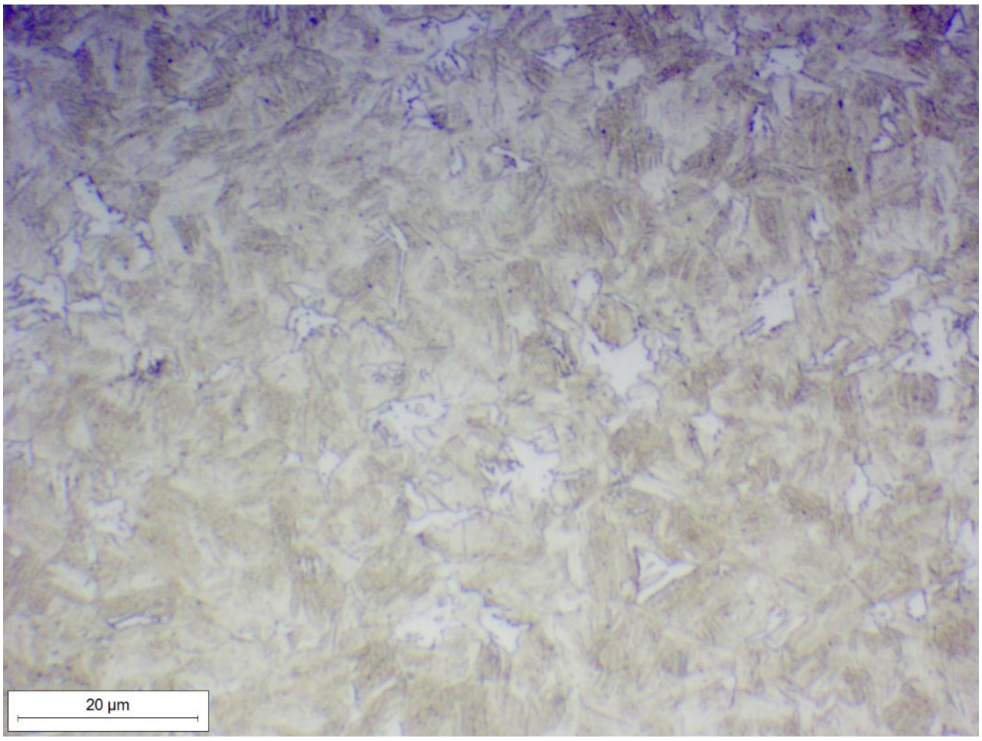

Fig. 94: Micrograph of the sample after hot pressing simulation and after the metallographic attack with Nital, at 100x1 magnification, side parallel to the direction of lamination.

In the micrograph showed in **Fig. 94** it is possible to note that, in addition to Martensite, Ferrite is still actually present: these are the white parts. This is due to the fact that in this case the process was just a laboratory reproduction, thus it is not easy to properly perform it like on an industrial level.

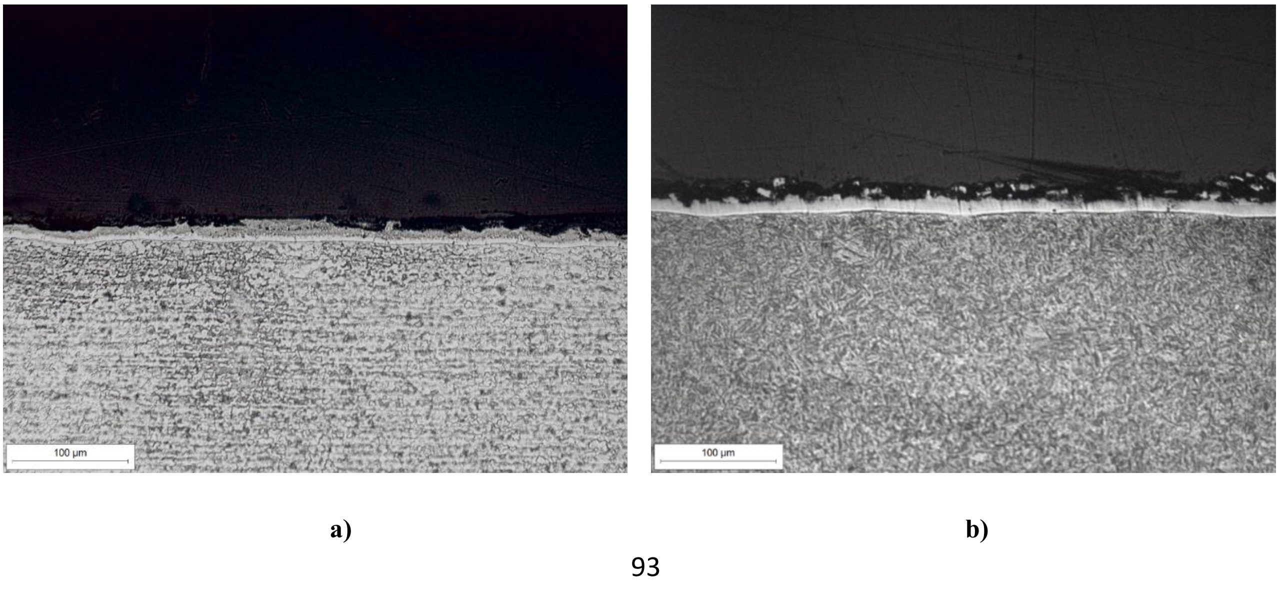

a) b)

Fig. 95: Comparison between the microstructure of the cold rolled steel B sample before and after hot pressing simulation, at 20x1 magnification, side parallel to the direction of lamination. Both micrographs are taken after metallographic attack with Nital.

a) Ferritic-pearlitic microstructure **before** hot pressing simulation;
b) Martensitic microstructure **after** hot pressing simulation, with some residual Ferrite.

3.3.2 – Hardness of the samples after hot pressing simulation

After the hot stamping simulation we carried out some Vickers hardness measurements on the obtained sample. We performed the test both at the sample edges (right side and left side) and at the sample centre.

We observed that hardness in the centre of the sample was a bit higher than hardness measured at the edges.

In fact, hardness at the edges was around 440 HV, while hardness in the centre resulted in values around 460 HV, on average.

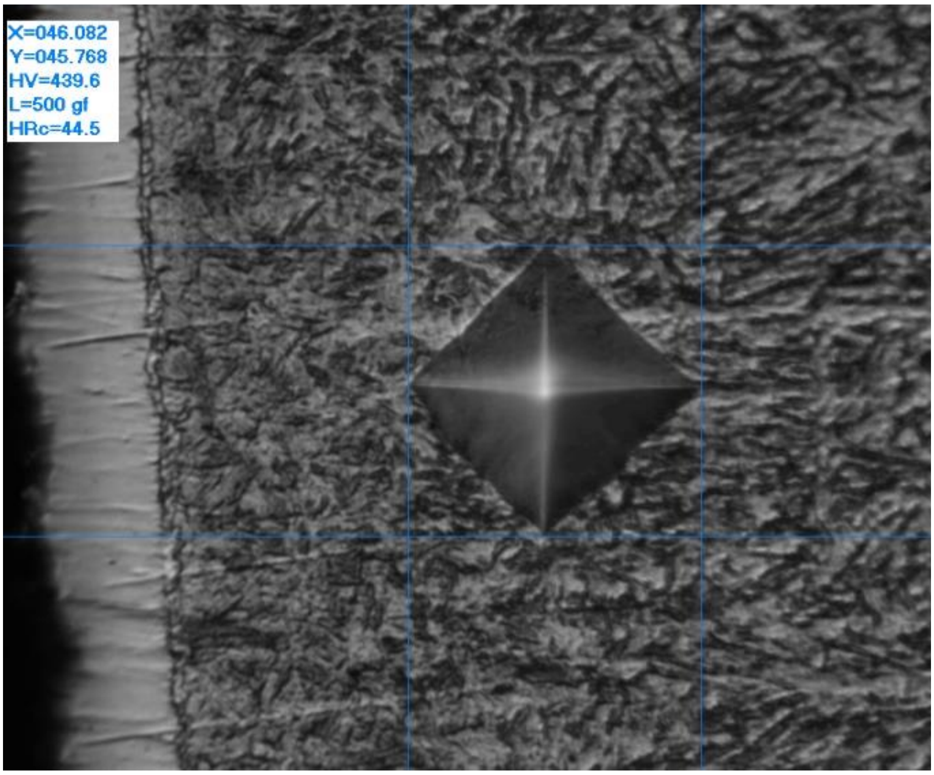

Fig. 96: Vickers incision on the left edge of the cold rolled steel B sample, after hot pressing simulation. Side perpendicular to the lamination direction. HV measured: 439.6.

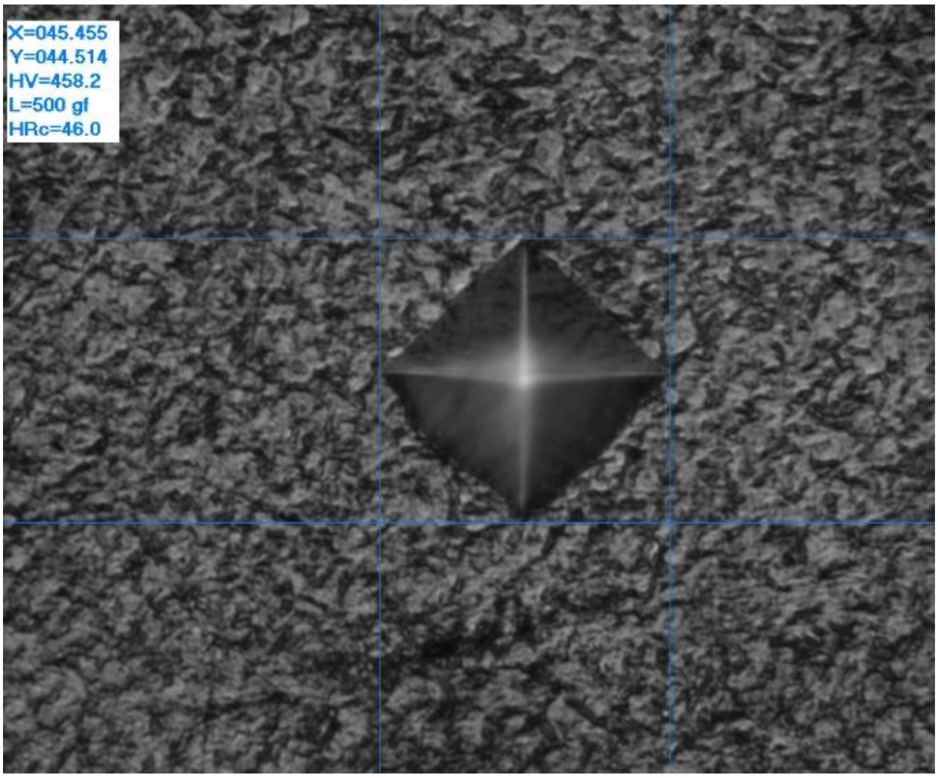

Fig. 97: Vickers incision in the centre of the cold rolled steel B sample, after hot pressing simulation. Side perpendicular to the lamination direction. HV measured: 458.2.

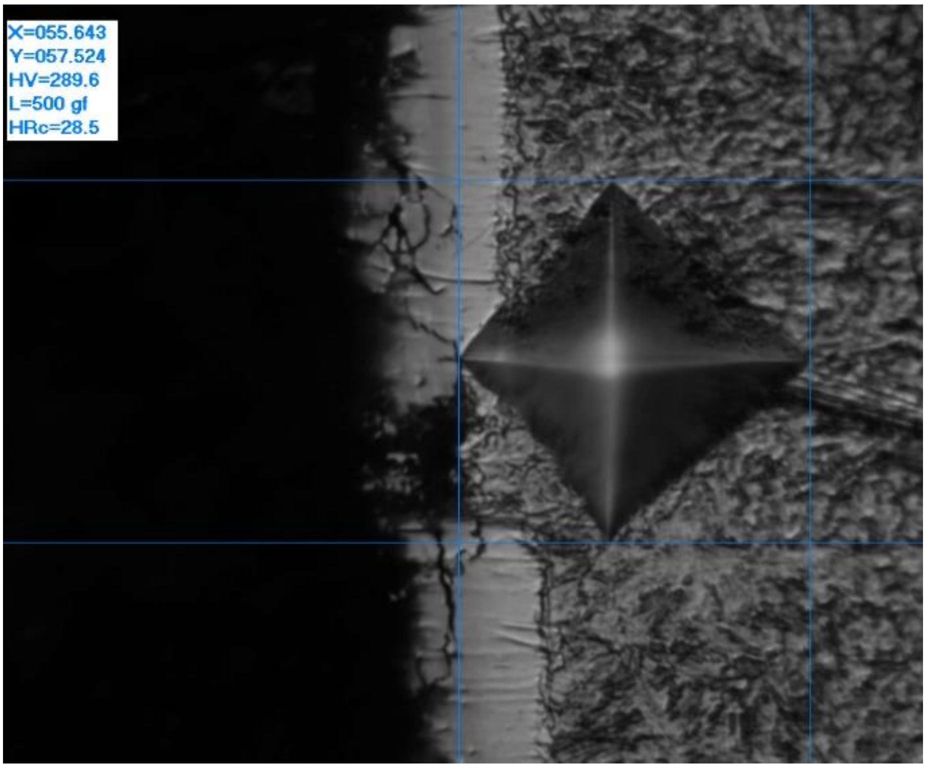

Fig. 98: Vickers incision on the left edge of the cold rolled steel B sample, after hot pressing simulation. Side perpendicular to the lamination direction. HV measured: 289.6.

In **Fig. 98** the measurement was not properly performed, since the incision was done too much close to the aluminised layer, thus the Vickers hardness necessarily had a lower value, 289.6 HV in this case, far lower than average 440 HV obtained in the other measurements. Hence, the value of 289.6 is not representative of the hardness of the sample.

3.4 – Microstructure of hot pressed samples after Bechet-Beaujard attack, to observe prior-Austenite grain boundaries

We eventually tried to observe the prior-Austenite grain boundaries of the hot pressed samples, both the steel A sample and the steel B sample, this last one after the hot pressing simulation. We did that by means of the Bechet-Beaujard attack, according to the normative ISO 643 and to the normative ASTM E407.

We prepared the etching solution as follows:

- 2 g of picric acid, in the form of solid powder;
- 1 g of Sodium dodecylbenzenesulfonate;
- 100 ml of water.

To prepare the solution, we put all the "ingredients" into a glass container and stirred them until everything was dissolved into the water.

After that, we immersed each sample into the solution and kept it there for about 5 minutes, taking a look to the microstructure under the microscope from time to time to check if in the meantime the prior-Austenite grain boundaries had become visible.

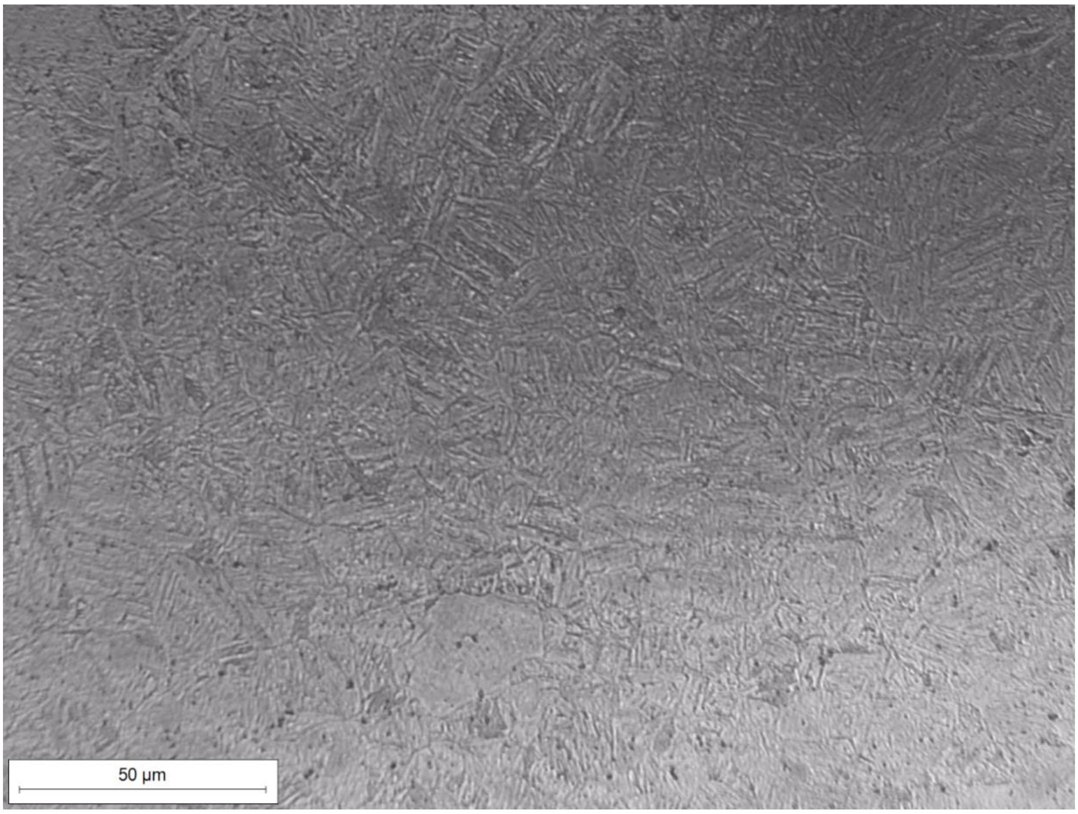

Fig. 99: Micrograph of the steel A sample after the Bechet-Beaujard attack, taken at 50x1 magnification, side perpendicular to the direction of lamination.

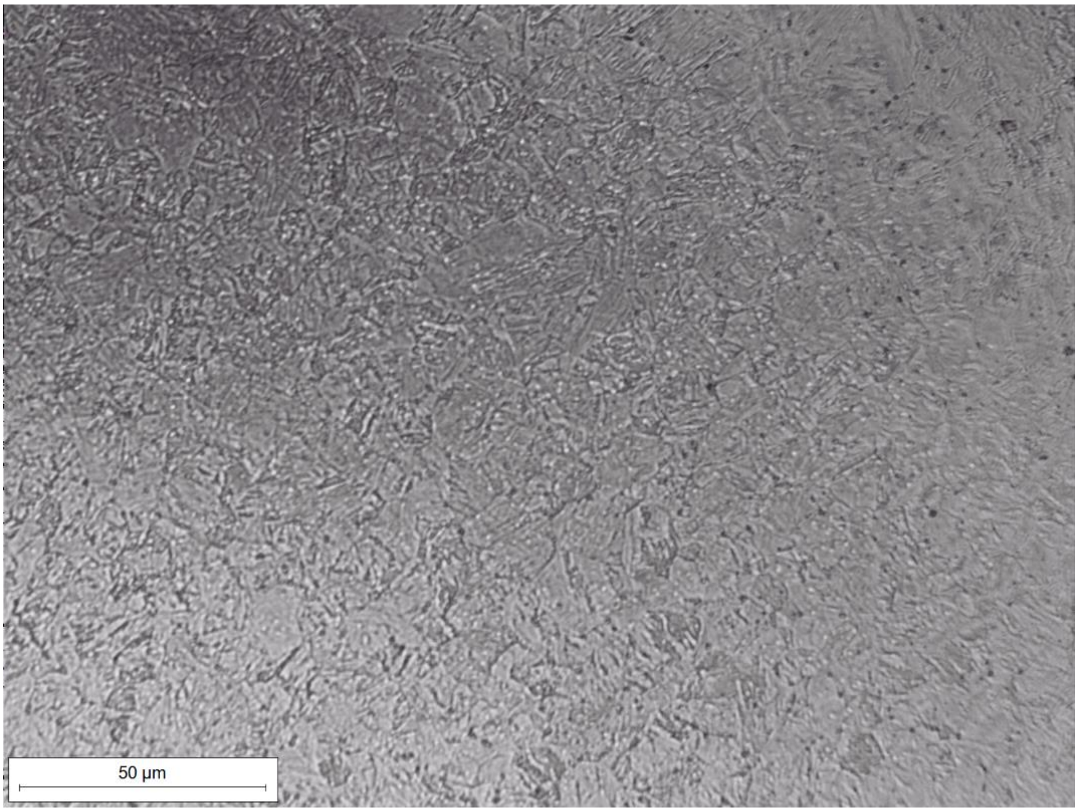

Fig. 100: Micrograph of the steel B sample (after hot pressing simulation) after the Bechet-Beaujard attack, taken at 50x1 magnification, side perpendicular to the direction of lamination.

In the micrographs obtained, showed in **Fig. 99** and **Fig. 100,** it is possible to glimpse the prior-Austenite grain boundaries, around which the Martensite grains have grown.

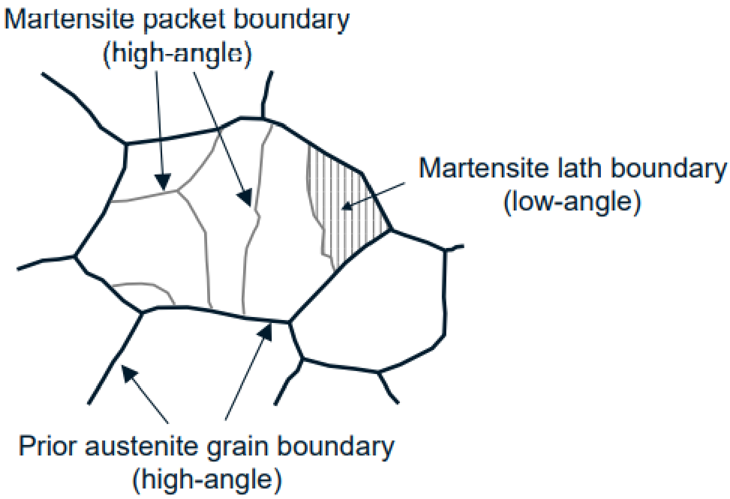

Fig. 101: Martensitic grains growth within the prior-Austenite grain boundaries.

Fig. 101 shows how martensitic grains are arranged. They follow the structure of the prior-Austenite grain boundaries.

Conclusions

Press hardening is a process used to produce ultra high strength steels used in the automotive sector for the production of the body-in-white. The steels produced in this way allow to reduce the weight of the vehicle, since they can assure the same resistance of heavier steels produced in other ways.

The typical hot stamped material for automotive application is the 22MnB5 steel grade. At the beginning of the process it has a ferritic-pearlitic microstructure, then it is austenitized and finally quenched, so that the resultant structure is Martensite, very strong.

On the other hand, press hardened steels are sensitive to several weaknesses, like Hydrogen embrittlement, low bendability, not so high toughness and small process window.

These cons can be partially reduced with the use of the element Niobium as a microalloying element. To be effective as a microalloyer, Niobium must precipitate in the form of Niobium carbides to the extent of at least 90% of Niobium dissolved in the supersaturated solid solution. Only in this way can Niobium bring the beneficial effects to press hardened steels.

By means of the experimental activity it was possible to directly observe the microstructure of hot-pressing steels and to measure their actual composition. The Vickers hardness measurements allowed us to see how hardness varies along the piece section, from the centre to the edge, while the Bechet-Beaujard attack gave us the possibility to observe the prior-Austenite grain boundaries.

Bibliography & sitography

- [1] Norrbottens Järnverk AB, Ridderstrale C.-E., *Manufacturing a hardened steel article*, UK patent GB 1490535 - A, Sweden, filed 1974, published 1977.
- [2] Kiani M, Gandikota I, Rais-Rohani M, et al., *Design of lightweight magnesium car body structure under crash and vibration constraints*, J Magnesium Alloys, 2014, p. 99 - 108
- [3] Philip T. V., *Ultra high strength steels*, Metals Handbook, 10th edition, Vol. 1, 1991, 428 – 430
- [4] Spindler, H., Klein, M., Rauch, R., Pichler, A., & Stiaszny, P. (2005). High strength and ultra high strength hot rolled steel grades–products for advanced applications. *Proceedings of Super-High Strength Steels,(Rome, Italy, Associazione Italian di Metallurgica, 2005)*.
- [5] GESTAMP, Jonsson, M. (2006). Products in hot stamped boron steel. In *Great Designs in STEEL Seminar*.
- [6] Macek, B. (2007). Developing a deep drawn hot stamped fuel tank guard. *Great Designs in Steel*.
- [7] Hashmi, S. (2014). *Comprehensive materials processing*. Newnes.
- [8] https://www.sciencedirect.com/topics/engineering/hot-stamping
- [9] Naderi, M., & Bleck, W. (2008). *Hot stamping of ultra high strength steels* (No. RWTH-CONV-112497). Lehrstuhl und Institut für Eisenhüttenkunde.
- [10] Taylor, T. A., & Clough, A. (2018). Critical review of automotive hot-stamped sheet steel from an industrial perspective. *Materials Science and Technology*, *34*(7), 809-861.
- [11] GM Worldwide Engineering Standards, GME Specification Center, Material Specification, Pre-Coated or Uncoated Low Carbon Heat-Treatable Boron Steel, GMW14400; 2011 Jan.
- [12] Renault Automobiles Standardisation, RE-DS/Department 67210, Product Specifications, Rolled Products Coated Steel for Hot Stamping, 11-04-822/-C; 2010 Oct.
- [13] https://www.thyssenkrupp-steel.com/en/company/the-route-to-steel/the-route-to-steel.html
- [14] https://www.wikiwand.com/en/Ellingham_diagram
- [15] Sun, J., Hensel, J., Klassen, J., Nitschke-Pagel, T., & Dilger, K. (2019). Solid-state phase transformation and strain hardening on the residual stresses in S355 steel weldments. *Journal of Materials Processing Technology*, *265*, 173-184.
- [16] https://www.sciencedirect.com/science/article/abs/pii/S0924013618304540

- [17] Hwang, B., Suh, D. W., & Kim, S. J. (2011). Austenitizing temperature and hardenability of low-carbon boron steels. *Scripta Materialia*, *64*(12), 1118-1120.
- [18] Rheingans, B., & Mittemeijer, E. J. (2015). Modelling precipitation kinetics: Evaluation of the thermodynamics of nucleation and growth. *Calphad*, *50*, 49-58.
- [19] Kapadia, B. M. (1977). Prediction of the Boron Hardenability Effect in Steel--A Comprehensive Review. *Hardenability Concepts with Applications to Steel*, 448-482.
- [20] Bhadeshia, H., & Honeycombe, R. (2017). *Steels: microstructure and properties*. Butterworth-Heinemann. Extract available at http://www.phase-trans.msm.cam.ac.uk/2004/z/3750-015.pdf
- [21] http://www.dierk-raabe.com/hydrogen-and-hydrogen-embrittlement/
- [22] *Materials Science and Technology*, 2017, Vol. 33, No. 13, p. 1481-1496.
- [23] https://www.piping-world.com/what-is-hydrogen-induced-cracking
- [24] http://www.dierk-raabe.com/hydrogen-and-hydrogen-embrittlement/
- [25] https://it.wikipedia.org/wiki/Columbite-tantalite
- [26] https://commons.wikimedia.org/wiki/File:Charles_Hatchett._Lithograph_by_W._Drummond,_1836,_after_T._Wellcome_V0002613.jpg
- [27] https://www.flickr.com/photos/internetarchivebookimages/14770308481/
- [28] https://www.gettyimages.ch/detail/nachrichtenfoto/tantalus-engraving-from-tableaux-du-temple-des-muses-nachrichtenfoto/646147148?language=it
- [29] Rammelsberg, C. (1872). VII.—On the composition of natural tantalates and niobates. *Journal of the Chemical Society*, *25*, 189-204.
- [30] https://www.researchgate.net/figure/Binary-phase-diagram-of-Fe-Nb-15_fig1_320129027
- [31] https://docplayer.com.br/144715333-Boas-vindas-relatorio-de-sustentabilidade-cbmm-2018.html
- [32] CBMM, Niobium Press Hardening Steels. Presentation available at https://niobium.tech/en/pages/gateway-pages/pdf/briefings/niobium_in_press_hardening_steels
- [33] https://www.niobelcon.com/NiobelCon/niobium/niobium_carbide/
- [34] https://sites.ualberta.ca/~ccwj/teaching/thermo/multicomp/
- [35] https://www.tf.uni-kiel.de/matwis/amat/iss/kap_b/advanced/ab_5_1.html

- [36] https://www.niobelcon.com/NiobelCon/niobium/niobium_in_automotive_flat_steel/auto_martensitic_steel/
- [37] Luperini, C. (2008). Delayed Fracture di Acciai Ultra Altoresistenziali, *Università di Pisa*, *Facoltà di Ingegneria*. Relatori: Dott. Ing. Renzo Valentini e Prof. Ing. Leonardo Bertini, a.a. 2007/2008.
- [38] CBMM, Mohrbacher, H., Niobium in Press Hardening (Hot Stamping) Steel, presentation.
- [39] NiobelCon, Mohrbacher, H., Precipitation of niobium in carbon steel: Fundamentals and application strategies, available at http://www.niobelcon.com/
- [40] Karbasian, H., & Tekkaya, A. E. (2010). A review on hot stamping. *Journal of Materials Processing Technology*, *210*(15), 2103-2118.
- [41] Namklang, P., & Uthaisangsuk, V. (2016). Description of microstructures and mechanical properties of boron alloy steel in hot stamping process. *Journal of Manufacturing Processes*, *21*, 87-100.
- [42] Kuhlmann, M., Schwedler, O., Holtschke, N., & Jüttner, S. (2015). Consideration of hydrogen transport in press-hardened 22MnB5. *Materials Testing*, *57*(11-12), 977-984.
- [43] Fan, D. W., Kim, H. S., Birosca, S., & De Cooman, B. C. (2007). Critical review of hot stamping technology for automotive steels. *MATERIALS SCIENCE AND TECHNOLOGY-ASSOCIATION FOR IRON AND STEEL TECHNOLOGY-*, *1*, 98.
- [44] DeArdo, A. J. (2003). Niobium in modern steels. *International Materials Reviews*, *48*(6), 371-402.
- [45] CBMM, *Sustainability report*, 2018. Document available at https://cbmm.com/-/media/CBMM/PDF/PDFs---Misc---Eng/CBMM_Sustainability-Report-2018.pdf
- [46] CBMM, *Cost-efficient Steel Alloy Design with Niobium*, 2018. Document available at https://cbmm.com/pt/Niobium-Resource-Center/-/media/CBMM/Resource-Center/PDFs/Structural---Estrutural/CBMM-Cost-Efficient-Steel-Alloy-Design-with-Niobium.pdf
- [47] Filho, A. I., Riffel, B. F., & Sousa, C. (2001, December). Some aspects of the mineralogy of CBMM niobium deposit and mining and pyrochlore ore processing- Araxa, MG- Brazil. In *International Symposium on Niobium 2001* (pp. 53-65).
- [48] Mori, K. I., Bariani, P. F., Behrens, B. A., Brosius, A., Bruschi, S., Maeno, T., ... & Yanagimoto, J. J. C. A. (2017). Hot stamping of ultra-high strength steel parts. *CIRP Annals*, *66*(2), 755-777.

- [49] Maeno, T., Mori, K. I., Ogihara, T., & Fujita, T. (2019). Removal of thin oxide scale by ultrasonic cleaning with diluted hydrochloric acid in hot stamping of bare 22MnB5 sheet using resistance heating. *Procedia Manufacturing*, *29*, 225-231.
- [50] Bergman, G., Berglund, D., & Isaksson, K. (2015). Thermo-mechanical Forming Analysis and Mapping of Material Properties in Press Hardened Components with Tailored Material Properties. In *Advanced Materials Research* (Vol. 1063, pp. 290-296). Trans Tech Publications Ltd.
- [51] Chamisa, A. (2014). *Development of ultra high strength steels for reduced carbon emissions in automotive vehicles* (Doctoral dissertation, University of Sheffield).
- [52] Çavuşoğlu, O., Çavuşoğlu, O., Yılmazoğlu, A. G., Üzel, U., Aydın, H., & Güral, A. (2020). Microstructural features and mechanical properties of 22MnB5 hot stamping steel in different heat treatment conditions. *Journal of Materials Research and Technology*, *9*(5), 10901-10908.
- [53] Flachstahl, S. (2014). 22MnB5 boron alloyed quenched and tempered steel. *Product catalogue*. Available at https://www.salzgitter-flachstahl.de/fileadmin/footage/MEDIA/gesellschaften/szfg/informationsmaterial/produktinformationen/warmgewalzte_produkte/eng/22mnb5.pdf
- [54] Khaira H. K., *Hardenability*, Bhopal. Presentation available at https://slideplayer.biz.tr/slide/11785831/
- [55] Atyam T., *Jominy End Quench Hardenability Test*. Presentation available at https://www.slideshare.net/TejasAtyam/jominy-end-quench-hardenability-test-40164217
- [56] Kiftaga L., *Performing Bench work*, 2005. Presentation available at https://www.slideshare.net/Lemmalove/performing-bench-work-ppt
- [57] Kumar S., *Hydrogen Embrittlement: Causes, Effects & Prevention*, 2011. Presentation available at https://www.slideshare.net/sidheshwar1988mm24/hydrogen-embrittlement-causes-effects-prevention
- [58] Herring, D., H., *Hydrogen Embrittlement*, 2010. Paper available at http://www.heat-treat-doctor.com/documents/hydrogen%20embrittlement.pdf
- [59] Haidemenopoulos, G. N., Kamoutsi, H., Polychronopoulou, K., Papageorgiou, P., Altanis, I., Dimitriadis, P., & Stiakakis, M. (2018). Investigation of stress-oriented hydrogen-induced cracking (SOHIC) in an amine absorber column of an oil refinery. *Metals*, *8*(9), 663.
- [60] *Hydrogen Embrittlement*, 2014. Presentation available at https://docplayer.it/38904696-Hydrogen-embrittlement-12-maggio-2014.html

- [61] deSouza Paraiso, O., & deFuccio, R. (1984). Mining, ore preparation and ferroniobium production at CBMM. In *Niobium-Proceedings of the international symposium*.
- [62] Marshall J. L., Marshall V. R., *Rediscovery of the Elements Niobium and Tantalum*, 2013. Research available at https://digital.library.unt.edu/ark:/67531/metadc306839/m2/1/high_res_d/2013-hexagon-niobium.pdf
- [63] Tina, A. (2020). Niobium micro-alloyed steels for automotive applications, *Politecnico di Torino*. Relatore: Prof. Paolo Matteis, a.a.2019/2020.
- [64] Gong, P., Nutter, J., Rivera-Diaz-Del-Castillo, P. E. J., & Rainforth, W. M. (2020). Hydrogen embrittlement through the formation of low-energy dislocation nanostructures in nanoprecipitation-strengthened steels. *Science advances*, *6*(46), eabb6152.
- [65] OHMORI, Y. (1975). Precipitation of Fine Niobium Carbide Particles in Low Carbon Steels. *Transactions of the Iron and Steel Institute of Japan*, *15*(4), 194-203.
- [66] CBMM, *Niobium Press Hardening Steels*. Presentation available at https://niobium.tech/en/pages/gateway-pages/pdf/briefings/niobium_in_press_hardening_steels
- [67] https://www.niobelcon.com/NiobelCon/niobium/
- [68] https://www.niobelcon.com/NiobelCon/niobium/niobium_carbide/
- [69] https://www.niobelcon.com/NiobelCon/niobium/niobium_in_automotive_flat_steel/auto_martensitic_steel/
- [70] Philip, T.,V., Ultra high strength steels, *Metals Handbook*, 10th edition, Vol. 1, 1991, 428-430
- [71] Rana, R., & Singh, S. B. (2016). *Automotive steels: design, metallurgy, processing and applications*. Woodhead Publishing.
- [72] NiobelCon, Mohrbacher, H., *Understanding martensitic steel*.
- [73] Private conversations with Dr Fabio D'Aiuto
- [74] https://www.machinedesign.com/materials/article/21834691/microalloying-strengthens-steel#:~:text=The%20most%20commonly%20used%20microalloying,particularly%20in%20combination%20with%20vanadium
- [75] https://www.industrialheating.com/articles/91318-segregation-and-banding-in-carbon-and-alloy-steel

Acknowledgements

This thesis has been a challenging work that allowed me to discover an interesting part of the steels sector.

I am fully grateful to my supervisor, the Professor Paolo Matteis, for his great and precious support and for his special willingness showed towards me throughout my entire work, both in theoretical and practical activities. I was extremely lucky to meet him on my way.

I thank Dr Fabio D’Aiuto a lot for his clear and interesting explanations relative to the world of Niobium, which is full of curiosities. Moreover, he provided me with a large amount of material, very useful to write my thesis, and has always been present and willing when I needed his help, so I wish to thank him very much for everything.

I greatly thank my family for all the efforts, for their support and patience demonstrated along these tough and unique years, hoping to be able to pay them back soon by giving them new satisfactions.

Last but not least, a special thought goes to all the people met at the Politecnico that in these years helped me in some way.